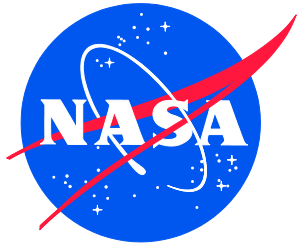


NASA/TM-2016-219214
NESC-RP-12-00795



Remote Imaging of Exploration Flight Test-1 (EFT-1) Entry Heating Risk Reduction

*David M. Schuster/NESC
Langley Research Center, Hampton, Virginia*

*Thomas J. Horvath
Langley Research Center, Hampton, Virginia*

*Richard J. Schwartz
Analytical Mechanics Associates, Hampton, Virginia*

NASA STI Program . . . in Profile

Since its founding, NASA has been dedicated to the advancement of aeronautics and space science. The NASA scientific and technical information (STI) program plays a key part in helping NASA maintain this important role.

The NASA STI program operates under the auspices of the Agency Chief Information Officer. It collects, organizes, provides for archiving, and disseminates NASA's STI. The NASA STI program provides access to the NTRS Registered and its public interface, the NASA Technical Reports Server, thus providing one of the largest collections of aeronautical and space science STI in the world. Results are published in both non-NASA channels and by NASA in the NASA STI Report Series, which includes the following report types:

- **TECHNICAL PUBLICATION.** Reports of completed research or a major significant phase of research that present the results of NASA Programs and include extensive data or theoretical analysis. Includes compilations of significant scientific and technical data and information deemed to be of continuing reference value. NASA counter-part of peer-reviewed formal professional papers but has less stringent limitations on manuscript length and extent of graphic presentations.
- **TECHNICAL MEMORANDUM.** Scientific and technical findings that are preliminary or of specialized interest, e.g., quick release reports, working papers, and bibliographies that contain minimal annotation. Does not contain extensive analysis.
- **CONTRACTOR REPORT.** Scientific and technical findings by NASA-sponsored contractors and grantees.

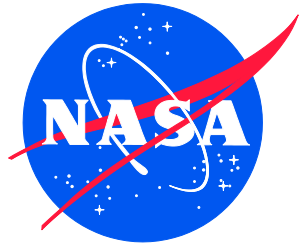
- **CONFERENCE PUBLICATION.** Collected papers from scientific and technical conferences, symposia, seminars, or other meetings sponsored or co-sponsored by NASA.
- **SPECIAL PUBLICATION.** Scientific, technical, or historical information from NASA programs, projects, and missions, often concerned with subjects having substantial public interest.
- **TECHNICAL TRANSLATION.** English-language translations of foreign scientific and technical material pertinent to NASA's mission.

Specialized services also include organizing and publishing research results, distributing specialized research announcements and feeds, providing information desk and personal search support, and enabling data exchange services.

For more information about the NASA STI program, see the following:

- Access the NASA STI program home page at <http://www.sti.nasa.gov>
- E-mail your question to help@sti.nasa.gov
- Phone the NASA STI Information Desk at 757-864-9658
- Write to:
NASA STI Information Desk
Mail Stop 148
NASA Langley Research Center
Hampton, VA 23681-2199

NASA/TM-2016-219214
NESC-RP-12-00795



Remote Imaging of Exploration Flight Test-1 (EFT-1) Entry Heating Risk Reduction

*David M. Schuster/NESC
Langley Research Center, Hampton, Virginia*

*Thomas J. Horvath
Langley Research Center, Hampton, Virginia*

*Richard J. Schwartz
Analytical Mechanics Associates, Hampton, Virginia*

National Aeronautics and
Space Administration

Langley Research Center
Hampton, Virginia 23681-2199

June 2016


Acknowledgments

The NESC team would like to recognize the Aerospace Corporation and the WB-57 High Altitude Research Program at the NASA JSC for support during this assessment. The services of these two organizations were activated deep into in the demonstration of capability (EFT-1 observation) phase of the assessment as a risk-reduction effort. While the primary aircraft was able to support the observation, the professional attitude and dedication to preparing a second aircraft to perform the mission on such short notice was remarkable. The NESC team would also like to recognize Surface Optics for providing laboratory measurements to quantify the surface optical properties of the MPCV TPS. The test results had a significant impact regarding the observation strategy to acquire the capsule at long range.

<p>The use of trademarks or names of manufacturers in the report is for accurate reporting and does not constitute an official endorsement, either expressed or implied, of such products or manufacturers by the National Aeronautics and Space Administration.</p>
--


Available from:

NASA STI Program / Mail Stop 148
NASA Langley Research Center
Hampton, VA 23681-2199
Fax: 757-864-6500

	NASA Engineering and Safety Center Technical Assessment Report	Document #: NESC-RP- 12-00795	Version: 1.0
Title:	Remote Imaging of EFT-1 Entry Heating Risk Reduction		Page #: 1 of 98

Remote Imaging of Exploration Flight Test-1 (EFT-1) Entry Heating Risk Reduction

May 19, 2016

	<h1 style="text-align: center;">NASA Engineering and Safety Center Technical Assessment Report</h1>	Document #: NESC-RP-12-00795	Version: 1.0
Title: Remote Imaging of EFT-1 Entry Heating Risk Reduction			Page #: 2 of 98

Report Approval and Revision History

NOTE: This document was approved at the May 19, 2016, NRB. This document was submitted to the NESC Director on June 10, 2016, for configuration control.

Approved:	<i>Original Signature on File</i>	6/15/16
	NESC Director	Date

Version	Description of Revision	Office of Primary Responsibility	Effective Date
1.0	Initial Release	Dr. David Schuster, NASA Technical Fellow for Aerosciences, LaRC	May 19, 2016



	NASA Engineering and Safety Center Technical Assessment Report	Document #: NESC-RP- 12-00795	Version: 1.0
Title:	Remote Imaging of EFT-1 Entry Heating Risk Reduction		Page #: 3 of 98

Table of Contents

Technical Assessment Report	7
1.0 Notification and Authorization	7
2.0 Signature Page.....	8
3.0 Team List	10
3.1 Acknowledgements.....	10
4.0 Executive Summary	12
5.0 Assessment Plan	15
6.0 Problem Description, Proposed Solutions, and Risk Assessment.....	15
6.1 Challenges with Heat Shield Thermocouples	16
6.2 Platform and Instrument Capability	18
6.3 Risk Characterization and Mitigation	24
6.3.1 Location of Peak Heating.....	25
6.3.2 Observation Location and Estimated Spatial Resolution.....	25
6.3.3 Asset Reliability and Schedule Conflict	29
6.3.4 Long-Range Acquisition.....	31
6.3.5 Obscuring Clouds	36
6.3.6 Effect of Shock Layer Emissions.....	39
6.3.7 Effects of Ablation.....	43
6.3.8 Mission Operations Readiness.....	45
7.0 Data Acquisition and Data Analysis.....	53
7.1 Data Collection during EFT-1 Thermal Observation	56
7.2 Unified Best Estimated Trajectory (BET)	68
7.3 Data Processing.....	68
7.3.1 Selection of Time Segments for Processing	70
7.3.2 Interpolation, Frame Co-Registration and Averaging.....	73
7.3.3 Radiometric Calibration.....	74
7.3.4 Atmospheric Compensation and Emissivity	76
7.3.5 Temperature Estimates	77
7.3.6 Uncertainty of Temperature Estimates	80
7.3.7 Comparison of TC Data to Image-Derived Temperature	82
8.0 Findings, Observations, and NESC Recommendations.....	87
8.1 Findings	87
8.2 Observations	88
8.3 NESC Recommendations	89
9.0 Alternate Viewpoint.....	91
10.0 Other Deliverables	91
11.0 Lessons Learned.....	91
12.0 Recommendations for NASA Standards and Specifications.....	91
13.0 Definition of Terms.....	91
14.0 Acronyms List	92
15.0 References.....	95
16.0 Appendices (separate volume)	98

	NASA Engineering and Safety Center Technical Assessment Report	Document #: NESC-RP- 12-00795	Version: 1.0
Title:	Remote Imaging of EFT-1 Entry Heating Risk Reduction		Page #: 4 of 98

List of Figures

Figure 6.1-1.	Schematic of EFT-1 Heat Shield DFI Instrumentation Layout (Subsurface TC Locations Identified in Blue and Red).....	17
Figure 6.1-2.	EFT-1 Heat Shield TC Plug (Side View Showing TC Junctions below the Surface with Outer Surface Shown on the Image Top)	18
Figure 6.2-1.	EFT-1 Proposed Reentry Flight Path (circa 2013) with Splashdown off the Coast of California.....	19
Figure 6.2-2.	Thermal Image of Endeavour During STS-134 Reentry Near the Point of Closest Approach, Mach 5.8, Slant Range ~32 nmi. (Estimated resolution ~4 inches per pixel.).....	20
Figure 6.2-3.	U.S. Navy NP-3D Cast Glance Aircraft (Bloodhound 300 (BH-300))	22
Figure 6.2-4.	Internal Layout of the Navy NP-3D Orion (BH-300).....	22
Figure 6.2-5.	NASA WB-57 with Nose-Mounted DyNAMITE Imaging Sensors	23
Figure 6.2-6.	NASA WB-57 with Nose-Mounted DyNAMITE Imaging Sensors	23
Figure 6.3-1.	Relative Size and Temperature Differences between SSP Orbiter and the MPCV Capsule	24
Figure 6.3.2-1.	Synthetic Image of MPCV Capsule near the Point of Peak Heating as Viewed from the Navy NP-3D Aircraft.....	27
Figure 6.3.2-2.	Estimated Spatial Resolution of the Cast Glance NIR as a Function of Time	28
Figure 6.3.2-3.	EFT-1 Ground Track and Hazard Keep-out Zone.....	28
Figure 6.3.3-1.	EFT-1 Ground Track and Hazard Keep-out Zone.....	30
Figure 6.3.4-1.	Blackbody Radiance Characteristics	32
Figure 6.3.4-2.	Predicted Surface Temperatures on the EFT-1 Capsule during Several Phases of Reentry	33
Figure 6.3.4-3.	TPS Samples Used to Obtain Surface Optical Properties.....	34
Figure 6.3.4-4.	Measured Emissivity of Aluminized Kapton® Tape.....	35
Figure 6.3.4-5.	Measured Emissivity of Charred/Ablated Avcoat.....	35
Figure 6.3.4-6.	Predicted Irradiance in SWIR Waveband at Time of Long-Range Acquisition. Distance to Capsule = 493 nmi. Elevation Angle = 3 deg. Signal-to-Sky Background ~1.5.	36
Figure 6.3.5-1.	Mean Total Cloud Cover	37
Figure 6.3.5-2.	SSP Orbiter Reentry Paths to KSC Superimposed on Predicted Cloud Cover Forecast in 2011.....	38
Figure 6.3.5-3.	General CFLOS Output Showing Relationships between a Target and Several Notional Observers and the Optical Blockage from Clouds.....	39
Figure 6.3.6-1.	Predicted Irradiance along Line-of-Sight from Heat Shield through Shock Layer toward an External Observer	40
Figure 6.3.6-2.	Predicted Shock Layer Radiance Relative to Total Radiance (Shock Layer and Heat Shield).....	41
Figure 6.3.6-3.	Predicted Irradiance in the NIR Waveband at the Time of Peak Heating. Distance to Capsule = 48 nmi. Elevation Angle = 27 deg. 850 nm Cut-on Filter.	42
Figure 6.3.6-4.	Predicted Irradiance from the Capsule Heat Shield Edge and Backshell in the NIR Waveband at the Point of Closest Approach to the Aircraft. Distance to Capsule = 35 nmi. Elevation Angle = 37 deg. 850 nm Cut-on Filter.	42


	<h1 style="text-align: center;">NASA Engineering and Safety Center</h1> <h2 style="text-align: center;">Technical Assessment Report</h2>	Document #: NESC-RP-12-00795	Version: 1.0
Title:	Remote Imaging of EFT-1 Entry Heating Risk Reduction		Page #: 5 of 98

Figure 6.3.7-1.	Predicted Emission and Transmission from SPURC for a Range of Surface- and Shock-Layer Temperatures.....	44
Figure 6.3.7-2.	Predicted Emission and Transmission from NEQAIR for a Range of Surface- and Shock-Layer Temperatures.....	44
Figure 6.3.7-3.	Predicted Emission and Transmission from SPURC for a Range of Surface Temperatures and Particulate Sizes	45
Figure 6.3.8.2-1.	Previous SCIFLI Operations Coordinated from the Auxiliary SSP Red Flight Control Room	47
Figure 6.3.8.2-2.	IPOC in the MCC	48
Figure 6.3.8.3-1.	BH-300 Aircraft Movements for JIS 1b Simulation where Several Anomalies with the MPCV Capsule and the BH-340 Imaging Aircraft Occurred	49
Figure 6.3.8.3-2.	SCIFLI Observation of a Flight Test Associated with the SpaceX Falcon 9 First Stage Recovery	51
Figure 7.0-1.	EFT-1 Altitude as a Function of Time from EI	54
Figure 7.0-2.	EFT-1 Mach Number as a Function of Time from EI	55
Figure 7.0-3.	EFT-1 Dynamic Pressure as a Function of Time from EI	55
Figure 7.0-4.	EFT-1 Velocity as a Function of Time from EI	56
Figure 7.1-1.	High-Temperature NASA Blackbodies Used to Calibrate the Cast Glance Sensors Delivered to the Navy Base at Point Mugu, California	57
Figure 7.1-2.	Assessment Mission Operations Team on Console at the JSC IPOC for the EFT-1 Observation (from left to right; MC, AC, and Mission Manager).....	58
Figure 7.1-3.	Calibration to Determine Spectral Characteristics of BH-300's Infrared Imaging System	59
Figure 7.1-4.	Locations of Descent Imaging Aircraft (BH-340) and NASA Ikhana UAV Relative to a Latitude-Based Line of No Transgression	61
Figure 7.1-5.	December 4, 2014 Satellite Imagery off California Coast at Time of Expected MPCV Capsule Recovery (Had Launch Been Successful)	63
Figure 7.1-6.	Forecasted CFLOS for Observer Looking up from 25,000 ft.....	64
Figure 7.1-7.	Forecasted CFLOS for an Observer Looking down from 25,000 ft	65
Figure 7.1-8.	MPCV Crew Capsule Reentry Track and Flight Path of the BH-300 Observation Aircraft (Planned, Yellow; Actual, Green).....	66
Figure 7.1-9.	Synopsis Slide Released to the General Public 24 Hours after Successful Reentry Observations	68
Figure 7.3-1.	Summary of Data Sources and Process for Inferring Temperature from Calibrated Imagery.....	70
Figure 7.3.1-1.	Sequence of Raw NIR Intensity Images Showing Perspective Change of Heat Shield as Capsule Approached the Aircraft.....	71
Figure 7.3.1-2.	Plot of Several Image-Derived Parameters to Highlight Selection of Imagery for Detailed Analysis.....	72
Figure 7.3.1-3.	The Selected Five Frames Used to Post-Process Imagery for Frame #8028.....	73
Figure 7.3.2-1.	Selected Five Frames Used to Post-Process Imagery for Frame 8028 after 8x Interpolation Has Been Applied	74
Figure 7.3.3-1.	Range of Integration Times Used During Collection of NIR Imagery during EFT-1 Observation.....	76



	NASA Engineering and Safety Center Technical Assessment Report	Document #: NESC-RP- 12-00795	Version: 1.0
Title:	Remote Imaging of EFT-1 Entry Heating Risk Reduction		Page #: 6 of 98

Figure 7.3.4-1.	Directional Emissivity Values as Measured on Charred/Ablated Avcoat TPS Sample	77
Figure 7.3.5-2.	Global Temperature Images Relative to EFT-1 Flight Path. Images of EFT-1 Parachute Deployment (far right)	79
Figure 7.3.5-3.	Comparison of Global Temperature Image with Post-Flight Image of the EFT-1 Heat Shield	80
Figure 7.3.6-1.	Influence of Emissivity on Computed Surface Temperature.....	81
Figure 7.3.6-2.	Influence of Atmospheric Transmittance on Computed Surface Temperature.	82
Figure 7.3.7-1.	Location of Two DFI In-Depth TCs Selected for Comparison to Image-Derived Surface Temperature.....	83
Figure 7.3.7-2.	Comparison of Image Derived Surface Temperature Distribution to Surface Temperature Derived from In-Depth TC Measurement Using Inverse Methods.....	83
Figure 7.3.7-3.	Plot Showing Selection of Two Time Segments Shaded (in blue) for Comparison of Cooling Rates	85
Figure 7.3.7-4.	Comparison of Temperature Cooling Rates during Two Selected Intervals of Reentry When Best Imagery Was Acquired.....	86

List of Tables

Table 6.2-1.	Initial Set of Aircraft Imaging Platforms Considered for the EFT-1 Thermal Observation.....	21
Table 7.0-1.	BH-300 Navy NP-3D Image Acquisition Times during Reentry	56
Table 7.3.5-1.	Final Global Temperature Images for Five Selected Times during EFT-1 Hypersonic Reentry	78
Table 7.3.7-1.	Summary of Temperatures Differences between Plug06 and Plug08 and the Five Selected Imagery Time Segments	84


	NASA Engineering and Safety Center Technical Assessment Report	Document #: NESC-RP- 12-00795	Version: 1.0
Title: Remote Imaging of EFT-1 Entry Heating Risk Reduction			Page #: 7 of 98

Technical Assessment Report

1.0 Notification and Authorization

Mr. Gavin Mendeck, the Entry, Descent, and Landing (EDL) Phase Engineer for the Multi-Purpose Crew Vehicle (MPCV) Program (Vehicle Integration Office/Systems & Mission Integration) at Johnson Space Center (JSC), requested a risk-reduction assessment pertaining to the use of quantitative imagery to independently provide Exploration Flight Test-1 (EFT-1) heat shield surface temperatures during reentry. A NASA Engineering and Safety Center (NESC) initial evaluation was approved on June 7, 2012. Dr. David Schuster, NASA Technical Fellow for the Aerosciences, was selected to lead this assessment. The assessment plan was approved by the NESC Review Board on June 28, 2012. The assessment plan identified the EFT-1 imagery team within the NESC and defined the team's mission, membership, responsibilities, and conduct of operations.

The key stakeholders for this assessment were Gavin Mendeck, the MPCV Program EDL Phase Engineer; Pete Huseman, MPCV Program Aerosciences Senior Manager (Lockheed Martin); Joe Olejniczak, MPCV Aerosciences Manager at Ames Research Center; and Stan Bouslog and John Kowal within the JSC Thermal Protection System (TPS) discipline area.

	NASA Engineering and Safety Center Technical Assessment Report	Document #: NESC-RP- 12-00795	Version: 1.0
Title: Remote Imaging of EFT-1 Entry Heating Risk Reduction			Page #: 8 of 98

2.0 Signature Page

Submitted by:

Team Signature Page on File – 6/22/16


Dr. David M. Schuster Date

Significant Contributors:


Mr. Thomas J. Horvath Date

Mr. Richard J. Schwartz Date

Signatories declare the findings, observations, and NESC recommendations compiled in the report are factually based from data extracted from program/project documents, contractor

	NASA Engineering and Safety Center Technical Assessment Report	Document #: NESC-RP- 12-00795	Version: 1.0
Title:	Remote Imaging of EFT-1 Entry Heating Risk Reduction		Page #: 9 of 98

reports, and open literature, and/or generated from independently conducted tests, analyses, and inspections.


	NASA Engineering and Safety Center Technical Assessment Report	Document #: NESC-RP- 12-00795	Version: 1.0
Title: Remote Imaging of EFT-1 Entry Heating Risk Reduction			Page #: 10 of 98

3.0 Team List


Name	Discipline	Organization
Core Team		
David M. Schuster	NESC Lead	LaRC
Thomas J. Horvath	Deputy Lead	LaRC
Adam Amar	Numerical Modeling	JSC
Frank Brody	NOAA/SMG	JSC
Melinda Cagle	Project Manager (EDL)	LaRC
Tim Garner	Spaceflight Meteorology Group	JSC/NOAA
David Gibson	CFLOS	JHU-APL
Wayne Hensley	Landing Support Officer	JSC/USA
Stephanie Hamrick	MTSO Program Analyst	LaRC
Jose Kalil	Lead Landing Safety Officer	JSC
Michael Kelly	CFLOS	JHU-APL
Stephen Kennerly	Night Vision and Electronic Sensors	JHU-APL
Robert Kerns	Communications	LaRC
Mark McDonald	EFT-1 Lead Flight Dynamics Officer	JSC/USA
Gavin Mendeck	EFT-1 Interface	JSC
David Mercer	Sensor Calibration	LaRC/Lites
Shann Rufer	Asset Coordinator	LaRC
Richard Schwartz	Mission Modeling	LaRC/AMA
Jan Shumaker	P-3 Test Manager	NAVAIR
Daniel Smith	MPCV Program Imaging Working Group	JSC/Jacobs
Thomas Spisz	Image Analyst	JHU-APL
Steve Tack	P-3 Imaging Specialist	NAVAIR
Jeff Taylor	Sensor Modeling & Analysis	JHU-APL
Daniel Winterhalter	Technical Lead for Robotics	JPL
Harry Verstynen	Asset Communications	LaRC
Joe Zalameda	Sensor Calibration	LaRC
Administrative Support		
Melinda Meredith	Project Coordinator	LaRC/AMA
Linda Burgess	Planning and Control Analyst	LaRC/AMA
Dee Bullock	Technical Writer	LaRC/AMA

3.1 Acknowledgements

The NESC team would like to recognize the Aerospace Corporation and the WB-57 High Altitude Research Program at the NASA JSC for support during this assessment. The services of these two organizations were activated deep into in the demonstration of capability (EFT-1 observation) phase of the assessment as a risk-reduction effort. While the primary aircraft was able to support the observation, the professional attitude and dedication to preparing a second aircraft to perform the mission on such short notice was remarkable. The NESC team would also

	NASA Engineering and Safety Center Technical Assessment Report	Document #: NESC-RP- 12-00795	Version: 1.0
Title:	Remote Imaging of EFT-1 Entry Heating Risk Reduction		Page #: 11 of 98

like to recognize Surface Optics for providing laboratory measurements to quantify the surface optical properties of the MPCV TPS. The test results had a significant impact regarding the observation strategy to acquire the capsule at long range.


	NASA Engineering and Safety Center Technical Assessment Report	Document #: NESC-RP- 12-00795	Version: 1.0
Title:	Remote Imaging of EFT-1 Entry Heating Risk Reduction		Page #: 12 of 98

4.0 Executive Summary

A Measure of Performance (MOP) identified with an Exploration Flight Test-1 (EFT-1) Multi-Purpose Crew Vehicle (MPCV) Program Flight Test Objective (FTO) (OFT1.091) specified an observation during reentry through external ground-based or airborne assets with thermal detection capabilities. The objective of this FTO was to be met with onboard Developmental Flight Instrumentation (DFI), but the MOP for external observation was intended to provide complementary quantitative data and serve as a risk reduction in the event of anomalous DFI behavior (or failure). Mr. Gavin Mendeck, the Entry, Descent, and Landing (EDL) Phase Engineer for the MPCV Program (Vehicle Integration Office/Systems & Mission Integration) requested a risk-reduction assessment from the NASA Engineering and Safety Center (NESC) to determine whether quantitative imagery could be obtained from remote aerial assets to support the external observation MOP. If so, then a viable path forward was to be determined, risks identified, and an observation pursued. If not, then the MOP for external observation was to be eliminated.

As part of this assessment:

- A review of measurement platforms and instrument capability was highlighted and aerial-based capabilities were preferred.
- Risks associated with the desired aerial observation were identified and described and mitigated during the observation.
- Available tools and techniques to characterize and reduce risk were described and exercised.
- A quantitative remote infrared-based observation from a crewed Navy NP-3D aircraft (referred to as BH-300) to provide engineering quality data was determined to be viable, and an observation campaign was successfully planned and executed. The coordination of the planning and mission operations was described.
- A request to expand the responsibilities of the NESC mission operations team to include the coordination of two additional aerial assets sponsored by the MPCV Program and NASA Public Affairs was identified along with steps taken to mitigate additional risk. The aircraft included a second Navy NP-3D aircraft (referred to as BH-340) to observe late stage recovery events such as the parachute deployment sequence, and an unmanned aerial vehicle (UAV) used for real-time video streaming.
- Risks that matured during the observation were identified and a chronology-based description of how the NESC mission operations team made informed decisions was presented.
- An optional analysis task to infer heat shield surface temperature from the calibrated thermal imagery was pursued based upon the quality of the acquired infrared imagery.
- Global surface temperature was inferred from calibrated infrared measurements and compared to surface temperatures reconstructed from in-depth measurements from two DFI thermocouples (TC). TC-derived temperatures were approximately 100 °F above the image-derived surface temperatures.


	NASA Engineering and Safety Center Technical Assessment Report	Document #: NESC-RP- 12-00795	Version: 1.0
Title:	Remote Imaging of EFT-1 Entry Heating Risk Reduction		Page #: 13 of 98

- Uncertainties of the image-derived surface temperature are dominated by uncertainties in the Avcoat surface emissivity and transmissivity of the atmosphere. Estimated uncertainty of the imaged derived surface temperature is ± 15 °F.
- Uncertainties in the surface-derived temperatures from the TCs was not in scope of this assessment but the large difference between the two measurement techniques suggests a high-fidelity uncertainty analysis is needed of the material properties of charred and ablated Avcoat that are currently used in the TC reconstruction process.
- The appendices provide further documentation of laboratory test results used to optimize the infrared sensor configuration, mission planning, data assimilation, and procedures associated with sensor calibration and aircraft operations.

Because the observation of the capsule at peak heating was expected to occur over a remote broad area of ocean, surface-based imaging assets were dismissed. Airborne platforms with imaging capability were identified and several eliminated due to their inability to reach the desired observation location with sufficient loiter time. The optical performance of the remaining aerial platforms to provide adequate spatial resolution was assessed. Tools developed to simulate optical performance were exercised. Risks associated with schedule availability of the aircraft to support the observation were balanced against cost, sensor requirements for long-range acquisition/tracking, and with crew operational experience. A recommendation was accepted by the MPCV Program Flight Test Management Office (FTMO) and the NESC Review Board to pursue a thermal observation using an existing imaging asset within the Department of Defense (DoD) with demonstrated capability.

To obtain the thermal imagery, the NESC team leveraged from mission planning tools developed under NESC assessment 07-048-E [ref. 1] and successfully utilized by the Space Shuttle Program (SSP)-sponsored Hypersonic Thermodynamic Infrared Measurement (HYTHIRM) team to provide global thermal images of seven SSP flights during hypersonic descent from 2009 to 2011 [refs. 2-19], the SpaceX Dragon capsule during its inaugural reentry in 2010, and the recovery of a SpaceX Falcon 9 first stage during a flight test in 2014 [ref. 20]. The concept of operations for the EFT-1 observation base lined the use of a Navy aircraft (BH-300). An Agency aircraft (WB-57) was later identified as a viable asset for risk mitigation if conflicts with the Navy asset developed. This risk was recognized several days before the EFT-1 launch; the WB-57 was activated as a backup but not flown because the conflict with the DoD asset was resolved. The team planned for but was not required to support off-nominal capsule reentry trajectories, nor were aircraft search and recovery services required. Opportunities to obtain spectral measurements of the afterbody wake and/or thermal measurements were considered but not pursued due to limitations of the existing Navy sensors. The assessment was considered complete with acquisition of the flight thermal imagery. However, subsequent approval of the optional data analysis extended the assessment timeline.


Based upon the success of the assessment, the MPCV Program requested the Scientifically Calibrated In-Flight Imagery (SCIFLI) team submit a budget request to perform an observation of the crew capsule's flight test Exploration Mission-1 (EM-1) that is targeted for September 2018 and planning has commenced. The DoD has entered into several collaborative efforts with

	NASA Engineering and Safety Center Technical Assessment Report	Document #: NESC-RP- 12-00795	Version: 1.0
Title:	Remote Imaging of EFT-1 Entry Heating Risk Reduction		Page #: 14 of 98

the SCIFLI team to develop a nationally managed unmanned aerial system (UAS) program to provide flexible, lower-cost, higher-quality measurement capability for civilian- and defense-related developmental/operational flight testing.

After the successful observation on December 5, 2014, the NESC team held internal reviews to identify and document lessons learned. The assessment findings, observations, and NESC recommendations presented in Section 8.0 can be summarized as:

- An external observation can provide unique non-evasive thermal protection system (TPS) performance data to complement in-situ instrumentation, which the latter often presents power, weight, and size challenges with limited spatial coverage.
- A crewed aircraft was used to successfully obtain engineering quality global surface temperature on a human-rated capsule of considerably smaller dimension than previously demonstrated.
- While capable, cost considerations of crewed platforms should be rigorously evaluated, with the flexibility in asset positioning to avoid weather constraints, endurance (time on station), and sensor limitations.
- The need for more affordable airborne imaging systems with enhanced capability is tied to future Agency and National flight test and evaluation (T&E) needs and the level of risk a development flight test program is willing to accept.
- NASA and DoD should explore and identify common interests and investments to maintain and advance flight (and in particular, hypersonic) T&E infrastructure.

	NASA Engineering and Safety Center Technical Assessment Report	Document #: NESC-RP- 12-00795	Version: 1.0
Title: Remote Imaging of EFT-1 Entry Heating Risk Reduction			Page #: 15 of 98


5.0 Assessment Plan

The assessment plan was initiated from concerns that the MOP specifying a quantitative, spatially resolved thermal observation of the EFT-1 capsule during reentry through external ground-based or airborne assets could not be met. The objective of this assessment was to provide recommendations to the MPCV Program on the ability to provide global heat shield temperature maps derived from engineering-quality thermal imagery obtained from an electro-optical asset during EFT-1 reentry. The assessment, as proposed, consisted of three phases: (1) an assessment of measurement capability, (2) a demonstration of capability through an infrared observation, and (3) an optional data analysis phase if imagery was successfully obtained. During the first phase, the NESC team reviewed capabilities of existing measurement platforms to support observations over broad areas of ocean where peak heating of the capsule was expected to occur. Then the team ascertained the performance of the optical measurement systems associated with these platforms. The performance of the optical systems was judged based upon past performance, likelihood of long-range acquisition from extreme distances, and determination of the expected spatial resolution of the resulting thermal imagery near the point of closest approach between the capsule and the imaging system.

Next, image degradation from atmospheric effects, shock-layer radiation, and the presence of the heat shield TPS ablation products was estimated using state-of-the-art tools. The NESC team's draft findings, observations, and recommendations from this initial assessment were presented to the stakeholders and the NESC Review Board (NRB) for approval. The recommendation to proceed to the second phase was approved. Based upon a successful infrared observation on December 5, 2014, the quality of the data was reviewed by the team and presented to the Aerosciences Technical Discipline Team (TDT) for approval to proceed to the final analysis phase, whereby surface temperatures derived by the remote-based observations were compared to heat shield surface temperatures inferred from in-depth TCs. The final review was the NESC peer-review cycle. A preliminary presentation was made to Mr. Tim Wilson, Director NESC, summarizing the observation and results. Recommendations were made to enable more affordable and enhanced measurement capability to support Agency and National priorities in, but not limited to, hypersonic flight T&E.

6.0 Problem Description, Proposed Solutions, and Risk Assessment

FTOs are technical statements defining objectives to be accomplished during a test flight. The MOPs often associated with FTOs describe specific types of measures to be collected and a description of the predicted behavior, value, or environment that the measures will be used to confirm. The MPCV Program FTO OFT1.091 identified the requirement to determine the capsule heat shield and backshell aerothermodynamic environment during reentry. This type of FTO generally requires quantitative data to be collected to validate a mathematical prediction of subsystem performance and/or environment. One of the three MOPs identified with OFT1.091 specified an observation during reentry through external ground-based or airborne assets with thermal detection capabilities.


	NASA Engineering and Safety Center Technical Assessment Report	Document #: NESC-RP- 12-00795	Version: 1.0
Title:	Remote Imaging of EFT-1 Entry Heating Risk Reduction		Page #: 16 of 98

The FTO objective was to be met with onboard DFI, and the MOP for external observation was intended to complement and serve as a risk reduction in the event of anomalous DFI behavior (or failure). For example, anomalous TC behavior in the form of large voltage fluctuations yielding non-physical temperatures has been documented in over 29 Shuttle hypersonic reentries. Root cause was never identified but was likely due to interactions of the TCs with plasma in the shock layer. Furthermore, failure of DFI recording hardware and loss of data was experienced during an early uncrewed Apollo test flight (AS-201) and the SSP during STS-1, STS-4, and STS-35. As such, Mr. Gavin Mendeck, the EDL Phase Engineer for the MPCV Program (Vehicle Integration Office/Systems & Mission Integration), requested a risk-reduction assessment from the NESC to determine whether quantitative thermal imagery could be obtained from remote aerial assets to support the external observation MOP. For the purposes of the assessment, thermal was interpreted as infrared signatures at sufficient accuracy to compare against in-situ TCs and at a spatial resolution to discern potential localized heating in the vicinity of heat shield surface features like the compression pads. If so, then a viable path forward was to be determined, risks identified, and an observation pursued. If not, then the MOP for external observation was to be eliminated. Time-resolved but spatially unresolved measurements of absolute spectral radiance from the MPCV capsule and its trailing wake during reentry were not considered.

6.1 Challenges with Heat Shield Thermocouples

Figure 6.1-1 shows the distribution of thermal measurement DFI on the heatshield: (19) four-junction TC plugs and (14) two-junction TC plugs are located on the heatshield. Also shown are the locations for the pressure instrumentation associated with Flush Air Data System (FADS) and radiometers. Because of the sparse TC spatial distribution on the heat shield as shown Figure 6.1-1, the nature of an image-derived global temperature map would make it possible to fill in these gaps for a brief time period during reentry. Also evident in the figure are the six compression pad locations near the periphery where the heat shield is attached to the service module. An example of a four-junction TC plug is shown in Figure 6.1-2. As viewed from the side of the plug, the TC junctions are not placed at the surface, but rather in depth in anticipation of heat shield recession and to protect them from the harsh conditions during reentry.

The desire to complement the TC DFI heat shield instrumentation with image-derived temperature inferred from remote infrared observation is coupled to the complex processes of collecting quality measurements and then reconstructing surface temperature from the in-depth TC measurements. It was anticipated that interpretation of the EFT-1 flight TC data would be challenging if past non-physical surface temperature, as exhibited by TC measurements during SSP orbiter reentry, was experienced during EFT-1. The non-physical temperatures resulting from large voltage fluctuations in the TCs can make it impossible to provide accurate data from which to validate engineering models and difficult, if not impossible, to reliably infer boundary layer transition from a temperature time history trace. The MPCV Program viewed the EFT-1 thermal observation as a risk reduction in the event of such DFI TC anomaly, recording hardware failure, or to aid in reconstruction in the event of a vehicle mishap during reentry.

	NASA Engineering and Safety Center Technical Assessment Report	Document #: NESC-RP- 12-00795	Version: 1.0
Title: Remote Imaging of EFT-1 Entry Heating Risk Reduction			Page #: 17 of 98

As discussed in a report issued 90 days after the EFT-1 recovery [ref. 21], the process to reconstruct surface temperature from in-depth TC temperature measurement requires an inverse heating method. The method necessitates accurate knowledge of the in-depth thermal properties of the material in which the TC is embedded so that an inverse heat transfer method can be applied to extrapolate the temperature measured at the junction to the surface. Post-processing of the flight TC measurements using an inverse heat transfer numerical method is complex and can be time-consuming to implement. Uncertainties arise from assumptions in time-dependent material properties and depth of the ablative TPS char layer in the vicinity of the in-depth TC. Surface temperatures derived by the remote-based observations associated with this assessment were presented as a direct and independent method to infer surface temperature and hence verify the performance of the material response methodology.

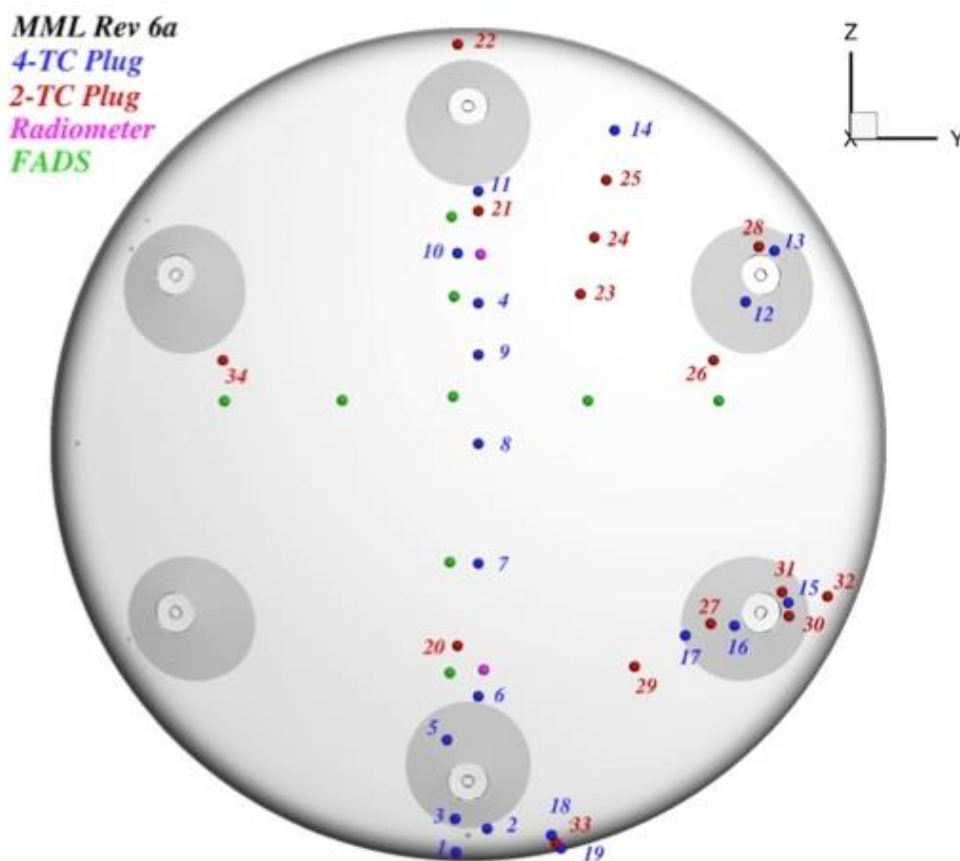



Figure 6.1-1. Schematic of EFT-1 Heat Shield DFI Instrumentation Layout (Subsurface TC Locations Identified in Blue and Red)

While nothing will replace the value of in-situ instrumentation, the challenges of minimizing DFI impacts to vehicle weight and internal complexity, and inherent instrument bandwidth limitations often restrict the ability to make high spatial density in-situ measurements. Thus, remote imaging at high spatial resolution can provide a synergistic opportunity to noninvasively obtain

	NASA Engineering and Safety Center Technical Assessment Report	Document #: NESC-RP- 12-00795	Version: 1.0
Title: Remote Imaging of EFT-1 Entry Heating Risk Reduction			Page #: 18 of 98

unique and critical flight data without interfering with nominal vehicle operations, weight, performance, and scheduling.

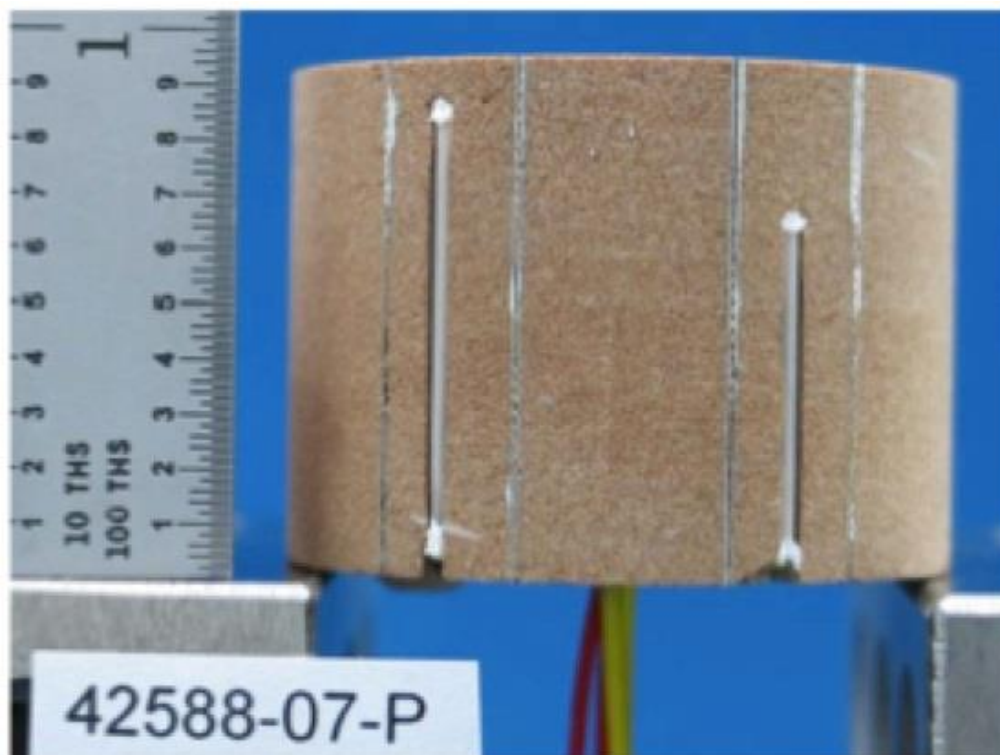



Figure 6.1-2. EFT-1 Heat Shield TC Plug (Side View Showing TC Junctions below the Surface with Outer Surface Shown on the Image Top)

6.2 Platform and Instrument Capability

At the heart of this assessment is the question of whether existing remote thermal sensing capabilities can address the MPCV Program's requirement of an observation as a risk reduction while providing useful, engineering-quality data. To answer this question, an analysis was undertaken to determine: where the observation would most likely occur, what type of imaging platform would be required, and whether the optical system associated with that platform would provide useful spatial resolution. Approximately 18 months prior to the EFT-1 launch, reentry trajectory information was provided to the NESC team to determine where the desired thermal observation would occur. The trajectories were imported into a synthetic virtual modeling environment from which to visualize the reentry path (herein referred to as the ground track) as shown in Figure 6.2-1. The inset graphic shows the 2 ½-orbit flight path from launch to recovery point. The synthetic modeling tool used to generate this graphic is discussed in more detail in Section 6.3, Risk Characterization and Mitigation.

	NASA Engineering and Safety Center Technical Assessment Report	Document #: NESC-RP- 12-00795	Version: 1.0
Title:	Remote Imaging of EFT-1 Entry Heating Risk Reduction		Page #: 19 of 98

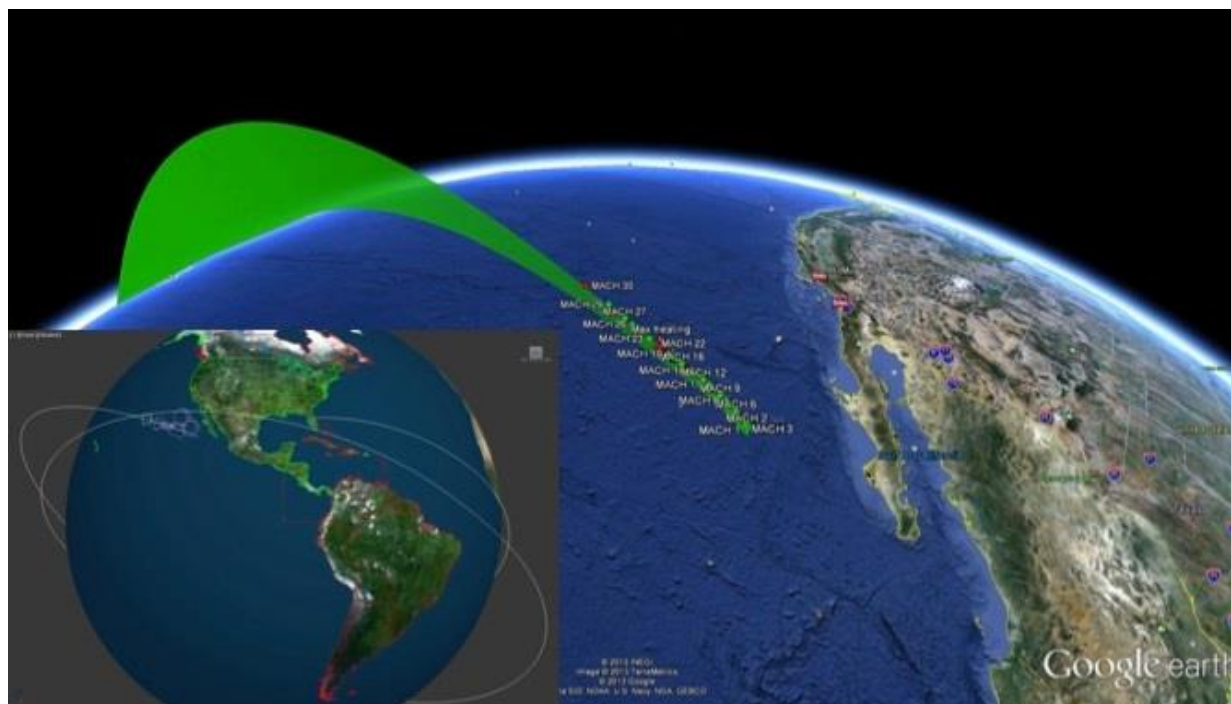



Figure 6.2-1. EFT-1 Proposed Reentry Flight Path (circa 2013) with Splashdown off the Coast of California

Ground-based systems have demonstrated superior spatial resolution performance and some level of mobility. The best spatial resolution obtained on a reentering spacecraft at hypersonic speeds was acquired with a mobile ground-based infrared imaging system during a reentry observation of the SSP orbiter *Endeavor* in 2011 [ref. 16], as shown in Figure 6.2-2. At a range of 32 nautical miles (nmi), the estimated spatial resolution on this thermal was approximately 4 inches per pixel. At this resolution, the individual carbon-carbon wing leading edge panels can be discerned.

	NASA Engineering and Safety Center Technical Assessment Report	Document #: NESC-RP- 12-00795	Version: 1.0
Title:	Remote Imaging of EFT-1 Entry Heating Risk Reduction		Page #: 20 of 98

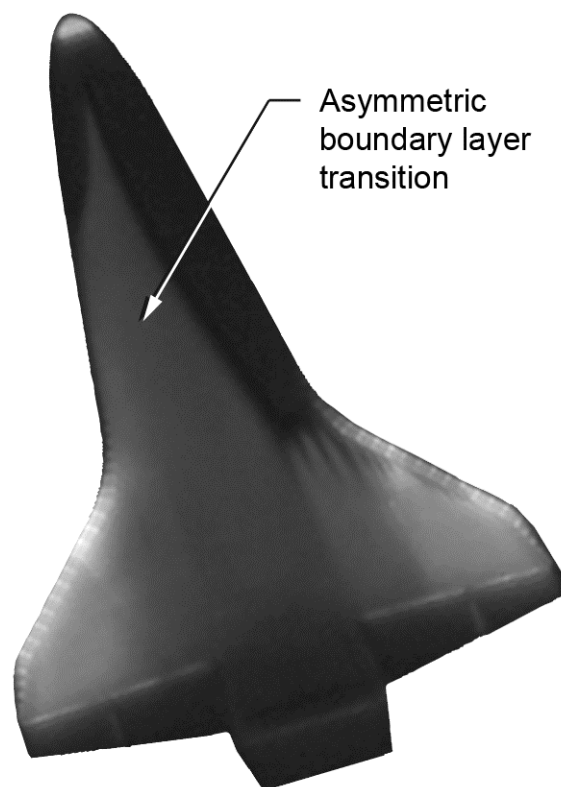


Figure 6.2-2. Thermal Image of Endeavour During STS-134 Reentry Near the Point of Closest Approach, Mach 5.8, Slant Range ~32 nmi. (Estimated resolution ~4 inches per pixel.)

However, experience has shown that mobile ground-based imagers are susceptible to longer atmospheric path lengths, turbulence near the ground, and obscuring clouds. As indicated in Figure 6.2-1, peak heating during EFT-1 reentry was anticipated to occur over the Pacific Ocean with crew capsule recovery approximately 600 nmi off the California coast, which is absent of any remote land islands capable of providing imaging from the ground. Therefore, any mobile or fixed ground-based imaging assets (e.g., the Air Force Maui Optical and Supercomputing observatory) were excluded from consideration. Sea-based imaging systems inherently possess all the challenges of a ground system along with other inherent concerns. In addition to making an observation through an image-degrading marine layer with high aerosol content, pointing stability requirements at sea associated with narrow field-of-view (FOV) optics represents a significant hardware integration challenge in terms of gyro-stabilization and isolation from the ship motion and engine vibrations. Therefore, sea-based imaging platforms were not evaluated.

Naturally, imaging strategies over remote bodies of water tend to favor the flexibility and range of airborne systems. Five aerial platforms were initially considered by the NESC team and are listed in Table 6.2-1.


	NASA Engineering and Safety Center Technical Assessment Report	Document #: NESC-RP- 12-00795	Version: 1.0
Title:	Remote Imaging of EFT-1 Entry Heating Risk Reduction		Page #: 21 of 98

Table 6.2-1. Initial Set of Aircraft Imaging Platforms Considered for the EFT-1 Thermal Observation

Aircraft	Transit Range, nmi	Endurance, hr	Max Altitude, ft
NASA DC-8	5,400	12	41,000
NASA WB-57	2,500	6.5	60,000
NASA SOFIA 747SP	6,600	9	45,000
NASA HU-25	2,000	7	40,000
L-3 HALO II GIII	3,500	7	51,000
Navy NP-3D (BH-300)	4,000	12	30,000

With the exception on the Navy NP-3D aircraft, all platforms initially considered operate at altitudes of greater than 40,000 ft. At these altitudes, risks from obscuring cloud coverage is essentially avoided and the undesirable optical absorption effects in the infrared spectrum from water vapor and scattering from aerosols is greatly diminished. Relatively speaking, aircraft at these altitudes are positioned closer to the intended target further mitigating detrimental atmospheric effects. Three aircraft (highlighted in red in Table 6.2-1) were eliminated from contention for several reasons. The DC-8 and Stratospheric Observatory for Infrared Astronomy (SOFIA) 747 aircraft serve as workhorse measurement platforms for NASA's Science Mission Directorate and they are used extensively for Earth/atmospheric science and astronomy, respectively. Schedule conflict risk was extremely high with these platforms. In addition, sensors and instrument operator expertise must be provided when utilizing the DC-8. The SOFIA 747 is configured with an infrared sensor, but since it is essentially staring for astronomical purposes, it is not possible to track a moving target at the high angular velocities required for an EFT-1 observation. The High-Altitude Observatory (HALO) II Gulfstream III platform supports observations associated with the Missile Defense Agency (MDA), but its sensor package could not be modified/optimized for the expected photon-rich infrared observation of the MPCV capsule heat shield.

Of the three remaining aircraft, the NASA HU-25, a converted Falcon business jet, was considered for a longer period of time during the assessment. It was eliminated from contention when it was determined that an imaging/tracking system being designed and built for use on this aircraft would not be operational on the projected EFT-1 launch date in December 2014.

The remaining two viable aircraft (i.e., BH-300 and the NASA WB-57) are multi-engine aircraft that routinely support over-water operations. Each hosts its own sensor package and provides instrument operational expertise. Following the optical analysis described in Section 6.3, these aircraft were shown to produce acceptable spatial resolution with their respective infrared imaging systems. Despite its larger susceptibility to weather constraints, the Navy NP-3D was selected as the primary imaging aircraft largely because of its demonstrated experience base tracking high-speed moving targets under the NESC HYTHIRM project, and its longer endurance/loiter time. The Navy NP-3D aircraft shown in Figure 6.2-3 is stationed at the Naval Air Warfare Center, Point Mugu Naval Air Station, California.


	<h1 style="text-align: center;">NASA Engineering and Safety Center Technical Assessment Report</h1>	Document #: NESC-RP- 12-00795	Version: 1.0
Title:	Remote Imaging of EFT-1 Entry Heating Risk Reduction		Page #: 22 of 98



Figure 6.2-3. U.S. Navy NP-3D Cast Glance Aircraft (Bloodhound 300 (BH-300))

The optical system on the BH-300, often referred to as Cast Glance, comprise a set of electro-optical platforms mounted within the aircraft pressurized section (Figure 6.2-4). A gyro-stabilized gimballed mirror tracks the target and directs the light toward a fixed telescope rather than moving the camera and lens. Through a series of beam splitters and pick-off mirrors, light is diverted to several video, digital and high-speed visual, and infrared imaging sensors. The gimballed mirror can be steered manually or assisted through the aid of a computer-aided pointing system. Aircraft flight data and target position information can be embedded into the video fields. A typical crew complement includes seven aircrew and four Cast Glance sensor operators. The aircraft operates nominally at an altitude of 25,000 ft but can climb higher as long as the internal cabin pressure can be maintained to a pressure equivalent to 10,000 ft (or below). The NP-3D is capable to reaching 40,000 ft, but it would require the supplemental use of oxygen to avoid hypoxia.

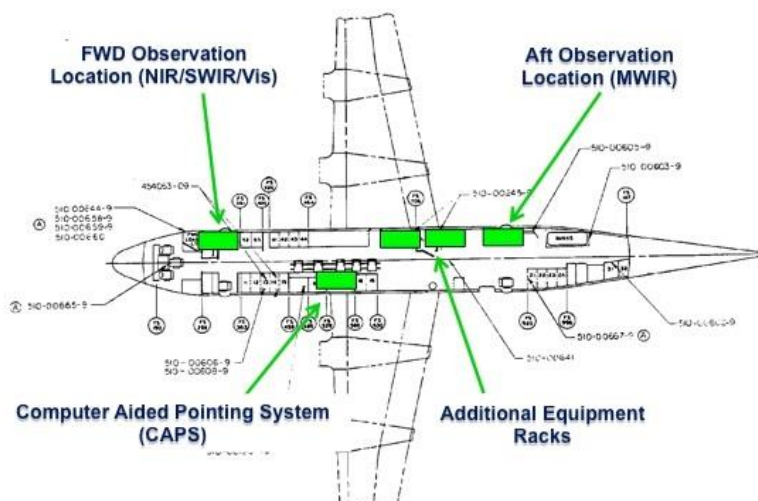



Figure 6.2-4. Internal Layout of the Navy NP-3D Orion (BH-300)

Spectral wavelengths of the Cast Glance systems include visible (0.4 μm to 0.7 μm), near-infrared (NIR) (0.7 μm to 1.1 μm), shortwave infrared (SWIR) (0.9 μm to 1.7 μm), midwave infrared (MWIR) (3.4 μm to 4.9 μm), and longwave infrared (LWIR) (7.5 μm to 13.0 μm).

	NASA Engineering and Safety Center Technical Assessment Report	Document #: NESC-RP- 12-00795	Version: 1.0
Title:	Remote Imaging of EFT-1 Entry Heating Risk Reduction		Page #: 23 of 98

The NASA WB-57, shown in Figure 6.2-5, is based at Ellington Field, Houston Texas and was maintained as a potential backup in the event mechanical or schedule issues precluded the use of the Navy NP-3D Orion aircraft. The platform from which this aircraft is derived was designed for high-altitude reconnaissance in the 1950s, and the NASA variant can reach an altitude in excess of 65,000 ft. The crew consists of the pilot and a sensor operator sitting inline in a front-and backseat configuration. As with Cast Glance, tracking is performed manually or with a computer-assisted auto tracking system. The WB-57 is capable of carrying a variety of electro-optical payloads in different locations on the airframe, including wing pods, a modified “bomb bay,” and a nose pod housing a gyro-stabilized ball turret referred to as the Day/Night Airborne Motion for Terrestrial Environments (DyNAMITE) ball turret imaging system (see Figure 6.2-6). Spectral wavelengths of the DyNAMITE system considered for EFT-1 imaging include high-definition visible (0.4 μm to 0.7 μm), and MWIR (3.4 μm to 4.9 μm) imagers.



Figure 6.2-5. NASA WB-57 with Nose-Mounted DyNAMITE Imaging Sensors

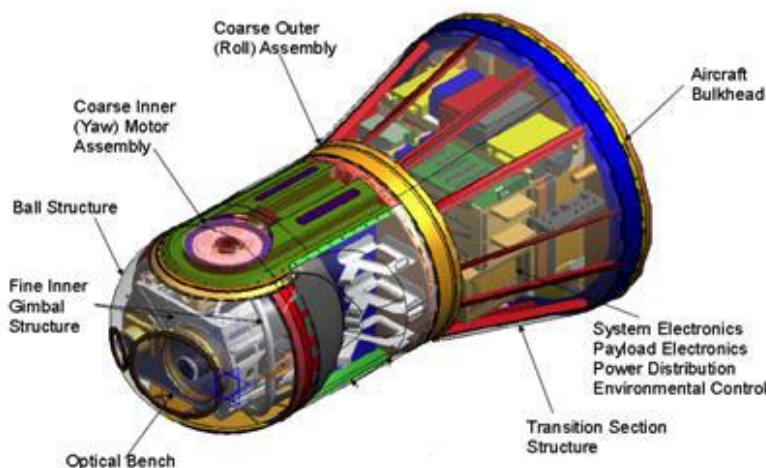



Figure 6.2-6. NASA WB-57 with Nose-Mounted DyNAMITE Imaging Sensors

	NASA Engineering and Safety Center Technical Assessment Report	Document #: NESC-RP- 12-00795	Version: 1.0
Title:	Remote Imaging of EFT-1 Entry Heating Risk Reduction		Page #: 24 of 98

6.3 Risk Characterization and Mitigation

The SSP observation campaigns from 2009 to 2011 resulted in remarkable thermal imagery yielding global surface temperature maps from seven successful infrared observations. Relative to the SSP orbiter, the EFT-1 capsule is significantly smaller in size and, as a result, surface temperatures were expected to be up to a factor of 2 higher during reentry. For comparative purposes, the relative size and expected temperature difference between the SSP orbiter and an early MPCV capsule configuration is shown in Figure 6.3-1. Given these fundamental differences, it was not clear at the beginning of the assessment if the target (MPCV capsule) could be acquired at extreme distances, if sufficient spatial resolution could be achieved at the point of closest approach, and/or if the higher surface temperatures and the ablative nature of the heat shield TPS would preclude useful surface temperatures derived from the infrared imagery.

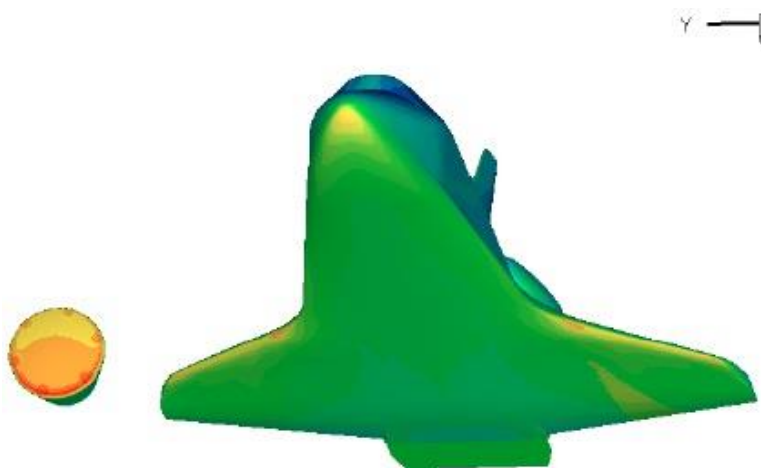



Figure 6.3-1. Relative Size and Temperature Differences between SSP Orbiter and the MPCV Capsule

To answer these and other questions, the NESC team utilized a number of simulation tools developed and tailored for use by the SCIFLI team prior to the observation. These simulation tools allowed the team to set expectations with the technical stakeholders and ultimately provide the sensor operators and flight planners with synthetic imagery from which to formulate deployment recommendations, determine pre-flight sensor configuration options, and locate optimal aircraft observation locations. The use of the modeling tools served as an essential element of risk mitigation. This section lists several risk topics identified by the team. A question is first stated pertaining to the risk topic. A risk statement is then presented (with risk context if appropriate). A description of the tools and how they were used to characterize and/or mitigate the risk is then provided. The risk topics are not necessarily listed in order of priority but more in terms of when the specific risk might be encountered during an observation campaign (e.g., in a chronological fashion).

	NASA Engineering and Safety Center Technical Assessment Report	Document #: NESC-RP- 12-00795	Version: 1.0
Title:	Remote Imaging of EFT-1 Entry Heating Risk Reduction		Page #: 25 of 98

6.3.1 Location of Peak Heating

Where along the EFT-1 reentry flight path does peak heating on the heat shield occur, and can an aircraft transit to and from that general location with sufficient loiter time?

Risk: Given the number of variables in determining when and where peak heating will occur, there is a possibility that the location will not be identified until the day of reentry.

Risk Context: Variables include, but are not limited to, final EFT-1 entry trajectory, vehicle weight, aerodynamic performance, when the onset of boundary layer transition will occur, and atmospheric uncertainties.


Assessment and Mitigations: In contrast to the SSP, where a 90-min (or 48-hour) delay in returning from low Earth orbit would significantly shift the ground track, the EFT-1 ascent and subsequent reentry ground track was not susceptible to these shifts. That is, for any given launch time, the location of the flight path relative to the Earth remains unchanged. Therefore, the process of determining the general location of the peak heating event relative to any fixed point on Earth was less complex. The position along the flight path where the EFT-1 capsule experiences maximum heat shield temperature (i.e., peak heating) was specified from a fixed point in time, either from capsule separation from the Delta IV upper stage or from Entry Interface (EI), which was designated as an altitude of 400,000 ft. Dispersions in the peak heating location resulting from uncertainties in the performance of the Delta IV Heavy launch vehicle upper stage, the capsule aerodynamics, and the upper atmosphere were later characterized by a series of Monte Carlo simulations. The uncertainty ellipse of the peak heating location provided to the NESC team was found to be relatively small (~50 nmi) compared to the required transit distances.

The Virtual Diagnostic Interface (ViDI) [refs. 22-25] tool was used to provide insights regarding the location of peak heating as identified by the EFT-1 Aerosciences team. In this software package, 6-degree of freedom trajectory information and the timing of critical events are imported and tied in with commercial off-the-shelf graphical software to visualize aspects of the entire trajectory on a virtual three-dimensional (3-D) Earth. Figure 6.2-1 represents an example of the output and shows the EFT-1 flight path relative to the west coast of California. Mach number or other desired information can be readily incorporated in the graphics. The initial peak heating location was approximately 600 nmi from the west coast of California, thus within reach of all the aircraft initially considered in Table 6.2-1. With the ability to stay aloft for approximately 11 hours, the Navy NP-3D would only require 2–3 hours of one-way transit time to reach the general area for the desired observation leaving 4–5 hours of loiter time.

6.3.2 Observation Location and Estimated Spatial Resolution

Where is the desired observation location from which peak heating is to be observed during EFT-1 reentry, and will spatially resolved thermal imagery be possible?


Risk: Given the number of variables in determining the final location of the aircraft, there is a possibility that the optimal test support point (TSP) will not be identified until the day of reentry.

	NASA Engineering and Safety Center Technical Assessment Report	Document #: NESC-RP- 12-00795	Version: 1.0
Title:	Remote Imaging of EFT-1 Entry Heating Risk Reduction		Page #: 26 of 98

Risk Context: Variables include, but are not limited to, local weather, EFT-1 launch timelines, aircraft performance parameters, Sun position, EFT-1 entry trajectory, and hazard zone boundaries. The geometry between the observing aircraft and the target vehicle determines elevation angle, system slewing rates, spatial resolution, aircraft maneuvers to maintain the capsule in the field of regard (FoR), and the total viewing time.

Assessment and Mitigations: Additional information in the form of surface computer-aided design (CAD) definition is imported into the ViDI tool to ascertain and then graphically display the spatial resolution performance of the imaging system. Lockheed Martin provided the EFT-1 surface CAD geometry for this phase of the assessment. The ViDI program pulls optical system specifications from an asset database (e.g., a particular telescope mount on an aircraft or a land-based system) and determines the view/orientation of the target based on the asset position and the location of the target during reentry. Information in a preliminary EFT-1 trajectory file, provided in 1-Hz increments, was used with the surface CAD to create dynamic synthetic imagery in the interactive 3-D virtual environment. A scaled representation of the flight test vehicle was located and orientated at each time step specified in the trajectory file. Entering latitude, longitude, and altitude defined the location for a virtual camera on the Navy NP-3D aircraft. Both the virtual camera FOV and the pixel resolution were matched to the performance of optical system carried on the aircraft, thus rendering a pixel-to-pixel accurate simulation of the expected imagery. A simulation of this nature only captures the expected spatial characteristics (e.g., viewing perspective, pixels on target) but is not radiometrically accurate.

An example of the ViDI output, Figure 6.3.2-1, depicts the spatial resolution performance of the Cast Glance NIR camera as configured for an observation near the expected point of peak heating. Based upon the sensor and telescope specifications and the capsule at a nominal slant range (i.e., distance from capsule to aircraft) of 37 nmi, each pixel associated with the NIR sensor represents approximately 10 inches. Some image degradation from the atmosphere and the optical system, and blurring due to jitter and motion of the aircraft, was expected to decrease the resolution of the unprocessed imagery to 12–15 inches per pixel. At this resolution, thermal features (e.g., the boundary layer transition if present during the observation period) could be readily identified. Localized temperature gradients expected within the compression pads (Figure 6.1-2) would not be spatially resolved, but the averaged elevated temperature in the general vicinity could be detected over several pixels. As such, the estimated spatial resolution and the heat shield viewing perspective obtained with the Cast Glance imaging system positioned for an observation near the peak heating event was acceptable to the FTMO and the MPCV engineering community.

	NASA Engineering and Safety Center Technical Assessment Report	Document #: NESC-RP- 12-00795	Version: 1.0
Title:	Remote Imaging of EFT-1 Entry Heating Risk Reduction		Page #: 27 of 98

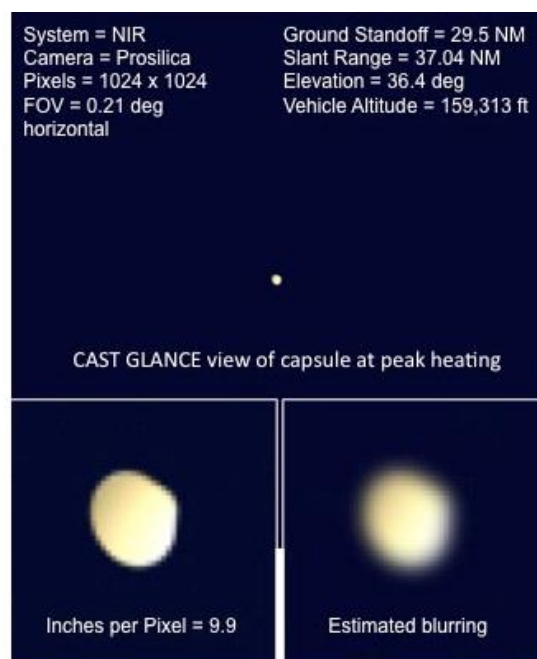



Figure 6.3.2-1. Synthetic Image of MPCV Capsule near the Point of Peak Heating as Viewed from the Navy NP-3D Aircraft

The synthetic imagery-based representation of spatial resolution as shown in Figure 6.3.2-1 is one point in time. The ViDI tool can output the estimated spatial resolution on the target as a function of time as shown in Figure 6.3.2-2 (aircraft position is located outside of the hazard zone and optimized for frontal view of capsule heat shield at peak heating). It is important to recognize the estimated 10-inch-per-pixel resolution will be experienced over a relatively brief time period (i.e., 10–15 sec) relative to the possible horizon-to-horizon observation time (i.e., 4–6 min).

For safety considerations and tracking constraints, the aircraft cannot be located directly under the EFT-1 flight path. Typically, the aircraft is positioned offset from the ground track some predetermined distance. The NAVY NP-3D standoff distance from the EFT-1 ground track was based upon elevation constraints looking through the aircraft window and keep-out zones imposed by hazard analysis of a potential capsule break up. Lockheed Martin and NASA analysts supporting the MPCV FTMO provided a Flight Dynamics Range Safety Data Package to the NESC team that detailed and enveloped all worst-case scenario debris during a failed crew capsule reentry. This keep-out zone dictated the standoff distance (and thus slant range) used in the spatial resolution analysis presented in Figure 6.3.2-1. To account for a hypersonic capsule breakup and dispersions in the atmospheric entry point, the aircraft standoff distance from the nominal EFT-1 ground track was required to be at least 27 nmi to ensure crew safety. In the unlikely event of an anomaly during reentry, communication to alert the aircraft via high-frequency (HF) radio and/or Iridium phone was planned at regular intervals. The relationship between the EFT-1 ground track, the keep-out zone boundary, and the Navy NP-3D flight is

	<h1 style="text-align: center;">NASA Engineering and Safety Center Technical Assessment Report</h1>	Document #: NESC-RP-12-00795	Version: 1.0
Title: <h2 style="text-align: center;">Remote Imaging of EFT-1 Entry Heating Risk Reduction</h2>			Page #: 28 of 98

shown in Figure 6.3.2-3. Blue points indicate timed locations of the Navy NP-3D as the capsule approached the point of peak heating.

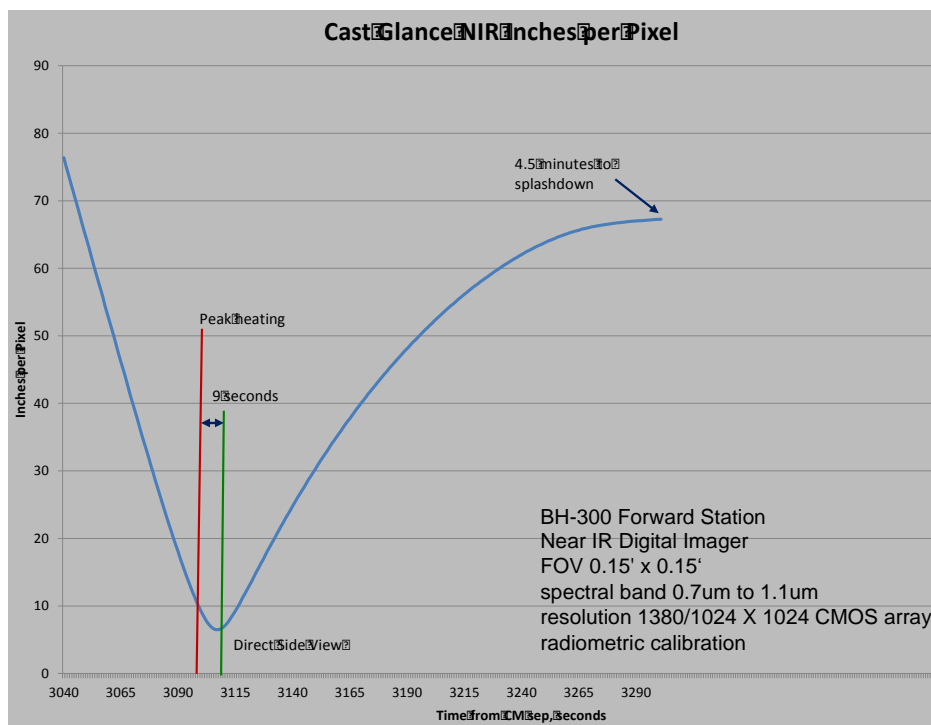


Figure 6.3.2-2. Estimated Spatial Resolution of the Cast Glance NIR as a Function of Time

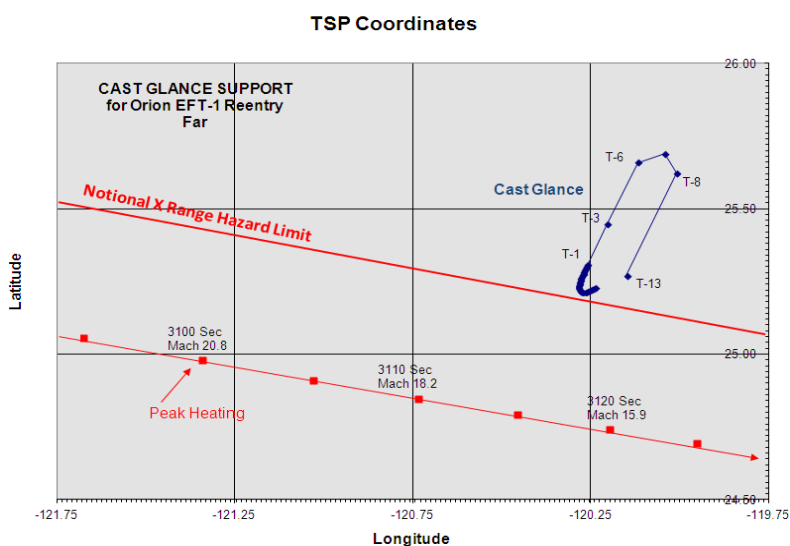



Figure 6.3.2-3. EFT-1 Ground Track and Hazard Keep-out Zone

The ViDI tool permits the user to determine the Sun's position as a function of time. Such advance knowledge is essential to avoid difficulties in long-range acquisition, or permanent

	NASA Engineering and Safety Center Technical Assessment Report	Document #: NESC-RP- 12-00795	Version: 1.0
Title:	Remote Imaging of EFT-1 Entry Heating Risk Reduction		Page #: 29 of 98

damage to the infrared sensors by inadvertent pointing into the Sun. The requirement to recover the capsule in daylight conditions dictated an early morning launch from Cape Canaveral Air Force Station, FL. The subsequent reentry, approximately 4.5 hours later in the Pacific, placed the Sun in a favorable position for imaging (i.e., the angular position between the Sun and the capsule as viewed from the aircraft was 20° or greater at all times). The Cast Glance personnel performed an independent analysis of optical tracking line-of-sight plotted against the Sun's azimuth and elevation throughout the planned observation interface. Should a conflict arise, positional shifts are considered to mitigate Sun influence. While repositioning is not always possible, it is important for the Cast Glance sensor operators to be cognizant of the Sun angle to determine proper sensor settings and to anticipate any visual difficulties in maintaining track. For MPCV's crew capsule proposed entry time, the Sun was expected to be in an advantageous location for imaging and acquisition. The anticipated rates for the gimballed mirror to maintain the capsule in the FoR were evaluated by the Navy personnel and were found to be acceptable (see Appendices F and G).

6.3.3 Asset Reliability and Schedule Conflict


Could mechanical failure or schedule conflict prevent the primary aircraft from supporting the observation?

Risk: Given that the Navy NP-3D supports DoD and other NASA missions, there is a possibility the aircraft will be unavailable to support the EFT-1 observation.

Risk Context: Navy NP-3D support to national priorities (e.g., support to MDA and DoD missions) take priority over NASA missions.

Assessment and Mitigations: Over a period of approximately 10 years, Cast Glance has supported over 25 observations of Expendable Launch Vehicle for the DoD (numerous classified DoD missions were not considered). During this timeframe, only three aircraft mechanical system failures have prevented an observation. All three incidents occurred when the squadron was forward deployed with limited access to maintenance. Aircraft mission readiness to support 10 NASA imaging missions since 2009 has been 100%. From this data set, Cast Glance mission readiness is approximately 93%. Given the general location of the EFT-1 observation off the coast of California, it was determined that the Navy NP-3D could support the EFT-1 observation from its home base at Naval Air Warfare Center Weapons Division located at Point Mugu Naval Air Station, California. Staging from its home base would provide readily available access to maintenance and was pivotal during the mission.

As the assessment evolved, the MPCV Program determined that an FTO associated with capsule visual photo-documentation during late-stage descent (i.e., parachute deployment sequence) required the use of a second Navy NP-3D. Normally, the second Navy NP-3D would serve as a backup to the primary Navy NP-3D for imaging. Tasking the second Navy NP-3D to descent imaging raised the question of aircraft priority. The MPCV Program determined that should a mechanical failure or schedule conflict develop with this second Navy NP-3D, the NESC-sponsored aircraft for peak heating would be re-tasked to support descent imaging. The NESC

	<h1 style="text-align: center;">NASA Engineering and Safety Center</h1> <h2 style="text-align: center;">Technical Assessment Report</h2>	Document #: NESC-RP-12-00795	Version: 1.0
Title:	Remote Imaging of EFT-1 Entry Heating Risk Reduction		Page #: 30 of 98

Aerosciences TDT lead was briefed on the MPCV Program priority and accepted the possibility of no thermal imagery should a schedule or mechanical risk mature.

Securing the services of the NASA WB-57 aircraft as a backup to the Navy NP-3D mitigated schedule risk. A few months from the scheduled EFT-1 launch, permission was granted by the NESC to allocate contingency resources toward securing WB-57 flight planning services. These planning services, obtained through The Aerospace Corporation, provided the pilot and sensor operator with sufficient background on the observation requirements in the event the aircraft had to be used. The flight path and optical performance of the NASA WB-57 was determined through the use of a custom tool developed by The Aerospace Corporation called Chase Plane Simulation (ChaPS). ChaPS provides similar functionality as the ViDI toolset, but was optimized for designing detailed flight paths for aircraft with gimballed turret sensors such as the WB-57. The target vehicle trajectory and aircraft sensor information are inputs, as are candidate aircraft flight paths. Similar to ViDI, the tool outputs detailed 3-D representations of the aircraft optical platform, with dynamically modeled gimbals. The simulated relationships between the aircraft, camera-pointing hardware, and the target vehicle are assessed with ChaPS. Figure 6.3.3-1 shows an example of the flight planning associated with the WB-57 aircraft. Yellow points in the figure indicate timed locations of the WB-57 as the capsule approached peak heating.

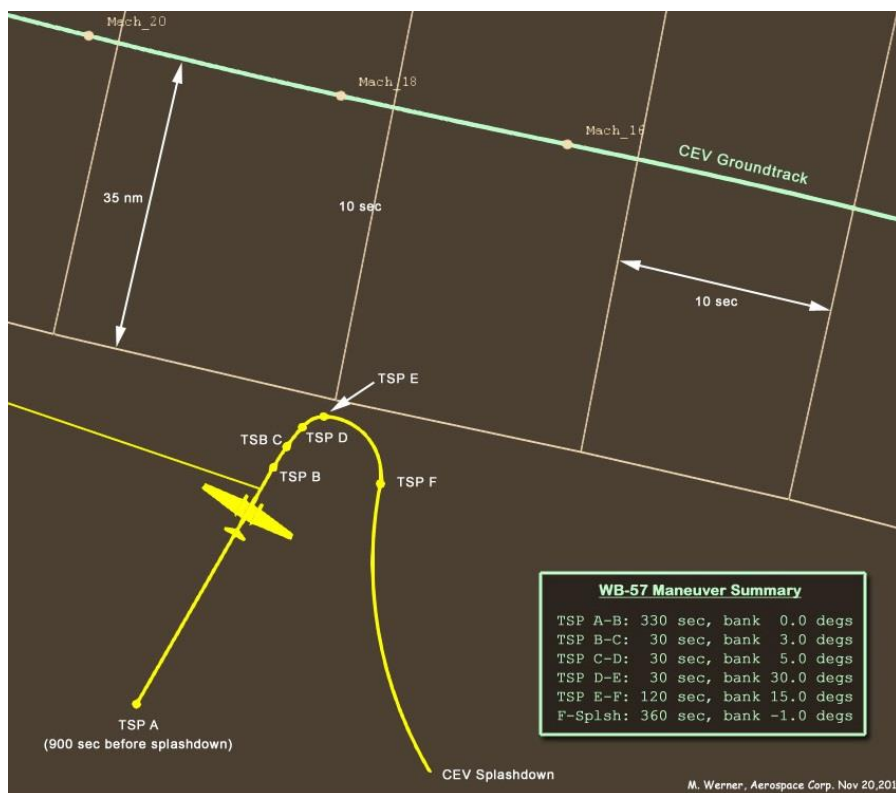



Figure 6.3.3-1. EFT-1 Ground Track and Hazard Keep-out Zone

	NASA Engineering and Safety Center Technical Assessment Report	Document #: NESC-RP- 12-00795	Version: 1.0
Title:	Remote Imaging of EFT-1 Entry Heating Risk Reduction		Page #: 31 of 98

6.3.4 Long-Range Acquisition

At the designated observation location, will the sensor instruments have sufficient sensitivity to acquire and track the capsule?

Risk: Given the expected low surface temperature of the MPCV capsule prior to EI, there is a possibility that the long-range wide field of view (WFOV) sensors will have insufficient sensitivity to acquire the target as it appears over the horizon.


Risk Context: The MPCV capsule will not broadcast a signal of its position. Positional data that are telemetered will experience time lags.

Assessment and Mitigations: Previous SCIFLI observations were successful at long-range acquisition because the vehicle surface temperatures were in excess of 1000 °F, providing high signal-to-noise ratio as the vehicle emerged over the hard Earth horizon. If the infrared signature of the capsule was too weak and it was not detected long-range at low angular velocities, then experience has shown it would be more difficult to acquire at higher angular velocities when the target approaches the aircraft.

The NESC team utilized a set of planning tools to establish processes and recommendations for reliably acquiring and tracking the EFT-1 capsule during reentry. In contrast to ViDI, these tool sets allowed the user to quantitatively characterize the optical signature presented by the capsule to infrared sensors, to assess the attenuating and image degrading effects of the atmosphere, and to determine the anticipated sensor response in the infrared. This section discusses how the optimal infrared waveband was determined for long-range acquisition and spatially resolved viewing at the point of peak heating. During the early stages of the assessment, the implications of the potentially attenuating effects of ablation and shock-layer radiation during the peak heating observation were recognized, but not considered due to the problem complexity. These effects will be discussed in Sections 6.3.6–7.

The basic principle behind infrared thermography is the measurement of surface emissions in the infrared radiation band by virtue of an objects temperature. The infrared radiation spectrum is classically divided into several bands as identified in Figure 6.3.4-1.

NIR	0.8–1.5 μm
SWIR	1.5–3.0 μm
MWIR	3.0–5.0 μm
LWIR	5–15 μm
Far Infrared	15–300 μm

	NASA Engineering and Safety Center Technical Assessment Report	Document #: NESC-RP- 12-00795	Version: 1.0
Title:	Remote Imaging of EFT-1 Entry Heating Risk Reduction		Page #: 32 of 98

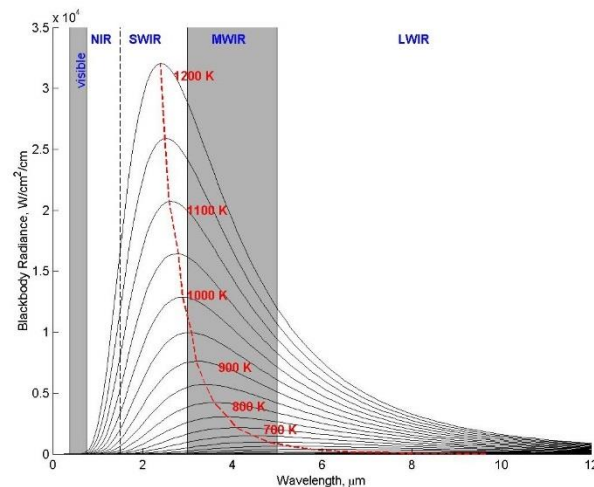



Figure 6.3.4-1. Blackbody Radiance Characteristics

The capsule optical signature (i.e., irradiance) was based on the predicted surface temperature provided by computational fluid dynamics (CFD). Predicted temperatures on the EFT-1 heat shield during several phases of reentry are shown in Figure 6.3.4-2. Time zero in this figure corresponds to when the capsule is separated from the Delta IV upper stage, with the capsule recovery in the Pacific occurring approximately 1 hour later. From the vantage point of the imaging aircraft, the capsule was expected to appear over the Earth's horizon (at a distance of 1,330 nmi) approximately 5 minutes before the capsule reached its maximum surface temperature. As the EFT-1 capsule would not be broadcasting its positional information real time, it was imperative to develop an acquisition strategy to permit the sensor operator to quickly locate the capsule and begin manual tracking. To initially locate the capsule, the optical system on the aircraft would be pointing at a predetermined point in the sky based upon a projected flight path. At the horizon break, the capsule heat shield was expected to be approximately 40 °F (277 K) because the initial line-of-sight view from the aircraft would occur when the capsule was exoatmospheric and before the frictional heating from the atmosphere. At this temperature, a perfect blackbody radiation source would have its irradiance peak in the LWIR waveband as shown, Figure 6.3.4-1, but its signal strength in this waveband would be relatively small and likely problematic from a detector sensitivity perspective. When the capsule was one minute from passing the observing aircraft, the heat shield temperature was expected to increase to approximately 1300 °F (977 K). At peak heating, the surface temperature was expected to increase by from its baseline temperature by two orders of magnitude, to approximately 4,000 °F (2,477 K). Extrapolation of the trends in Figure 6.3.4-1 to this temperature level suggested the NIR waveband would likely be targeted for the desired spatially resolved thermal measurement. Given the rapidly changing surface temperature during this time period, it was apparent the sensor operator would need to be prepared to monitor detector saturation levels and adjust the sensor exposure time should these levels be approached.

	NASA Engineering and Safety Center Technical Assessment Report	Document #: NESC-RP- 12-00795	Version: 1.0
Title: Remote Imaging of EFT-1 Entry Heating Risk Reduction			Page #: 33 of 98

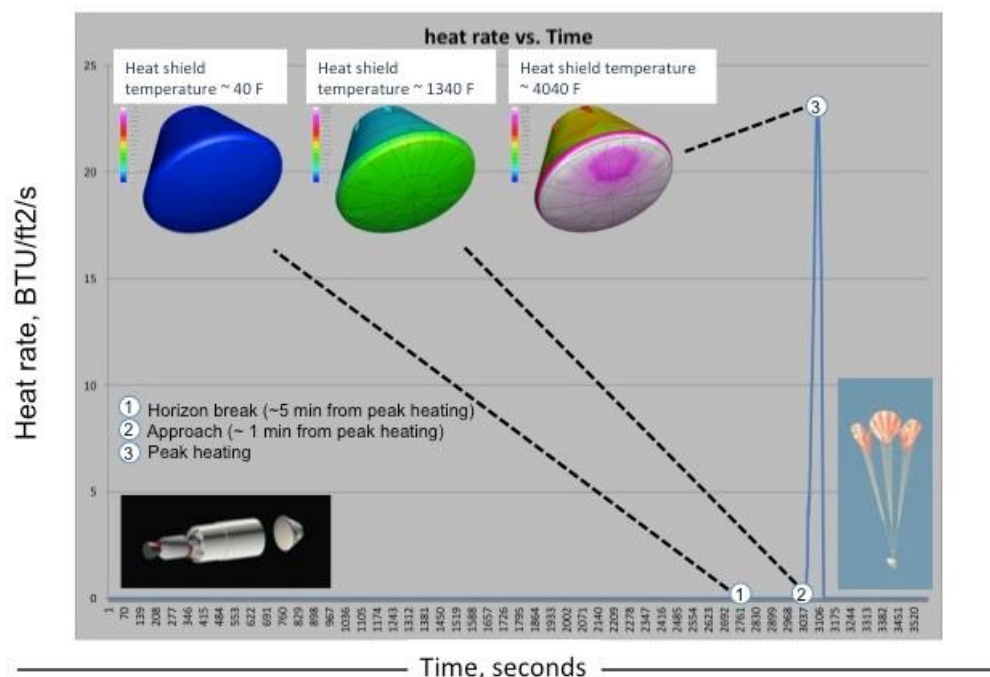



Figure 6.3.4-2. Predicted Surface Temperatures on the EFT-1 Capsule during Several Phases of Reentry

During an SSP observation using the same Navy NP-3D and NIR sensor, the high temperature capsule windward surface ($\sim 1,500^{\circ}\text{F}/1,089\text{ K}$) presented a strong photon-rich emission in the NIR waveband as it emerged over the horizon. In these observation campaigns, a WFOV NIR imager would manually acquire, track, and provide pointing instructions to the narrow FOV NIR imager utilized to provide the spatially resolved thermal data. It was initially assumed this long-range acquisition strategy would be viable during the EFT-1 flight test. When it was determined the capsule heat shield would have a surface temperature an order of magnitude lower than the SSP orbiter at horizon break ($\sim 40\text{--}50^{\circ}\text{F}$), it was concluded the capsule would be significantly more difficult to distinguish from the sky background using the Cast Glance NIR WFOV sensor. It was assumed sufficient signal strength would appear in the more photon-rich MWIR band for acquisition and tracking purposes when the capsule was at extreme distance, spatially unresolved (i.e., a point source), and at low temperature. Through high-fidelity radiance modeling, this assumption was proved incorrect.

The high-fidelity radiance modeling tools used by Johns Hopkins University Applied Physics Laboratory (JHU-APL) are derived from an off-the-shelf code [refs. 26-27] traditionally used by the DoD to support an advanced scene generation capability. Under a previous NESC assessment [ref. 1], the code has been tailored for use by NASA and it was used for this assessment to produce simulated capsule heat shield infrared signatures. This radiance model is fundamentally built around capsule laminar and turbulent CFD surface-temperature predictions over a range of Mach numbers. The radiance modeling simulated the infrared sensor response to

	NASA Engineering and Safety Center Technical Assessment Report	Document #: NESC-RP- 12-00795	Version: 1.0
Title:	Remote Imaging of EFT-1 Entry Heating Risk Reduction		Page #: 34 of 98

the estimated target vehicle irradiance based on surface temperature, emissivity, and reflectance. Because the Sun's radiation, aerosols, and molecular scattering are particularly important background sources, the atmospheric absorption and radiation emission are additional parameters that must be considered when inferring the target surface temperature from infrared emission. Characteristics of the infrared sensor and associated optical system were considered. The radiometric analysis by JHU-APL determined the ability of a particular sensor to obtain measurements with acceptable signal-to-noise ratios under given camera settings. In the waveband of interest, atmospheric effects (e.g., radiance and transmittance) were estimated with the radiative transfer code MODTRAN® [ref. 28], which is designed to model the propagation of electromagnetic radiation through the atmosphere.

Surface optical properties are critical for accurately predicting the thermal irradiance from the capsule in the desired waveband of interest (i.e., spectrally integrated surface emissivity across several wavebands is insufficient). Emissivity is a measure of how closely the radiation emitted from a heated body corresponds to that of a perfect blackbody. Laboratory material testing was required to determine in-band surface emissivity of the EFT-1 capsule heat shield. Surface roughness and reflectance characteristics can strongly influence emissivity, so EFT-1 specific TPS surface material samples were provided to the Surface Optics laboratory to conduct laser-based measurements to characterize their respective surface optical characteristics both spectrally and angularly (see Appendix A). The Avcoat TPS samples represented the virgin and charred/ablated state after exposure to a high-temperature environment produced in an arcjet. Images of the TPS samples used in these laboratory measurements as shown in Figure 6.3.4-3.

During this phase of the assessment, it was learned that to control the heat shield thermal environment while in orbit, the Avcoat surface would be coated with a white epoxy enamel paint and covered by a thin aluminized Kapton® film. While these materials would ablate after EI, it would be present during the long-range acquisition from the aircraft. This had implications in terms of the long-range acquisition strategy.

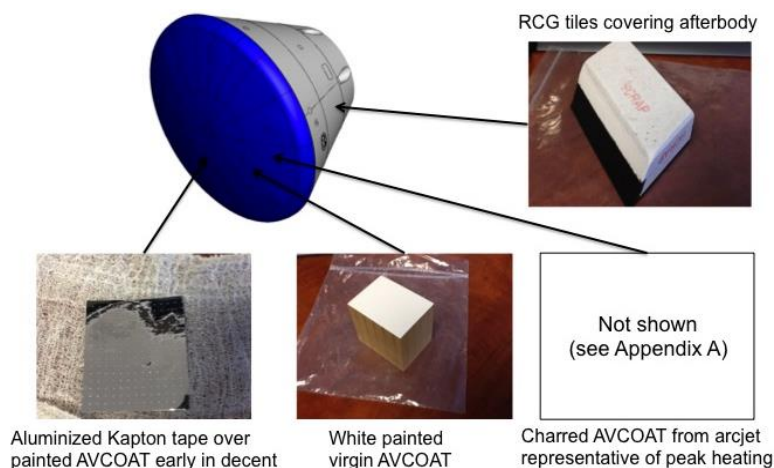



Figure 6.3.4-3. TPS Samples Used to Obtain Surface Optical Properties

	NASA Engineering and Safety Center Technical Assessment Report	Document #: NESC-RP- 12-00795	Version: 1.0
Title: Remote Imaging of EFT-1 Entry Heating Risk Reduction			Page #: 35 of 98

The laboratory measurements revealed the aluminized surface would significantly attenuate the capsule irradiance in the MWIR, thus presenting significant risk in an acquisition strategy using the MWIR waveband as had been assumed. As shown in Figure 6.3.4-4, the metallic tape measurements over a range of viewing angles indicate a low value of emissivity for wavelengths greater than 2 μm (i.e., the MWIR/3.0-5.0 μm and LWIR/ 5-15 μm wavebands).

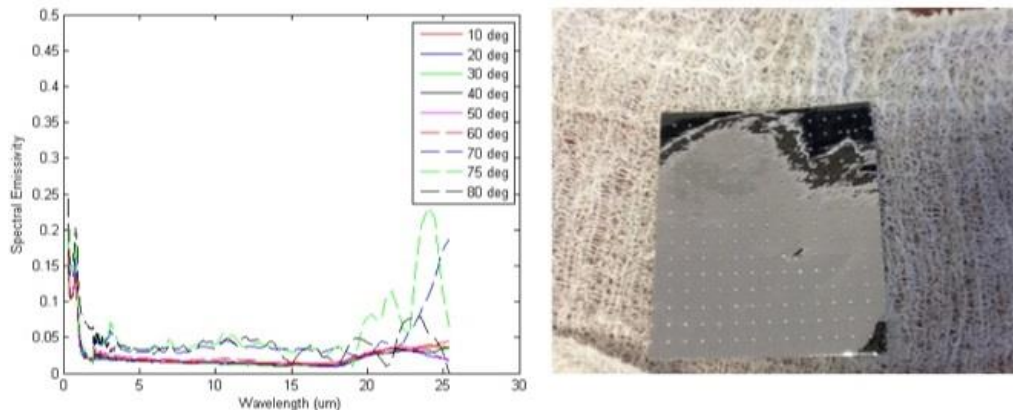


Figure 6.3.4-4. Measured Emissivity of Aluminized Kapton[®] Tape

The emissivity measurements on the charred Avcoat yielded higher values, as shown in Figure 6.3.4-5, confirming the NIR waveband as suitable for the spatially resolved thermal observation after long-range acquisition and tracking had been achieved.

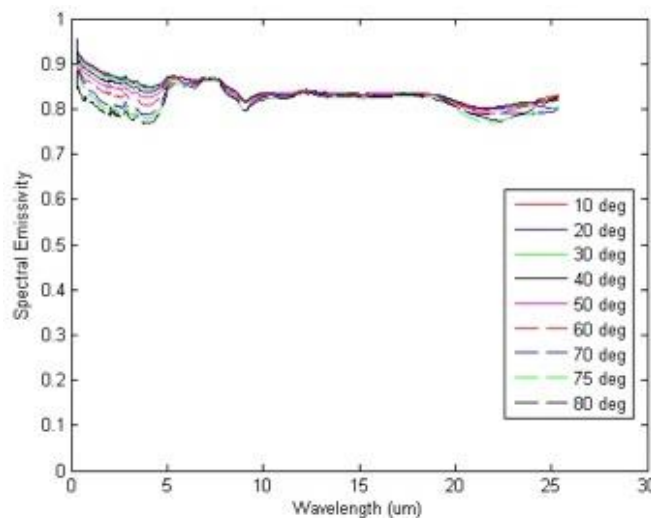


Figure 6.3.4-5. Measured Emissivity of Charred/Ablated Avcoat

Based upon the laboratory measurements, it was decided to develop a long-range acquisition strategy centered around the Cast Glance SWIR WFOV sensor where a higher signal-to-noise ratio provided a better opportunity to distinguish the capsule from the sky background.


	NASA Engineering and Safety Center Technical Assessment Report	Document #: NESC-RP- 12-00795	Version: 1.0
Title: Remote Imaging of EFT-1 Entry Heating Risk Reduction			Page #: 36 of 98

Figure 6.3.4-6 provides an example of the radiance model output. At a range of approximately 500 nmi, the capsule is spatially unresolved. The effects of blurring from the atmosphere and aircraft motion estimated and yielded a signature that is a factor of approximately 1.5 higher than the background sky irradiance. The corresponding signature for the MWIR waveband (not shown) was less than 50% of the background sky radiance that rendered acquisition of the capsule in this waveband improbable. For estimating the atmospheric attenuation and atmospheric radiance background, the 1976 U.S. Standard Atmospheric model was used with optimistic maritime settings (e.g., maritime haze and no clouds).

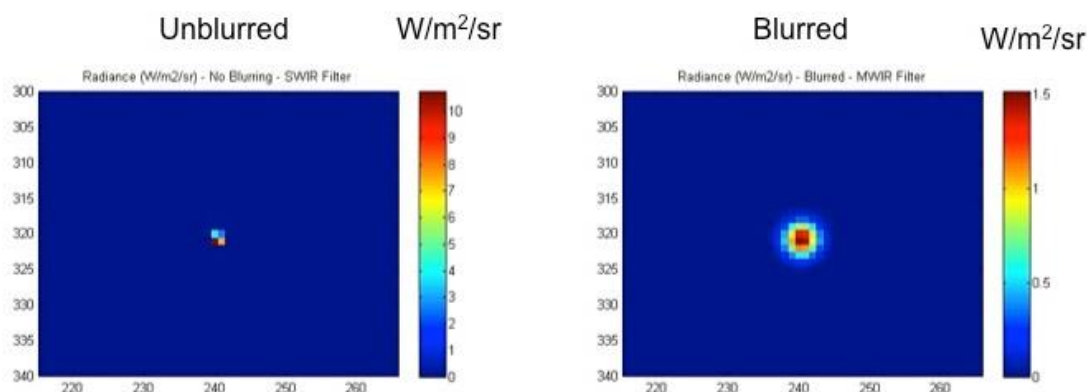


Figure 6.3.4-6. Predicted Irradiance in SWIR Waveband at Time of Long-Range Acquisition.
Distance to Capsule = 493 nmi. Elevation Angle = 3 deg. Signal-to-Sky Background ~1.5.

Additional analysis showed that during the long-range acquisition phase when the aluminized tape was in place and highly reflective, the irradiance from the capsule would be dominated, particularly in the SWIR waveband, by solar reflectance and not thermal emission. This solar irradiance, which is the result of a favorable Sun/capsule orientation would enhance the signal-to-sky background, thereby increasing the probability of observing the capsule at long range.


6.3.5 Obscuring Clouds

Will clouds interfere or prevent long-range acquisition or the desired spatially resolved thermal observation?

Risk: Given the expected Navy NP-3D operational ceiling (i.e., ~30,000 ft), there is a possibility variable cloud layers in the observation location will obscure the view of the capsule leading to loss of data.

Risk Context: A SCIFLI mission in support of the SSP encountered partial loss of imagery data because clouds prevented the sensor operator from tracking the orbiter. In addition, low-level clouds provided further operational challenges during SpaceX flight test launch phase observations.

Assessment and Mitigations: Long-range (e.g., climatic) weather forecasting is desired to evaluate asset deployment options. Knowledge of the expected local weather close to the time of observation is required to mitigate the likelihood of clouds obscuring the desired view (the presence of water vapor has an attenuating effect on the propagation of infrared radiation through

	NASA Engineering and Safety Center Technical Assessment Report	Document #: NESC-RP- 12-00795	Version: 1.0
Title:	Remote Imaging of EFT-1 Entry Heating Risk Reduction		Page #: 37 of 98

the atmosphere). The National Weather Service Spaceflight Meteorology Group (SMG) provided forecasting support to the NESC team. Months in advance of the anticipated observation, SMG provided historical satellite cloud and water vapor climatology data to assess the challenges of potential observation locations. Monthly cloud-cover data provided an outlook of expected impacts on the potential EFT-1 operations in the Pacific just off the coast of California. Such statistical cloud coverage information is essential when ground- or sea-based platforms are being considered, or for aerial systems with an operating ceiling below 25,000 ft. The climatology information included percentage of sky cloud cover at various altitudes and winds aloft, giving the assessment team and flight crews an appreciation for the potential weather challenges. An example of cloud coverage at flight altitude in the expected area of operations for September 2014 (the month of launch at the time of early mission planning) is provided in Figure 6.3.5-1. The anticipated aircraft and the EFT-1 recovery locations are designated off the coast of Baja, California. If launch had occurred in September 2014 as originally planned, the historical data suggested the operations team would likely need to be prepared to deal with obscuring clouds. The historical data indicated that the percentage of cloud coverage in the planned observation area would increase if the EFT-1 launch were later in the calendar year.

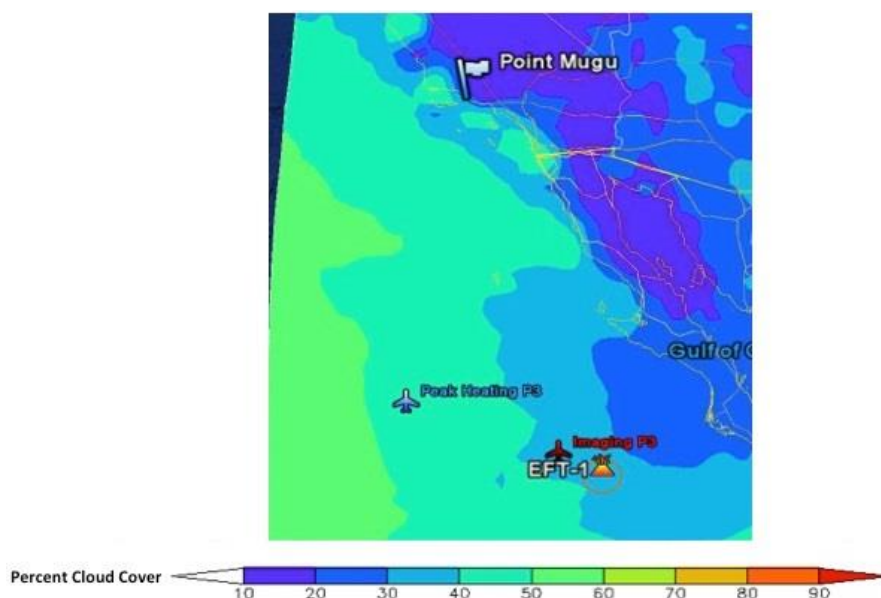



Figure 6.3.5-1. Mean Total Cloud Cover

Tactical weather information in the form of short-range forecasts from the SMG meteorologists permitted the NESC team to successfully anticipate possible actions on the part of the EFT-1 Launch Director to delay or scrub the launch. Information of this nature would be an important consideration in terms of making informed decisions during aircraft pre-flight. When mission operations would commence, SMG would utilize a customized Advanced Weather Interactive Processing System to superimpose the EFT-1 reentry flight path (sometimes referred to as ground track) onto satellite imagery and numerical model forecast data. These graphics created

	NASA Engineering and Safety Center Technical Assessment Report	Document #: NESC-RP- 12-00795	Version: 1.0
Title: Remote Imaging of EFT-1 Entry Heating Risk Reduction			Page #: 38 of 98

highly effective weather visualization for rapid decision-making. An example of such short-term graphically based forecast information is shown in Figure 6.3.5-2 from an SSP observation. In the figure, red corresponds to low relative humidity (no cloud cover); green to medium relative humidity (some cloud cover); and purple to high relative humidity (high cloud cover). The reentry flight paths associated with the primary flight path of the SSP orbiter returning to the Kennedy Space Center (KSC) and an alternate path associated with a one-orbit wave-off are shown superimposed on information used to predict the development of clouds.

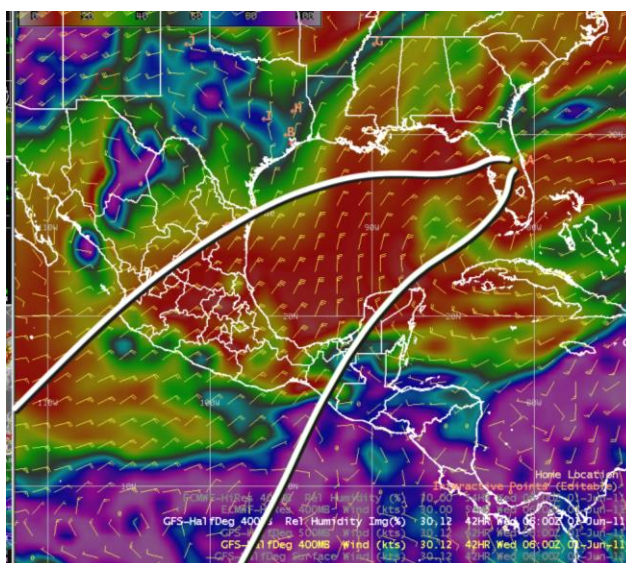



Figure 6.3.5-2. SSP Orbiter Reentry Paths to KSC Superimposed on Predicted Cloud Cover Forecast in 2011

Graphics-based briefings showing relevant weather conditions relative to the anticipated reentry path provided the operations team the required flexibility to factor in the time needed to reposition an imaging system if required. During mission pre-flight, the NP-3D aircrew would be briefed on weather conditions in the mission operation areas. Just prior to takeoff, Cast Glance personnel are provided with the latest predictions and satellite images. Alternate aircraft observation locations are pre-negotiated if the viewing conditions are expected to be poor.

When significant cloud coverage is anticipated or encountered at the time of an observation, satellite information is used to determine an alternate imaging asset position that would present cloud-free line-of-sight (CFLOS) to the target. A CFLOS software package developed by JHU-APL [ref. 29] infers cloud tops and bases from real-time satellite measurements and indicates the level of obstruction by clouds along the line of sight from the observer to the target. If an obscured line of sight to the target is anticipated, then a new observation position can be identified and relayed to the asset personnel. An example of graphical output from this tool is shown in Figure 6.3.5-3. The colors signify percentage within any particular cell ($\sim 30 \times 30$ nmi) that clouds will prevent a line of site from the observer to the target. Depending on the type of inputs used, the tool can be used in a real time or forecast mode.

	NASA Engineering and Safety Center Technical Assessment Report	Document #: NESC-RP- 12-00795	Version: 1.0
Title:	Remote Imaging of EFT-1 Entry Heating Risk Reduction		
			Page #: 39 of 98

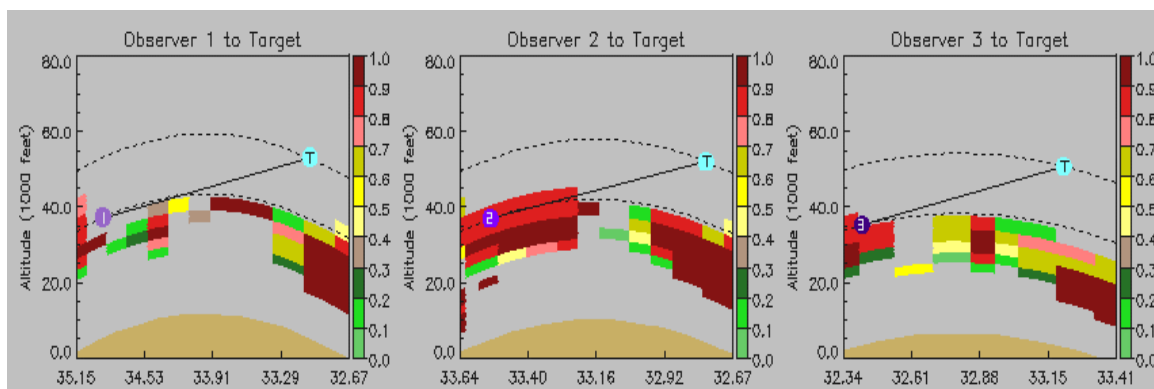
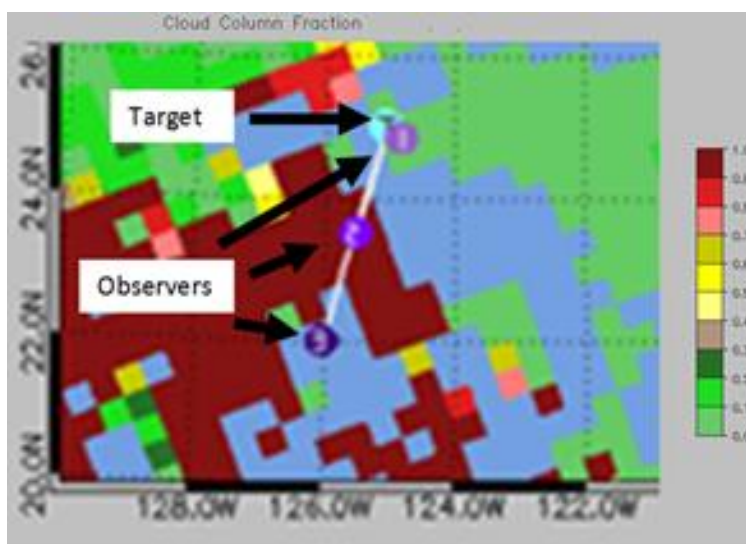



Figure 6.3.5-3. General CFLOS Output Showing Relationships between a Target and Several Notional Observers and the Optical Blockage from Clouds

In general operational practice, the observing aircraft will fly to the primary TSP and make a real-time assessment. If the weather is below minimums to satisfy imaging requirements, then the aircraft will fly parallel to the capsule trajectory toward or away from the recovery point to find acceptable viewing while avoiding or coordinating hazardous airspace. Real-time communications to the aircraft during a mission will allow the operations team to pass recommendations to the crew as to the direction toward more favorable viewing conditions.

6.3.6 Effect of Shock Layer Emissions

Will the shock layer emissions from the hot gas cap interfere with the infrared signature from the capsule heat shield?

Risk: Given the uncertainty in the in-band irradiance of the MPCV Program capsule heat shield and high-temperature shock layer during reentry, there is a possibility that (1) the shock emissions from the shock layer will be a significant fraction of the emissions expected from the

	<h1 style="text-align: center;">NASA Engineering and Safety Center</h1> <h2 style="text-align: center;">Technical Assessment Report</h2>	Document #: NESC-RP-12-00795	Version: 1.0
Title:	Remote Imaging of EFT-1 Entry Heating Risk Reduction		
			Page #: 40 of 98

heat shield, and (2) the optimal sensor configuration will not be determined, resulting in saturation of the infrared imager and subsequent data loss.

Risk Context: Variables include, but are not limited to, uncertainties in surface emittance of the MPCV Program crew capsule heat shield, atmospheric attenuation, and optical path transmission losses. Quantifying the radiance reaching the focal plane array pre-flight provides the necessary situational awareness to determine optimal gain and exposure (integration) times.

Assessment and Mitigations: For the accurate capsule heat shield temperature determination as inferred from infrared intensity measurements, accurate book keeping of the photons collected at the detector focal plane array must be performed. Surface temperature is inferred from the photons emitted from the heat shield by virtue of its temperature. However, there are other sources of photons that must be identified and potentially accounted for. One of these sources is irradiance from the high-temperature shock layer between the heat shield and the observing aircraft.

The planned return velocity during the EFT-1 flight test was approximately 80% that experienced during a nominal lunar return. To determine whether irradiance from the high-temperature shock layer during reentry might represent a considerable fraction of the total radiance from the heat shield due to its temperature, a first-order estimate was made. Figures 6.3.6-1 and 6.3.6-2 summarize a computational study that was performed using the Data Parallel Line Relaxation CFD code [ref. 30]. First, total radiance was computed along lines of sight outward from the heat shield surface, through the shock layer, and toward a notional observing aircraft (Figure 6.3.6-1). The computational prediction was made at the anticipated reentry conditions of 4.87 mi/sec (7.84 km/sec) and 34.4 mi (55.4 km) altitude for peak heating. A hot wall assumption quantified the total irradiance from the heat shield and shock layer. A companion cold wall assumption of 80 °F (300 K) provided the irradiance contribution from the shock layer only.

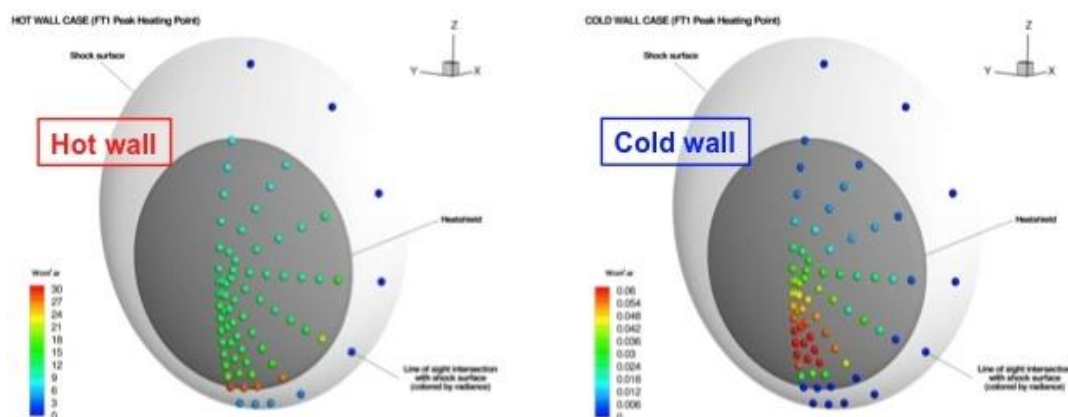



Figure 6.3.6-1. Predicted Irradiance along Line-of-Sight from Heat Shield through Shock Layer toward an External Observer

	NASA Engineering and Safety Center Technical Assessment Report	Document #: NESC-RP- 12-00795	Version: 1.0
Title:	Remote Imaging of EFT-1 Entry Heating Risk Reduction		Page #: 41 of 98

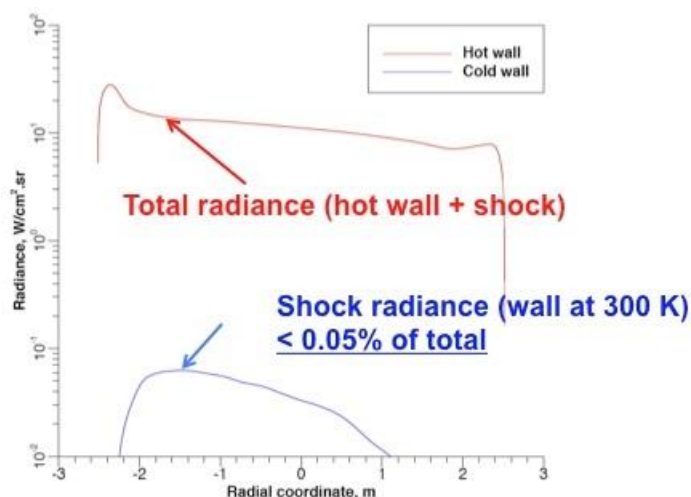



Figure 6.3.6-2. Predicted Shock Layer Radiance Relative to Total Radiance (Shock Layer and Heat Shield)

Figure 6.3.6-2 summarizes the results by presenting irradiance as a function of the radial position along the heat shield. The conclusion from this assessment was that while the radiative heating from the shock is not negligible, it was two orders of magnitude less than that from the heat shield. That is, the radiation from the high-temperature heat shield would dominate that emanating from the shock layer.

These conclusions were supported by higher-fidelity analysis (see Section 6.3.7). During the same period of maximum heating, analysis with the JHU-APL radiance model indicated that, in the NIR waveband, there would be no shortage of photons. This analysis implied that during the observation either the use of a neutral density filter or reduced camera integration times would be required to avoid saturation of the detector. Figure 6.3.6-3 provides an example of the radiance model output. At a range of approximately 48 nmi, the capsule is spatially resolved. On the left, the capsule irradiance estimated to reach the NIR focal plane array using a filter and an exposure time of 20 msec is displayed graphically. The corresponding image of what the sensor operator would observe on his tracking display (intensity/counts) is shown on the right. The estimates assumed blurring due to the atmosphere and aircraft motion. Estimated pixel resolution in these radiometrically accurate synthetic images was consistent with earlier ViDI results.

	<h1 style="text-align: center;">NASA Engineering and Safety Center Technical Assessment Report</h1>	Document #: NESC-RP-12-00795	Version: 1.0
Title: Remote Imaging of EFT-1 Entry Heating Risk Reduction			Page #: 42 of 98

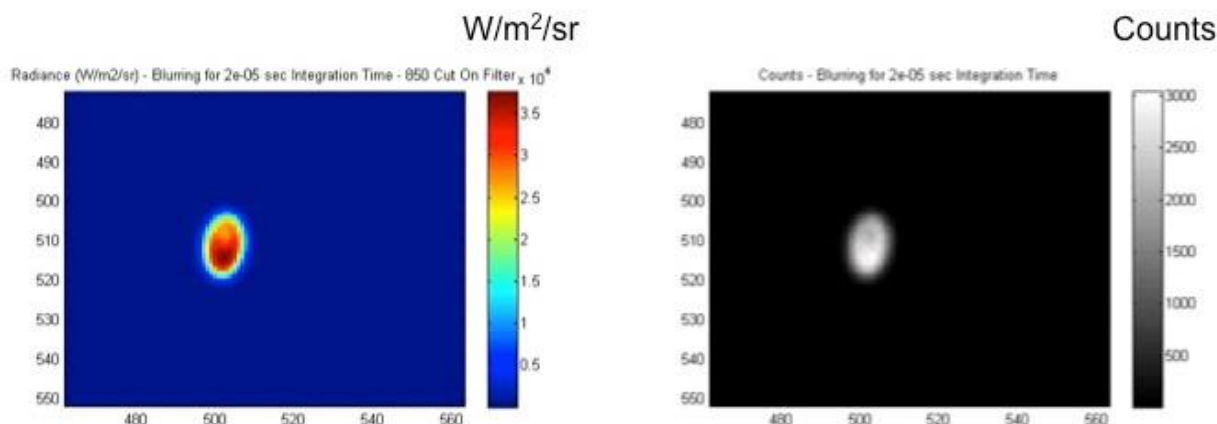


Figure 6.3.6-3. Predicted Irradiance in the NIR Waveband at the Time of Peak Heating. Distance to Capsule = 48 nmi. Elevation Angle = 27 deg. 850 mm Cut-on Filter.

A backshell temperature measurement was not an objective for this observation. However, estimates were made to determine whether useful information could be obtained from the infrared imagers after the peak heating measurement was obtained as the capsule passed by the imaging aircraft presenting a side-on view. Backshell temperatures were expected to be a factor of 3–8 lower than the heat shield. Radiometric analysis, shown in Figure 6.3.6-4, indicated that insufficient photons in the NIR waveband from the backshell would be available to successfully detect the capsule afterbody. The MWIR imager had better sensitivity at the expected lower backshell temperatures, but insufficient spatial resolution. No useful information on the capsule backshell was expected.

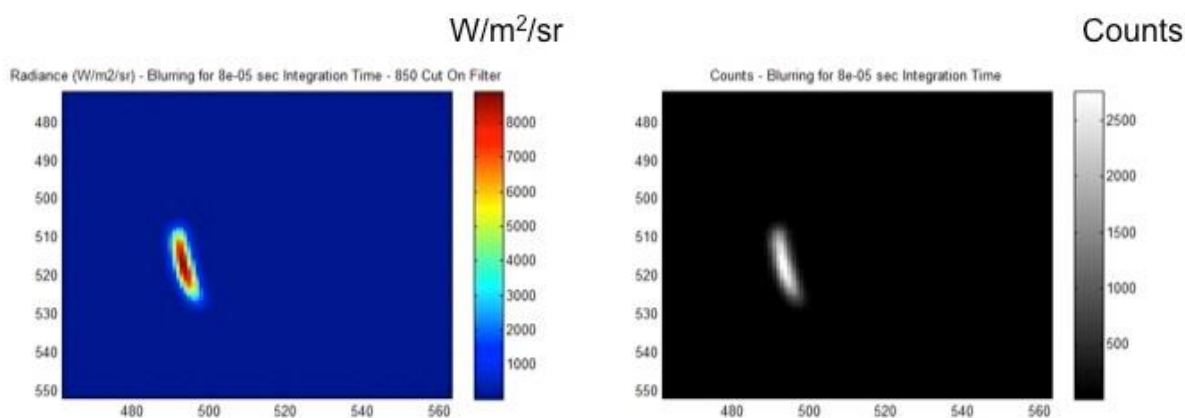



Figure 6.3.6-4. Predicted Irradiance from the Capsule Heat Shield Edge and Backshell in the NIR Waveband at the Point of Closest Approach to the Aircraft. Distance to Capsule = 35 nmi. Elevation Angle = 37 deg. 850 mm Cut-on Filter.

	NASA Engineering and Safety Center Technical Assessment Report	Document #: NESC-RP- 12-00795	Version: 1.0
Title:	Remote Imaging of EFT-1 Entry Heating Risk Reduction		Page #: 43 of 98

6.3.7 Effects of Ablation

Will the TPS ablative nature interfere with the capsule heat shield infrared signature?


Risk: Given the uncertainty in the in-band irradiance of the MPCV crew capsule heat shield and the presence of TPS ablation material in the shock layer, there is a possibility that the optimal sensor configuration will not be determined resulting in subsequent data loss.

Risk Context: Variables include, but are not limited to, uncertainties in surface emittance of the MPCV crew capsule heat shield, the optical transparency of the heat shield ablation products, atmospheric attenuation, and optical path transmission losses. Quantifying the irradiance reaching the detector focal plane array pre-flight provides the necessary situational awareness to determine optimal gain and exposure (integration) times.

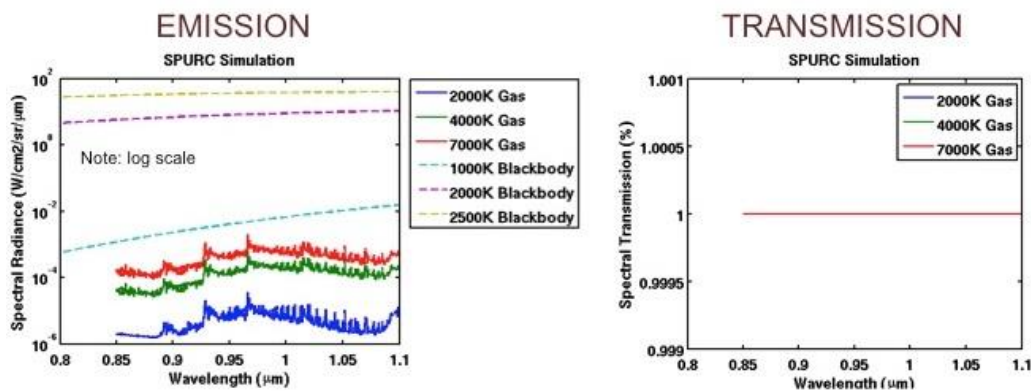
Assessment and Mitigations: To ascertain the potential attenuation of the heat shield irradiance from the presence of ablation products (or additional emissions from ablation particulates) in the wavebands of interest, a supplementary analysis was performed. Two Agency-developed radiation transport tools were exercised to assess the levels of expected emission in the NIR and MWIR. These codes were the Standard Plume Ultraviolet Radiation Code (SPURC) [ref. 31] and Nonequilibrium Air Radiation Code (NEQAIR) [ref. 32]. Near-surface flowfield properties provided by computational prediction near the point of peak heating were used as inputs to these codes. SPURC is tailored to compute emissions from the ultraviolet to LWIR region of the spectrum from particulate (e.g., soot or alumina) and was developed for characterizing rocket plume signatures using band models. NEQAIR computes radiation in the same part of the spectrum, but uses line methods instead of bands for temperatures approaching 17,500 °F (9,978 K). NEQAIR is specifically tailored for assessing hypersonic shock layer radiation, but does not address particulate emissions.

An estimate of the boundary-layer edge properties and chemical species was provided by the MPCV Aerosciences team. The chemical composition provided was from an equilibrium calculation using Avcoat ablation products mixed and reacted with with boundary layer air species at representative boundary layer conditions. A simplified problem was constructed to investigate the effects of this layer on the NIR measurements. A homogenous slab of gas was assumed with the species concentrations provided at the edge pressure over a range of representative temperatures. The thickness of the slab was chosen to be slightly larger than three times the maximum momentum thickness to ensure that the extent of the ablation products into the flowfield would be captured. Inspection of non-ablating CFD predicted flowfields at peak heating conditions indicated the slab thickness was approximately 20% of the stagnation line shock standoff distance.

The results from SPURC and NEQAIR are shown in Figures 6.3.7-1 and 6.3.7-2, respectively, for the NIR waveband. A range of heat shield surface temperature and shock layer temperatures are presented.

	NASA Engineering and Safety Center Technical Assessment Report	Document #: NESC-RP- 12-00795	Version: 1.0
Title: Remote Imaging of EFT-1 Entry Heating Risk Reduction			Page #: 44 of 98

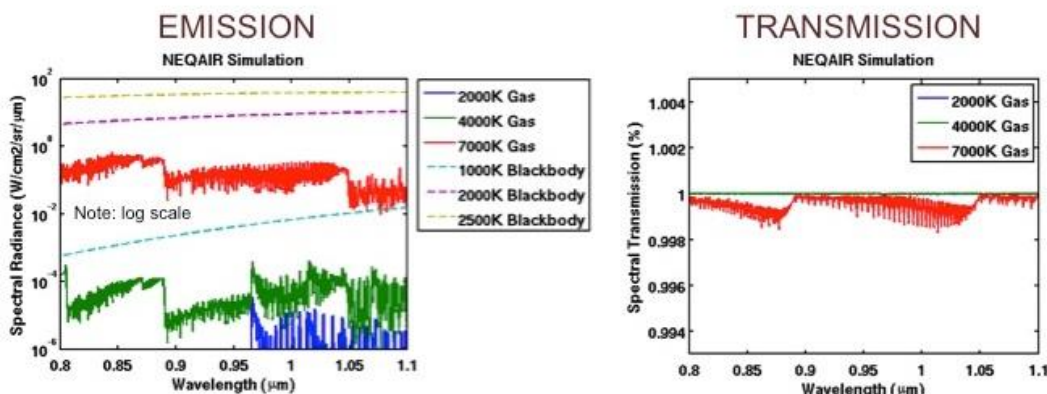
SPURC Results for NIR Region



Wavelength region: 0.85-1.1 μm (NIR)

Figure 6.3.7-1. Predicted Emission and Transmission from SPURC for a Range of Surface- and Shock-Layer Temperatures


NEQAIR Results for NIR Region



Wavelength region: 0.8-1.1 μm (NIR)

Figure 6.3.7-2. Predicted Emission and Transmission from NEQAIR for a Range of Surface- and Shock-Layer Temperatures

The predicted emission data from both codes (left plots) compare the magnitude of the NIR emissions from the heat shield surface relative to those from the high-temperature gas in the shock layer. Note a log scale was used due to the large differences in magnitude between the two photon sources. The SPURC emission predictions (Figure 6.3.7-1) indicate the photons from the heat shield by virtue of its temperature are dominate. Increases in NIR emissions from the presence of water vapor in the shock layer are predicted with SPURC. For a gas temperature of 12,140 °F (7,000 K), the companion NEQAIR results indicated a significant increase in NIR emissions from nitrogen (1+) that was not captured by SPURC. However, the emission level is approximately an order of magnitude less than those from the heat shield at a surface temperature of 3,150 °F (2,000 K).

	NASA Engineering and Safety Center Technical Assessment Report	Document #: NESC-RP- 12-00795	Version: 1.0
Title: Remote Imaging of EFT-1 Entry Heating Risk Reduction			Page #: 45 of 98

The transmission data from these two codes suggest little to no absorption of the heat shield emissions in the NIR waveband within the high-temperature shock layer. A value of unity indicates the emissions leaving the heat shield surface are transmitted through the high-temperature gas cap with no loss. The NEQAIR results, Figure 6.3.7-2, indicate an absorption in the NIR waveband for the higher-temperature gas that the SPURC does not capture.

The presence of ablation particulate could represent an additional source of NIR emission and/or serve as an attenuating effect by blocking the heat shield emissions through the shock layer. SPURC was used to assess this potential effect, and the results are shown in Figure 6.3.7-3.

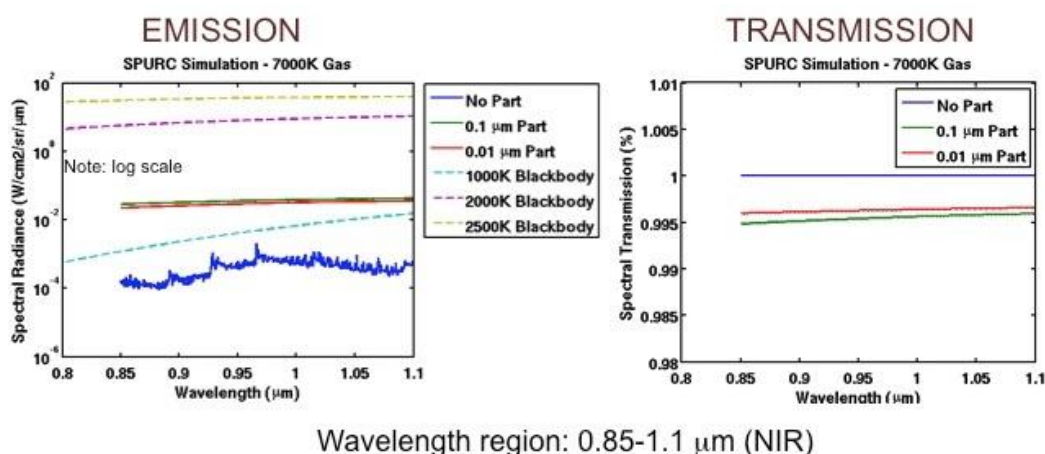


Figure 6.3.7-3. Predicted Emission and Transmission from SPURC for a Range of Surface Temperatures and Particulate Sizes


The SPURC results suggested that emission in the NIR waveband from small ablation particulate in sufficiently large amounts could exceed those emanating from the heat shield if its surface temperature was below 1,300 °F. At peak heating, heat shield temperatures were expected to be 3,150 °F (2,000 K) or greater and, as such, the NIR emissions from the heat shield were predicted to be several orders of magnitude larger.

The final outcome of the JHU-APL assessment study determined (1) the presence of ablation would not introduce large uncertainties in surface temperatures derived from the NIR imagery, and (2) while the shock layer radiation needed to be accounted for during the period of peak heating, the correction would be only on the order of 3%. Corrections of this nature could be accounted for in the post-flight data processing, and would not alter the method of data acquisition.

6.3.8 Mission Operations Readiness

How will the execution of the observation be coordinated?

Risk: Given the complex nature of the observation and level of communications required, there is the risk that timely decisions will not be made and the NESC team will not be prepared for the observation campaign.

	NASA Engineering and Safety Center Technical Assessment Report	Document #: NESC-RP- 12-00795	Version: 1.0
Title:	Remote Imaging of EFT-1 Entry Heating Risk Reduction		Page #: 46 of 98

Risk Context: In previous SCIFLI observations, the operations team operated out of the JSC Mission Control Center (MCC). Full access to control-room consoles and communications paths were provided and were considered critical to mission success.

Assessment and Mitigations: Upon approval of an EFT-1 thermal observation campaign, a wide array of activities began to prepare for the scientific, logistic, hardware, software, and human aspects of the observation. These activities and associated procedures have evolved over 17 observations spanning more than 10 years under HYTHIRM and SCIFLI. This section describes the primary elements of planning and training to familiarize the NESC team with the tasks leading to a successful imaging campaign on December 5, 2014. Operations the day of reentry are described in Section 7.0, Data Acquisition and Analysis.


6.3.8.1 Mission Execution Plan (MEP)

Coordination of a remote observation is a dynamic logistical effort that requires the gathering, analysis, and dissemination of time-critical information. To assure critical information is developed, received, and distributed to the appropriate team member at the proper time, an MEP is created. It is a comprehensive document encompassing a wide range of reference information tailored to specific events and requirements for coordination of an observation campaign. The EFT-1 MEP was initially drafted in August 2013, in anticipation of a spring 2014 launch. Because the launch for EFT-1 was slipped from this first quarter CY2014 date, a majority of the NESC team went into a semi-hibernation mode to conserve resources. The NESC team was reactivated in late 2013 when the revised launch date of December 2014 was announced. The last MEP revision (see Appendix B) was made in November 2014 to reflect the revised launch date of December 4, 2014.

The EFT-1 MEP defines the observation objectives and identifies the operations team roles and responsibilities. The MEP describes processes and procedures for conducting the observation and outlines the long-term schedule (e.g., 14 weeks prior to launch) for training opportunities and the delivery of critical items (e.g., hardware, software, and trajectory information). The intermediate MEP schedule (e.g., ~4 weeks prior to launch) describes the requirements and/or delivery schedule for weather information, trajectory file naming and formatting conventions, plans for airspace coordination, approved incursions into foreign airspace (if necessary), communications protocols with the Navy NP-3Ds, and scheduling of the dress rehearsal flight(s). The short-term MEP schedule (day of launch), was managed under a separate Microsoft® Excel®-based document that identified critical events during the EFT-1 flight test and provided a detailed checklist as a guide for the EFT-1 operations team (see Appendix C). The MEP coordinator is the individual responsible for the maintaining the MEP, and ensuring the MEP procedures and timelines are being followed as the mission progresses.

6.3.8.2 Mission Operations Facilities

In a majority of SCIFLI imaging campaigns, the operations team consisting of personnel leading trajectory processing, communications, and weather were co-located with a JSC flight dynamics officer liaison, the technical lead, and appropriate program management. For SSP observations, mission operations were conducted from one of the backup JSC mission control rooms as shown

	<h1 style="text-align: center;">NASA Engineering and Safety Center Technical Assessment Report</h1>	Document #: NESC-RP-12-00795	Version: 1.0
Title:	Remote Imaging of EFT-1 Entry Heating Risk Reduction		Page #: 47 of 98

in Figure 6.3.8.2-1. For the EFT-1 thermal observation, the assessment team's recommendation to the NESC was to staff the assessment operations team in a similar manner.



Figure 6.3.8.2-1. Previous SCIFLI Operations Coordinated from the Auxiliary SSP Red Flight Control Room

For the EFT-1 observation, the NESC assessment operations team operated out of the Imagery Payload Operations Center (IPOC) of the JSC MCC as shown in Figure 6.3.8.2-2. The IPOC provided the required communications and workspace in a central location, contributing to the ability to successfully coordinate the EFT-1 observation. The IPOC was initially developed as a control room for SSP payloads, and was left relatively unchanged following program termination. The room contained numerous consoles, computer terminals, monitors, landline phones, and counter space. In addition, each console had access to the digital voice intercommunications equipment audio distribution system used to communicate with elements of the EFT-1 Flight Operations team. The IPOC was to be minimally occupied for EFT-1, which provided ample workspace for the NESC team prior to and during the mission.

The assessment operations team worked with the Landing Support Officer (LSO), the SMG, and the Flight Dynamics Officer (FDO). The IPOC hosted the MPCV Program FTMO and the JSC imagery group, responsible for the image-documentation requirements associated with the second Navy NP-3D, and the Ikhana UAV representative from Armstrong Flight Research Center (AFRC) who coordinated the Public Affairs Office (PAO) UAV. The IPOC was ideal for the assessment operation team, as it would provide and facilitate electronic and face-to-face communication with key personnel at critical times during the mission.

Following the EFT-1 mission, the JSC imagery group was responsible for the IPOC refurbishment. Ideas for developing a state-of-the-art control environment for NASA missions requiring imaging were solicited from the assessment team and will be implemented for future use during the EM-1 flight and other Agency flight test opportunities.


	NASA Engineering and Safety Center Technical Assessment Report	Document #: NESC-RP- 12-00795	Version: 1.0
Title:	Remote Imaging of EFT-1 Entry Heating Risk Reduction		Page #: 48 of 98



Figure 6.3.8.2-2. IPOC in the MCC

6.3.8.3 Simulation and Training

Mission simulations were a key part of EFT-1 mission operations personnel training. The NESC assessment operations team was more closely integrated into the flight operations for EFT-1 than in any previous imaging mission, with the status of the observation aircraft being relayed to the EFT-1 Launch Director, the NASA Recovery Coordinator, and the Navy recovery forces. A series of Agency-level simulations were conducted for training and proficiency purposes, and the assessment operations team was fortunate to have the ability to participate in and benefit from these formal training exercises.


Joint Integrated Simulation (JIS) 1a:

The first opportunity for NESC assessment operations team to participate in a major simulation training exercise was the JIS 1 a/b, which was held on consecutive days. The exercise, involving all personnel providing imaging support (launch to recovery) was conducted approximately 8 months prior to the launch. The EFT-1 observation Mission Coordinator (MC) was sent to the JSC MCC to participate. In this exercise, the Navy NP-3D aircraft squadron and the Cast Glance imaging personnel did not participate.

JIS 1a was a relatively simple training exercise, which began in the minutes prior to launch and continued through splashdown. There were no mission anomalies introduced into the exercise that would effect a reentry observation. Numerous communications requirements and protocol were identified, and the assessment operations MEP mission timeline was updated based upon the experiences of this training exercise.

JIS 1b

Initially, the JIS 1b training exercise paralleled the 1a training. However, a “green card,” or anomaly, was posted by the simulation leader to the NESC assessment team. The second Navy NP-3D (BH-340), intended to observe the parachute deployment sequence, developed engine

	<h1 style="text-align: center;">NASA Engineering and Safety Center</h1> <h2 style="text-align: center;">Technical Assessment Report</h2>	Document #: NESC-RP-12-00795	Version: 1.0
Title: Remote Imaging of EFT-1 Entry Heating Risk Reduction			Page #: 49 of 98

problems and was returned to base. This information was propagated appropriately through the lines of communication. Shortly thereafter, a problem developed on the MPCV capsule while in orbit, and it became evident the capsule would land hundreds of nmi downrange from the planned splashdown point. The key exercise for the JSC FDO was to prevent the capsule from landing on Mexican soil. However, it became apparent the only one U.S. Government asset that could possibly reconnoiter the capsule once in the water was the NESC-sponsored Navy NP-3D (BH-300). Working with the MPCV Program FTMO, the decision was made to send the Navy NP-3D to a holding location and await information on the splashdown location. Ultimately, the scenario progressed where the Navy NP-3D was able to reach the capsule, which splashed down just off the Mexican coast, approximately 900 nmi downrange from the planned recovery location. To accomplish this scenario, the Navy NP-3D had to land in Mexico to refuel as shown in Figure 6.3.8.3-1.

The responses of the NESC assessment team mission operations representative to reposition the NESC-sponsored Navy NP-3D were based on aircraft performance estimates and assumptions. The resulting lessons learned led to the creation of a formal, documented protocol on how contingencies would be handled through NASA, the Navy NP-3D commanders, and Navy leadership. These revised protocols and associated risks to loss of imagery were approved by the NESC. Another key issue identified in the simulation was the choice of holding location for the NESC aircraft (BH-300). During the training exercise, this holding location required the NESC-sponsored Navy NP-3D to cross under the flight path of the capsule, but did not coordinate the time when the crossover would be made. This decision potentially placed the aircraft within a hazard boundary at a time the capsule would be flying over. Protocols to coordinate such a repositioning during the real observation were implemented.

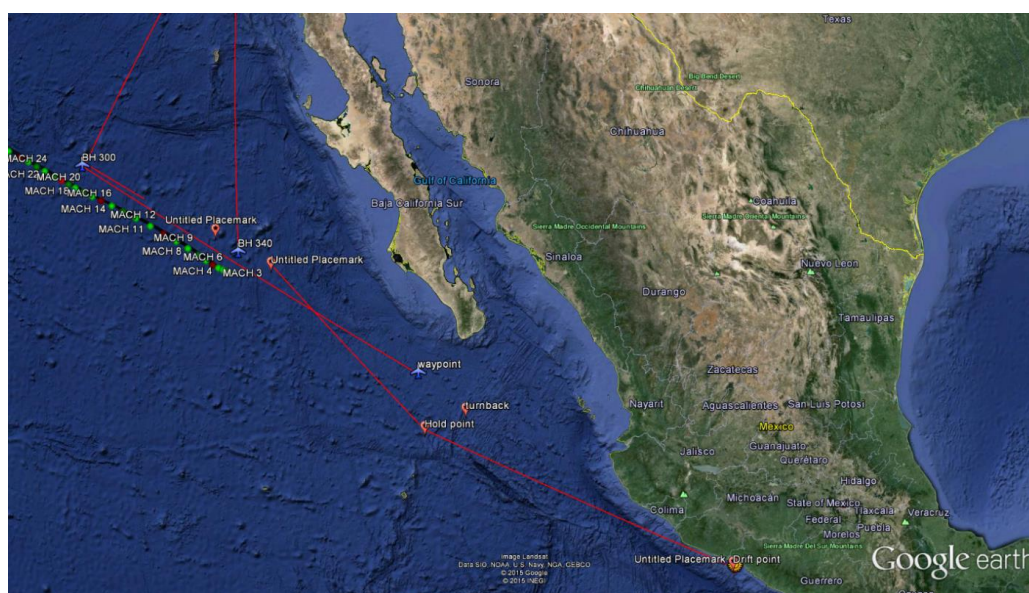



Figure 6.3.8.3-1. BH-300 Aircraft Movements for JIS 1b Simulation where Several Anomalies with the MPCV Capsule and the BH-340 Imaging Aircraft Occurred

	NASA Engineering and Safety Center Technical Assessment Report	Document #: NESC-RP- 12-00795	Version: 1.0
Title: Remote Imaging of EFT-1 Entry Heating Risk Reduction			Page #: 50 of 98


Assessment Team Internal Simulations

Following the JIS exercise, two lower-fidelity simulations were conducted at Langley Research Center (LaRC) for the benefit of the extended assessment mission operations team members. No direct interfaces with the JSC MCC team or Navy NP-3D personnel existed during these local training exercises. In the first training mission scenario, the EFT-1 launch and recovery mission proceeded without anomalies, allowing the NESC assessment operations team to practice the critical MEP time-lined events, communications, and notifications.

The second simulation was performed with the NESC operations team responding to a launch delay. After the anomaly was resolved and the Delta IV Heavy launched, the capsule encountered an issue in orbit necessitating a potential capsule recovery downrange of the planned site. At that critical decision point in the training exercise, the assessment team MC became incapacitated for the remainder of the mission. This required the other team members to change their roles and responsibilities and continue to work through the series of contingency plans (see Appendix D) developed after JIS 1b and carry on the interface with the EFT-1 flight controllers. This internal exercise exposed the team members to cross training and was useful in identifying and working out issues with the MEP mission timelines and protocols.

Observation of SpaceX Flight Test

An observation campaign in 2014 by the SCIFLI team provided several opportunities for mission operations training under the conditions and demands of an observation. The Propulsive Descent Technologies Project managed by the Game Changing Development Office/Space Technology Mission Directorate had a requirement to obtain spatially resolved thermal imagery of the SpaceX Falcon 9 first stage as it conducted a Supersonic Retro-Propulsion flight maneuver during a flight test to demonstrate recovery techniques. The SCIFLI team supported three observation attempts during 2014 to collect the desired thermal imagery. The successful observation in September 2014, summarized in Figure 6.3.8.3-2, highlights the use of the tools and infrastructure that would be utilized approximately 3 months later during EFT-1 mission operations. The details of the observation are not reported herein, but the multiple deployments by the SCIFLI team to support the imaging served as a training opportunity under the demanding conditions of an observation. While the SpaceX campaign was instrumental in mitigating risk with the EFT-1 observation, the nearly concurrent observation schedules created scheduling demands on and workload challenges for the NESC team. Through careful schedule management, the SpaceX observation enabled a new forecast capability with the JHU-APL CFLOS cloud prediction tool to anticipate the presence of unfavorable viewing conditions (see Section 6.3.5), and increased the overall readiness of the EFT-1 operations team. Coordinated by SCIFLI, the first use of the NASA WB-57 for calibrated infrared imaging positioned the aircraft and crew as a viable backup asset during the EFT-1 observation.

	<h1 style="text-align: center;">NASA Engineering and Safety Center Technical Assessment Report</h1>	Document #: NESC-RP-12-00795	Version: 1.0
Title: Remote Imaging of EFT-1 Entry Heating Risk Reduction			Page #: 51 of 98

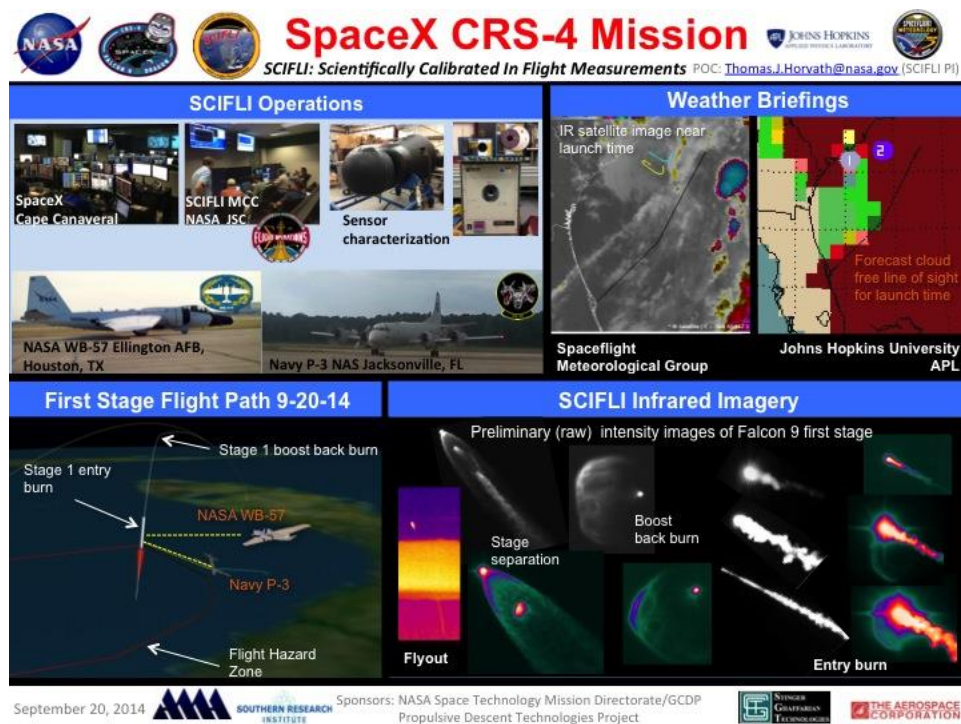



Figure 6.3.8.3-2. SCIFLI Observation of a Flight Test Associated with the SpaceX Falcon 9 First Stage Recovery

JIS 4

JIS 2 and 3 focused on only post-splashdown recovery procedures, and the NESC team was not involved. Several weeks before the EFT-1 launch in December 2014, the JIS 4 training exercise was held. The NESC assessment mission operations team deployed to the IPOC, entering this simulation with a series of finalized procedures and documents. Additions made from prior training exercises included the detailed contingency list, the use of the MCC Electronic Flight Notes to provide aircraft updates, the use of two weather forecasting models to predict cloud conditions, and the inclusion of the NASA Ikhana UAV into the mission operation. The training exercise revealed discrepancies in the weather forecasts that led to the realization data in one of the models not being input correctly. The issue was resolved post training exercise. During this simulation, the assessment team did not directly receive green “anomaly” cards, and the MPCV Program capsule remained on course and on time for a recovery off the California coast. While in orbit, an anomaly associated with the DFI batteries was identified. The NESC team technical lead participating in the exercise suggested the possibility of repositioning the Navy NP-3D peak heating aircraft in the event of battery failure and loss of DFI instrumentation. The battery issue was resolved and the Navy NP-3D remained at its designated observation location. The real-time simulation, which began at T-minus 6 hours and continued past splashdown, resulted in a 12-hour exercise that solidified the mission planning and provided confidence for the mission operations.

	NASA Engineering and Safety Center Technical Assessment Report	Document #: NESC-RP- 12-00795	Version: 1.0
Title:	Remote Imaging of EFT-1 Entry Heating Risk Reduction		Page #: 52 of 98

6.3.8.4 Aircraft Flight Dress Rehearsals

Dress rehearsals with the aircraft, the crew, and the sensor operators are an important part of the training and risk mitigation process. When an aerial asset becomes involved, it provides the mission operations team, flight crew, and instrument operators the opportunity to rehearse procedures and become familiar with timing cues used during the mission. Mission day operations will be conducted during the flight simulation in accordance with the MEP where events, communications calls, and decisions are scripted. A dress rehearsal flight is generally performed 2 or 3 days prior to an imaging mission. The specific flight training exercise for EFT-1 will be reviewed in Section 7.1.

Prior to EFT-1 launch, the MPCV Program made the decision the Navy NP-3Ds (i.e., BH-300 and BH-340) would not be requested to transit into foreign airspace. Therefore, exercising the processes of obtaining foreign airspace requests with the appropriate airspace controllers would not be required. During a dress rehearsal, each asset generally simulates an observation and data capture with a virtual target. The health of the aircraft, instrumentation, and associated hardware/software were assessed and performance verified. During the flight dress rehearsal, the camera operator coordinates with the pilot and aircrew to perform timed maneuvers in a pre-determined precision racetrack-like pattern to position the aircraft and its gimballed mirrors for the data acquisition.

The aircraft communication systems are verified through a full check with HF radio and Iridium-based satellite phones. The HF communications are generally provided by Cape Radio, an element of the U.S. Air Force Eastern Test Range located at Cape Canaveral. Cape Radio has access to a worldwide network of HF transmitters and receivers, and works interactively with the aircrews to switch between HF radio ground stations and frequencies that would provide the optimal communications at any given time.


Space weather is provided to the squadron to determine whether unusual Sun activity may inhibit HF radio communication. During the dress rehearsal flight, the aircraft will call the IPOC via Iridium phone at regular intervals. Real-time test event calls will be given in accordance with the Cast Glance and MEP mission script and timelines. Status reports will be generated from the IPOC, then relayed to both aircraft. Time to EFT-1 launch will be provided to the aircraft crew. Once launch occurs, a splashdown time will be calculated and provided to aircrew. Cast Glance will synchronize all subsequent events to that time.

6.3.8.5 Logistics of Additional Assets

Can the NESC operations team handle the additional workload associated with management of a second (MPCV-sponsored) Navy NP-3D and a NASA Ikhana UAV?

Risk: Given the initial six of the NESC operations team, there is the possibility that inadequate staff can be provided to reliably and effectively support the use of additional aerial assets desired by FTMO.

Risk Context: The SpaceX observation campaign supported by the SCIFLI team required the management of multiple aircraft. Based upon a survey of the team post mission, a lesson learned

	NASA Engineering and Safety Center Technical Assessment Report	Document #: NESC-RP- 12-00795	Version: 1.0
Title:	Remote Imaging of EFT-1 Entry Heating Risk Reduction		Page #: 53 of 98

was adequate mission operations team staffing was essential to provide reliable and effective support.


Assessment and Mitigations: Early in the assessment process, the NESC team was asked by the MPCV Program FTMO to coordinate pre-flight logistical planning and communications with a second Navy NP-3D on the day of launch. This aircraft (BH-340) was tasked to provide photo-documentation of critical events associated with the late-stage recovery process (e.g., capsule forward bay cover jettison, drogue chute deployment, parachute reefing and inflation, and if the recovery was off nominal, marking of the final splash coordinates). The implications of this requirement and aircraft priority were discussed with the NESC and the NESC operations teams. Because the NESC operations team was to be in place coordinating the BH-300 aircraft with its thermal imaging task, the NESC operations personnel accepted coordination and management responsibilities of this asset. The FTMO provided additional resources to cover the logistical support required of the asset coordinator to assist VX-30 with flight planning and communications with both aircraft on the day of launch. The additional workload and risk were both accepted by NESC Aerosciences TDT lead.

Logistical risk was further escalated when the NASA PAO introduced an Ikhana UAV several months prior to the EFT-1 launch to support a real-time video feed of the splashdown. The NESC operations team was asked to facilitate coordination of the UAV with all other airborne systems in the recovery area (i.e., BH-300, BH-340, and two FTMO-sponsored Navy helicopters). Additional resources were requested from FTMO to permit the NESC assessment team asset coordinator for mission operations to develop and implement air space separation and safety protocols and contingency plans. This was required as Navy leadership expressed reservations concerning the operation of their NP-3Ds and helicopters in close proximity to the NASA UAV operating from Edwards Air Force Base (AFB).

A comprehensive contingency matrix (see Appendix D) was developed to facilitate efficient and timely decisions. A section of the matrix addresses the protocols to maintain safe and efficient operations and communications in the event an off-nominal situation developed. To further mitigate risk, it was requested that a representative from the Ikhana UAV operations team have a physical presence with the NESC operations team at the IPOC during EFT-1 launch and recovery.

7.0 Data Acquisition and Data Analysis

On December 5, 2014, at 7:05 Eastern Standard Time, the EFT-1 capsule was successfully launched by a Delta IV Heavy launch vehicle from Space Launch Complex 37B at Cape Canaveral Air Force Station. The approximately 4.5-hour flight took the MPCV crew capsule on two orbits around the Earth. Peak altitude was approximately 3,130 nmi (5,800 km). The high altitude coupled with an additional propulsive boost from the Delta IV upper stage allowed the spacecraft to reach reentry speeds of 20,000 mi/hr (8.90 km/sec), which exposed the heat shield to temperatures to approximately 4,000 °F (2,477 K). Figures 7.0-1 to 7.0-4 provide a summary of several capsule performance parameters (e.g., altitude, Mach, dynamic pressure, and velocity)

	NASA Engineering and Safety Center Technical Assessment Report	Document #: NESC-RP- 12-00795	Version: 1.0
Title:	Remote Imaging of EFT-1 Entry Heating Risk Reduction		Page #: 54 of 98

as a function of time during reentry starting from EI at 400 kft (121,920 m) to splashdown. The red circle designated “max heating” indicates the approximate time when the capsule heat shield reached its maximum peak heating.

For context, the green colored portion of the plotted time segment indicates the period when the capsule was under observation by the NESC-sponsored Navy NP-3D (BH-300) during reentry. Table 7.0-1 summarizes the times during the observation at which BH-300 had sensor acquisition of signal (AOS) and Loss of Signal (LOS). The span of time between 155.15 and 215.10 sec represents the observation period when quality thermal imagery was collected. As described in Section 7.1, the initial thermal imagery was acquired approximately 40 sec after the peak heating event because of a large weather system producing widespread overcast skies. During this time segment, there was a period of approximately 3 sec where the capsule image was not within the focal plane array. At 215.10 sec, after the capsule had passed by the aircraft, observation was obscured by clouds. The time period between 375.55 and 570.25 sec represents the duration the capsule was reacquired and imaged at extreme range. During this period, the capsule parachute sequence was observed and complemented the information obtained from the BH-340 NP-3D aircraft located in the recovery zone.

The five vertical line segments near 200 sec represent the times where the thermal analysis of the imagery was performed. Section 7.3 will discuss the rationale and basis for selection of these times for subsequent analysis.

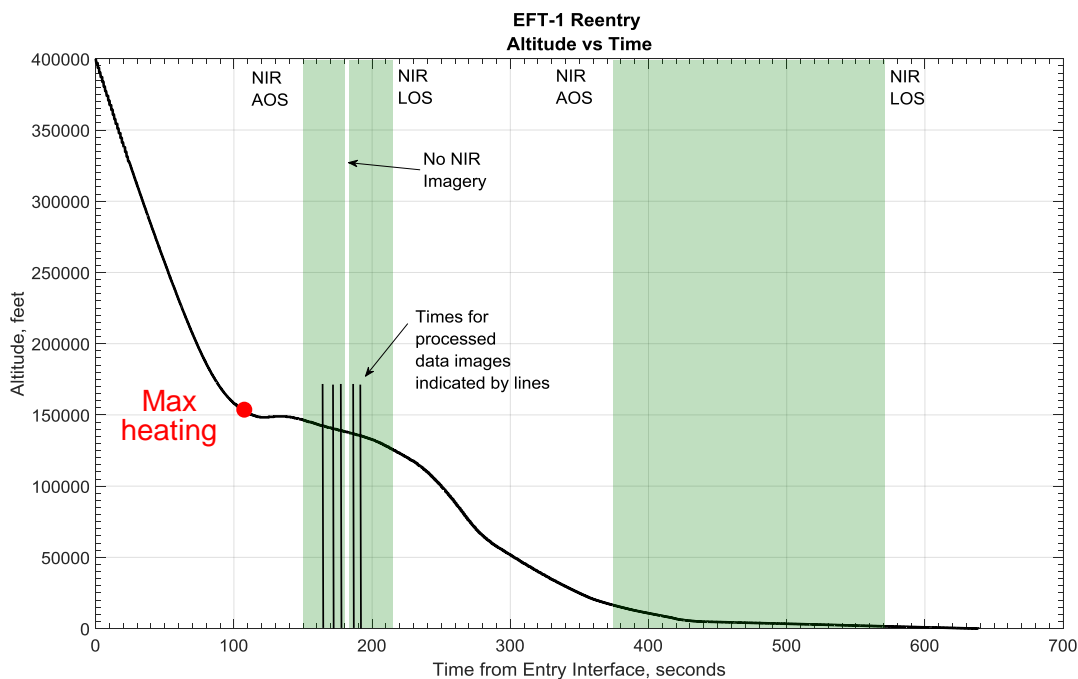



Figure 7.0-1. EFT-1 Altitude as a Function of Time from EI

	NASA Engineering and Safety Center Technical Assessment Report	Document #: NESC-RP- 12-00795	Version: 1.0
Title: Remote Imaging of EFT-1 Entry Heating Risk Reduction			Page #: 55 of 98

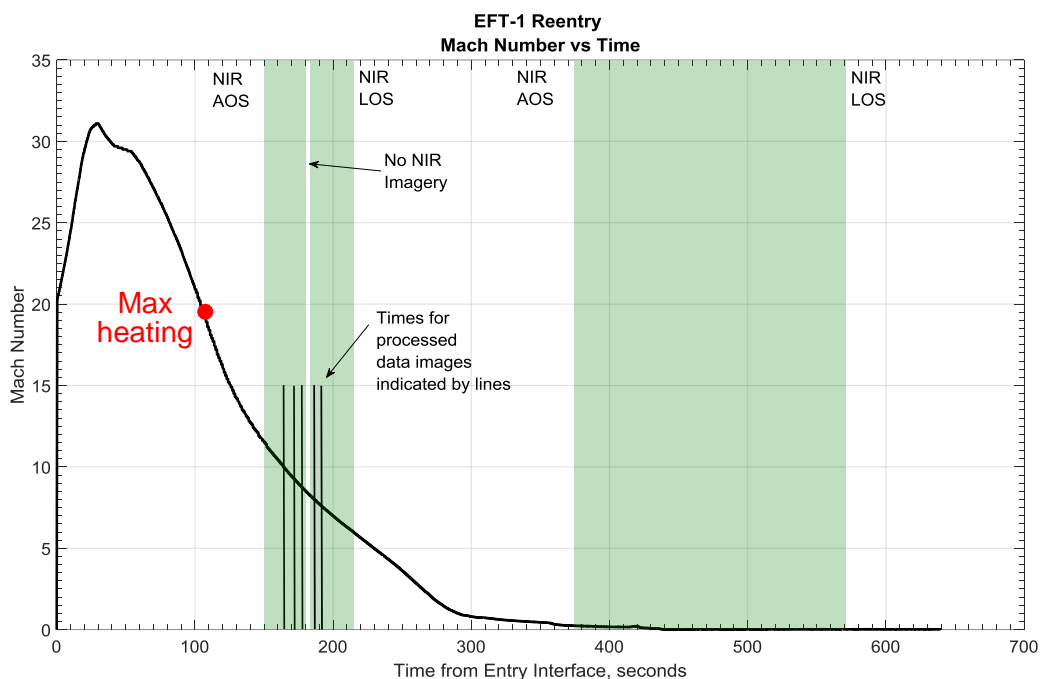


Figure 7.0-2. EFT-1 Mach Number as a Function of Time from EI

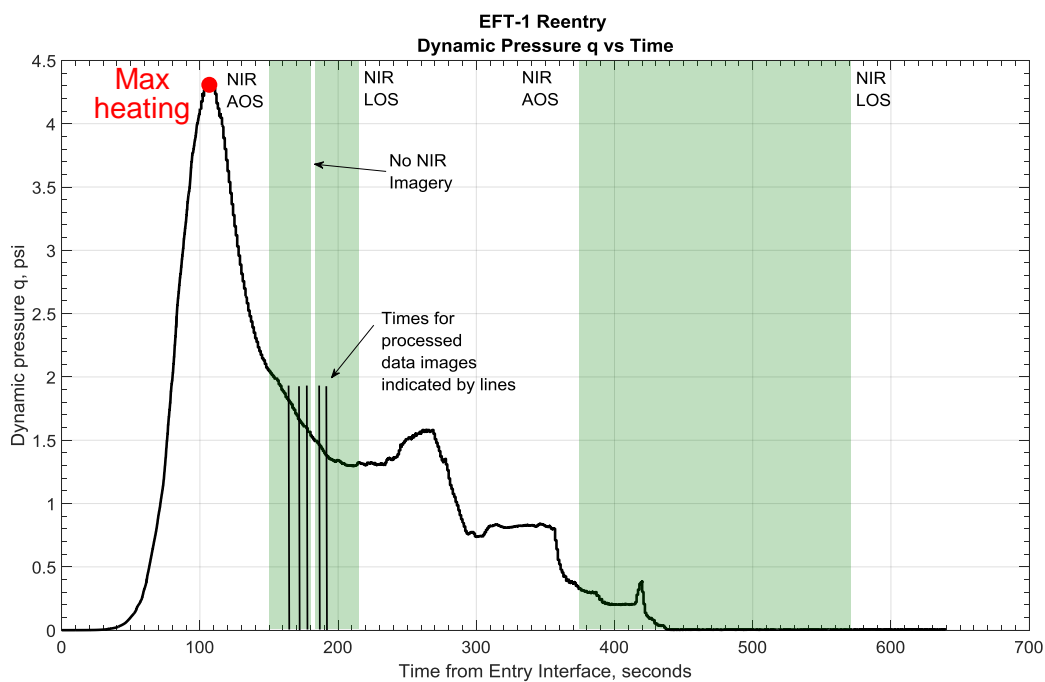


Figure 7.0-3. EFT-1 Dynamic Pressure as a Function of Time from EI

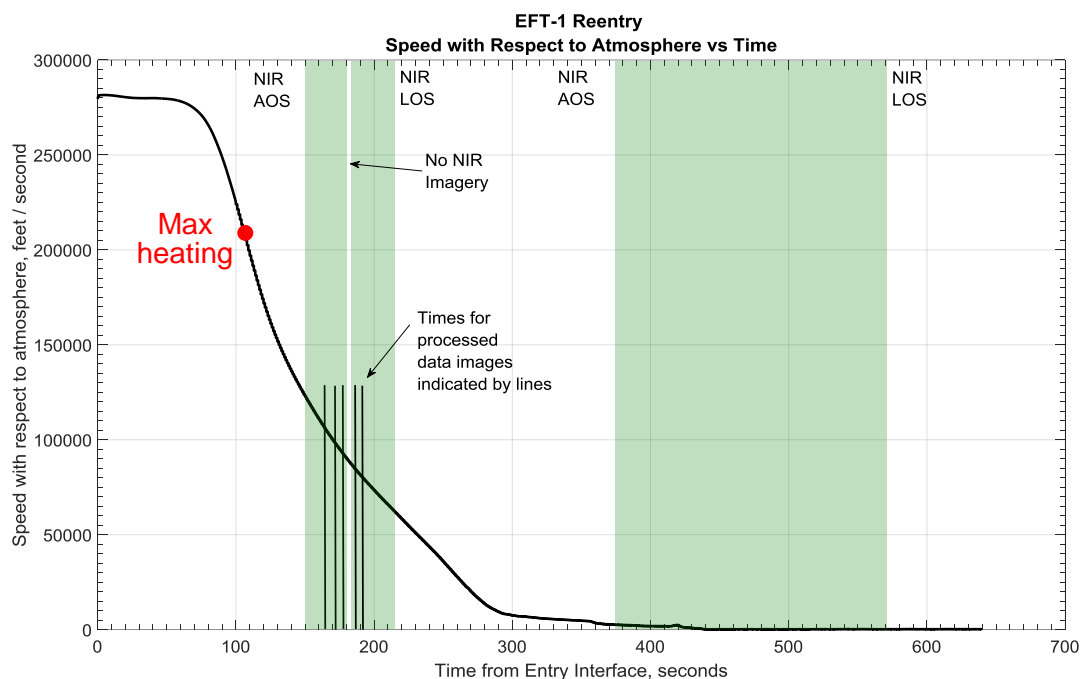


Figure 7.0-4. EFT-1 Velocity as a Function of Time from EI


Table 7.0-1. BH-300 Navy NP-3D Image Acquisition Times during Reentry

	Time from EI (sec)	Coordinated Universal Time (UTC) (hr, min, sec)
AOS	155.15	16:21:19.57
LOS	181.63	16:21:46.42
AOS	184.52	16:21:49.32
LOS	215.10	16:21:19.89
AOS	375.55	16:21:00.35
LOS	570.25	16:21:15.05

Section 7.1 details the chronology of events during the days leading to the observation. Section 7.2 provides a description of how the time stamped imagery was correlated to critical events during the flight test. Section 7.3 documents the process by which individual infrared image frames were selected for analysis, and highlights the processes from which global surface temperature was inferred from the collected infrared intensity measurements.

7.1 Data Collection during EFT-1 Thermal Observation

This section describes the general chronology of events during the thermal observation campaign conducted by the NESC assessment mission operations team. Where appropriate, operations associated with the FTMO sponsored aircraft (BH-340 NP-3D and two Navy helicopters) and NASA PAO-sponsored Ikhana UAV are mentioned, but the reader is referred to reference 33 for more details on the imagery obtained with these aerial platforms.

	<h1 style="text-align: center;">NASA Engineering and Safety Center Technical Assessment Report</h1>	Document #: NESC-RP- 12-00795	Version: 1.0
Title:	Remote Imaging of EFT-1 Entry Heating Risk Reduction		Page #: 57 of 98


In early November of 2014, a delta Critical Mission Review (CMR) was held to review risks and status the readiness of the NESC assessment team to proceed with the observation campaign. The participants included representatives from JSC FTMO, assessment stakeholders, the NESC, and the primary and backup aircraft organizations. No outstanding hardware and software issues were identified. A review of sensor configuration recommendations based upon JHU-APL radiance modeling was made with no changes identified. The risk associated with a Navy NP-3D aircraft schedule conflict was re-evaluated and characterized as low. To protect in the event of a mechanical failure of one or both of the Navy NP-3Ds, the NESC approved the forward deployment of the NASA WB-57 to March AFB in southern California in advance of the EFT-1 launch. The WB-57 aircraft and its crew would remain on standby at its home base at Ellington Air Field ready to transit to March AFB in the event the aircraft mechanical risk matured. The Navy continued to evaluate protocols for safe operations of the BH-340 NP-3D for descent imaging in the presence of the NASA Ikhana UAV. Dialogue between the AFRC personnel and Navy leadership was facilitated by the NESC operations team Asset Coordinator (AC). At the conclusion of the delta CMR, the NESC team was polled and it was determined that deployment to JSC for missions operations would commence on November 30, 2014.

Between November 30 and December 1, 2014, the NESC assessment operations team reported to their respective duty stations. The NESC operations team Calibration Coordinator (CC) departed for the Point Mugu Naval Air Station NP-3D home base to support advanced calibration logistics and acquisition of the calibration data, and to collect, duplicate, and disseminate the imaging data. The CC is shown in Figure 7.1-1 delivering the blackbodies used for calibration of the infrared sensor on the Navy NP-3D several days in advance of the EFT-1 launch.



Figure 7.1-1. High-Temperature NASA Blackbodies Used to Calibrate the Cast Glance Sensors Delivered to the Navy Base at Point Mugu, California

The MC arrived at JSC in advance of the NESC operations team to configure the console stations in the IPOC. An image of the IPOC control room with the assessment operations team at their

	NASA Engineering and Safety Center Technical Assessment Report	Document #: NESC-RP- 12-00795	Version: 1.0
Title:	Remote Imaging of EFT-1 Entry Heating Risk Reduction		Page #: 58 of 98

duty stations is shown in Figure 7.1-2. Live weather updates from SMG and EFT-1 flight information were fed to the display monitors.

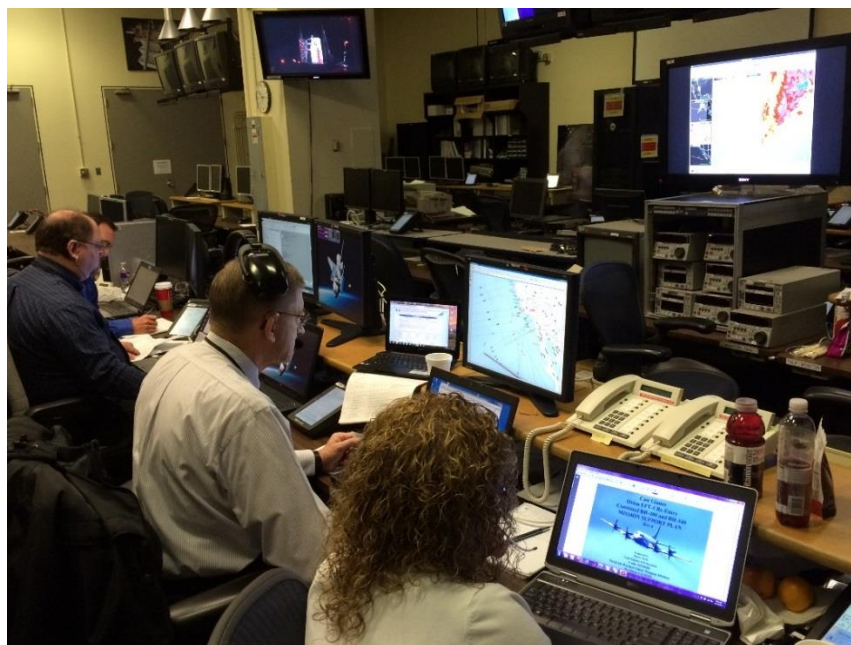



Figure 7.1-2. Assessment Mission Operations Team on Console at the JSC IPOC for the EFT-1 Observation (from left to right; MC, AC, and Mission Manager)

December 1, 2014: Three days before a scheduled December 4 EFT-1 launch the mission operations team assembled in IPOC for the dress rehearsal flights with of the Navy NP-3D aircraft. Both aircraft were to depart from their home base with the NESC-sponsored BH-300 NP-3D taking off after a simulated EFT-1 launch confirmation. The plan during the launch was to hold the descent imaging NP-3D BH-340 on the ground until confirmation that BH-300 was successfully airborne. In contrast to the EFT-1 mission, the aircraft were not required to transit to the planned observation location. For the rehearsal flights, the aircraft were to perform their suite of timing and optical tracking maneuvers using a virtual target. As such, the maneuvers were to be performed over water off the coast of their home base. The aircraft call signs were to be designated by their military designations BH-300 and BH-340 with flight plans filed with the Federal Aviation Administration (FAA) used their corresponding civilian designations as NASA 500 and NASA 501 to permit following the flight of these aircraft on <http://flightaware.com/>.

Weather for the check-out flights was favorable. During dress rehearsal pre-flight checks, a cracked propeller was identified on BH-340. To protect the schedule and provide the necessary proficiency flight opportunity to the respective crews and sensor operators, it was decided to perform both dress rehearsal procedures on BH-300. This was accomplished by flying both flight and sensor crews on this aircraft and running through their respective flight plans in a serial fashion. The LSO coordinated HF radio communication with the BH-300 via Cape Radio. All alternate forms of communication were exercised (i.e., Iridium SatPhone, Global Positioning System tracker) and were successfully demonstrated. A mock countdown was held, with verbal

	NASA Engineering and Safety Center Technical Assessment Report	Document #: NESC-RP- 12-00795	Version: 1.0
Title:	Remote Imaging of EFT-1 Entry Heating Risk Reduction		Page #: 59 of 98


updates sent to the aircraft. The Navy NP-3D crews practiced their respective racetrack patterns to be flown during the EFT-1 observation, working to position the aircraft at the desired location when the capsule would encounter EI. The exercises went without incident, and the BH-300 had an uneventful return to base.

Later that evening, sensor calibrations were performed on BH-300 NIR and MWIR sensors at Point Mugu Naval Air Station, California. The calibration was moved up a day from its originally scheduled time as adverse weather was predicted. Evening calibrations were desired to minimize the effects of solar illumination/scattering. In addition, the suspension of particulates in the atmosphere is generally less than found during the day when local winds at ground level are higher. During the calibration data acquisition process, ambient air temperature and relative humidity were recorded for later use in the calibration data analysis. The atmospheric measurements are used as inputs for MODTRAN® to generate the atmospheric spectral transmittance at the time the calibration data were recorded.

To calibrate the infrared systems, two blackbodies were setup at approximately 500 ft (152 m) from the Cast Glance aircraft observation window. The cameras were pointed such that the blackbodies were near the center of the FOV, and each camera was adjusted so that both blackbodies were in focus. Once the blackbody temperatures were stabilized, a calibration data set was collected. A calibration data set consisted of infrared intensity data captured over the range of anticipated sensor integration times. The blackbody set-point temperatures representative of those expected on the EFT-1 heat shield were adjusted and the process repeated. Using two blackbodies simultaneously reduced the volume of image-based calibration data, and the time required to systematically vary the temperatures of the blackbody sources over the desired range. An image of a white light source used in the determination of the spectral response is shown in Figure 7.1-3. BH-300 with its infrared imaging systems is located on the tarmac out of view. The high-temperature blackbodies are housed in the van.



Figure 7.1-3. Calibration to Determine Spectral Characteristics of BH-300's Infrared Imaging System

	NASA Engineering and Safety Center Technical Assessment Report	Document #: NESC-RP- 12-00795	Version: 1.0
Title:	Remote Imaging of EFT-1 Entry Heating Risk Reduction		Page #: 60 of 98

All calibration data were post-processed using MATLAB® and Microsoft® Excel®. The preliminary sensor calibration data determined no significant changes to the infrared camera responses had occurred. A detailed description of the calibration data collection process, the hardware used, and the subsequent analysis to convert measured infrared intensity counts to in-band radiance values and temperature is documented in Appendix E.


The situation involving the cracked propeller on BH-340 activated a contingency plan where the NASA WB-57 crew was put on alert in the event the mechanical issue was not resolved. At the time the calibration was concluded on December 1, 2014, the maintenance crew for BH-340 reported the defective propeller had been successfully removed and a spare located. Installation was to occur the next day.

The long-range weather forecasts at Point Mugu Naval Air Station, California and the observation locations off the coast of San Diego began to converge and suggested clouds at the observation locations could become problematic. Local conditions at Point Mugu were expected to deteriorate and potentially threaten the required check-out flight on the BH-340 following propeller replacement. Weather conditions were expected to continue to be dynamic over the following days.

December 2, 2014: The BH-340 propeller was successfully replaced and low revolutions per minute testing indicated a successful installation. A required check flight was scheduled for December 3, 2014. Communications with the NASA WB-57 crew continued and the weather situation regarding the BH-340 check flight was monitored. If the check flight could not be completed or resulted in the grounding of BH-300, then the contingency plan involving the forward deployment of the NASA WB-57 would be activated. The contingency plan called for the BH-300 to be re-tasked to provide the parachute and recovery image documentation. The NASA WB-57 would be forward deployed to March AFB and utilized for the NESC-sponsored thermal observation.

A Flight Readiness Review (FRR), led by the NESC operation team AC, was held with the Navy. In this briefing, the status of the launch was provided (green) and the science/engineering objectives were reviewed with the crew. All assets (BH-300, Ikhana UAV, and Navy helicopters) were “go” with the exception of BH-340. In the event BH-340 was not available, a delta FRR operations brief would be held with the NASA WB-57 flight crew on December 3, 2014. The expected delivery timelines of EFT-1 reentry trajectory updates were presented and how they would be communicated to the crew was reviewed. The NESC team reported a successful rehearsal flight the previous day. Contingency plans were reviewed with a special emphasis on BH-300 NP-3D being re-tasked to provide descent imaging. Hazard zone boundaries and protocols pertaining to a capsule break up or an abnormal propulsive burn of the Delta IV upper stage prior to capsule separation were highlighted. Flight planning for the UAV included compliance with additional airspace restrictions associated with transiting the UAV through the National Airspace System.

Noteworthy during the FRR was concurrence by Navy leadership regarding operation of BH-340 in proximity to the Ikhana UAV. Flight plans for transiting to the observation location and

	NASA Engineering and Safety Center Technical Assessment Report	Document #: NESC-RP- 12-00795	Version: 1.0
Title:	Remote Imaging of EFT-1 Entry Heating Risk Reduction		Page #: 61 of 98

subsequent loitering developed for the BH-300 and BH-340 aircraft were reviewed with details of the airspace separation plan articulated. To satisfy safety concerns, a plan to provide positive altitude separation of at least 2,000 ft between the BH-340 aircraft and the Ikhana was required at all times for safe operations. Negotiations continued up until the FRR before Navy leadership was satisfied all safety concerns were addressed. A latitude-based “line of no transgression” was established (see Figure 7.1-4) and protocols were determined for the safe exit of the Ikhana UAV should the BH-340 be required to reposition within the UAV area of operations.

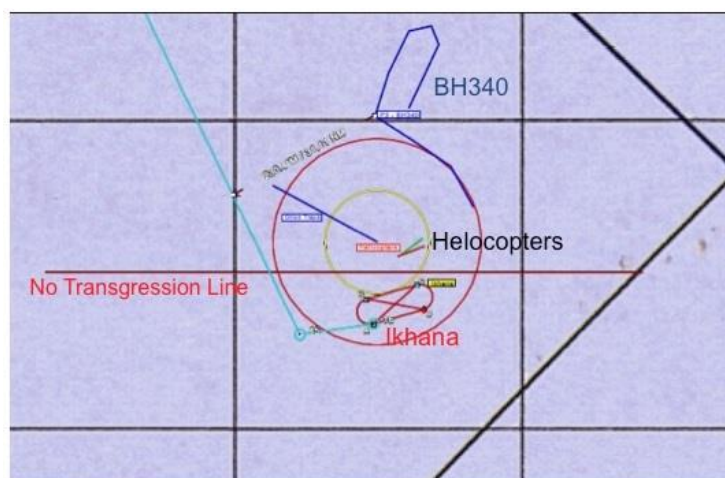



Figure 7.1-4. Locations of Descent Imaging Aircraft (BH-340) and NASA Ikhana UAV Relative to a Latitude-Based Line of No Transgression

Launch weather at the Cape Canaveral Air Force Station continued to look favorable with concerns noted that flight through precipitation and ground winds at lift off could become an issue. Forecasted weather at the recovery site indicated precipitation and considerable cloudiness at the splashdown location on December 4. Local weather at the planned observation location several hundred nmi up-range, indicated favorable viewing with scattered broken clouds below the nominal BH-300 25,000 ft operating altitude. At this point in time (i.e., 2 days before launch), the SMG and JHU-APL weather forecasting tools suggested unfavorable viewing conditions at the peak heating observation location should the launch slip by 24 hours. As such, the NESC operations team began discussion alternate locations for imaging.

December 3, 2014: Despite marginal weather conditions at the Point Mugu Naval Air Station, the BH-340 check flight was successfully completed approximately 24 hours from EFT-1 launch and the aircraft list as “green.” While no longer necessary, forward deploying the NASA WB-57 to March AFB would mitigate the risk associated with a mechanical failure with one or both Navy NP-3D aircraft in the hours before EFT-1 launch. Loss of either aircraft from this point forward would prevent thermal imaging. The option to forward deploy the WB-57 was presented to the NESC and the FTMO, but was not accepted. The WB-57 was stood down as a backup aircraft and it remained at Ellington Air Field in Texas.

	NASA Engineering and Safety Center Technical Assessment Report	Document #: NESC-RP- 12-00795	Version: 1.0
Title:	Remote Imaging of EFT-1 Entry Heating Risk Reduction		Page #: 62 of 98

December 3, 2014, was a mandated day of rest for the imaging crews, so communication between the operation team and the squadron was minimal. No additional information regarding trajectory updates was anticipated or received.


The weather prognosis for a December 4, 2014, launch at the Cape Canaveral Air Force Station remained favorable with some concerns of ground wind violations. In the recovery area, precipitation and considerable cloudiness was expected in and around the splashdown area on December 3, 2014. Sprinkles or virga (i.e., rain not hitting the ground) was expected to move through the projected splashdown area 2 to 6 hours prior to launch making capsule observations around the time of final descent challenging. All guidance at this time indicated improving sky and weather conditions at the recovery site as the morning progressed on December 4, 2014. Observation conditions at the planned peak heating location continued to look favorable with a scattered low and high clouds expected in the general area.

If the EFT-1 launch was unsuccessful on the morning of December 4, 2014, then the forecast for December 5, 2014, at the peak heating observation area around the time of the recovery window called for an increase in the presence of high, thick obscuring clouds. This prediction was supported with the CFLOS tool. In contrast, the weather at the local splashdown location showed significant improvement with broken scattered clouds and no precipitation or lightning forecast.

December 4, 2014: As per pre-defined timelines, a majority of the assessment operations team arrived on console in IPOC at 2:30 a.m. Central Daylight Time (CDT). Sleep shifting was required by select team members to support post-imaging operations (e.g., data transfer) in the event the observation was successful. The entire team was in place several hours before the scheduled launch window opened at 6:05 am CDT. Winds aloft information off the California coast provided by SMG permitted the AC to verify that transit times with each aircraft reaching their respective observation locations to allow them to be held on the ground until confirmation of EFT-1 launch was received. This would avoid aircraft recall due to a launch scrub or delay deep into the launch window. Navy safety protocol dictates a NP-3D cannot land with a full fuel load and the fuel must be expended or discharged. As per mission timelines, the aircraft crews were periodically provided updates on weather along their expected transit routes and at the observation locations.

The local weather at Edwards AFB, where the Ikhana UAV was based, was unacceptable for takeoff, and its departure in advance of the EFT-1 launch time was delayed by several hours. At the Cape Canaveral Air Force Station, the EFT-1 countdown proceeded nominally, but was halted twice due to ground-wind violations. The Ikhana UAV, now airborne, continued toward its planned TSP while the BH-300 and BH-340 NP-3Ds were held on the ground, awaiting EFT-1 launch. Mechanical issues associated with a fuel valve on the Delta IV Heavy ultimately led to a launch scrub with a 24-hour recycle to another attempt. The Ikhana UAV was recalled and returned to base without incident.

Had a launch occurred, the local weather at the desired peak heating observation location was ideal. Based upon satellite thermal imagery, scattered broken clouds were present but estimated

	NASA Engineering and Safety Center Technical Assessment Report	Document #: NESC-RP- 12-00795	Version: 1.0
Title:	Remote Imaging of EFT-1 Entry Heating Risk Reduction		Page #: 63 of 98

to be below the operating altitude of the BH-300 NP-3D. No significant high-altitude cirrus clouds were identified. Figure 7.1-5 shows an infrared image from the Geostationary Operational Environmental Satellite LWIR where the cold cloud tops are indicated in bright white. A significant weather system was present inland of the Baja Peninsula. The next approaching storm system is seen in this image. The clear area in between is the general area where the thermal observation was to have occurred. The remainder of the day was spent monitoring the predicted weather at the Cape Canaveral Air Force Station, the staging locations for the aircraft and the planned observation sites. Unfortunately, the prognosis for a clear line of site for thermal imaging on December 5 was poor.

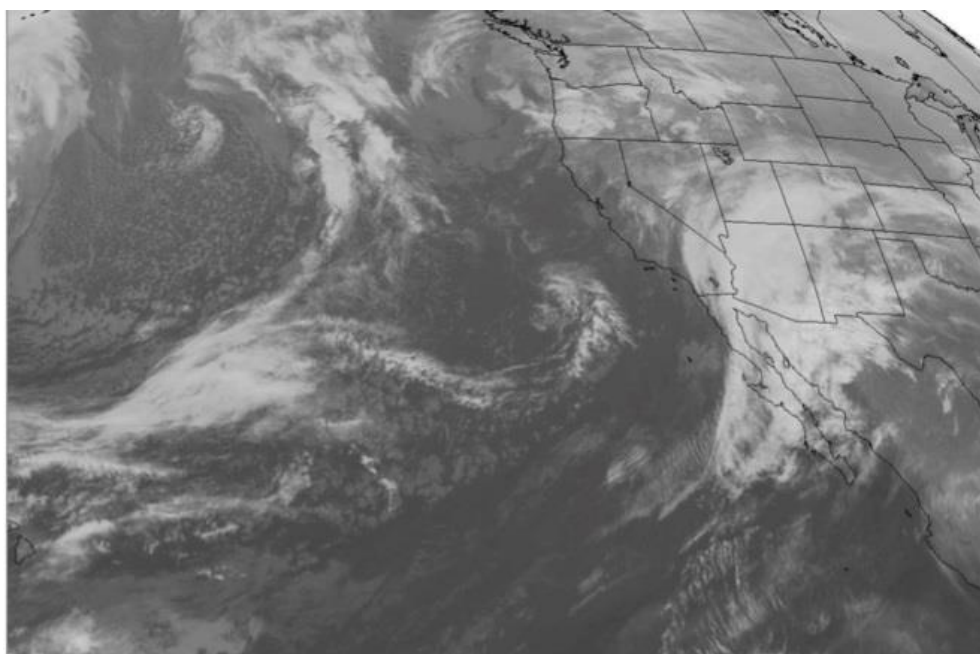



Figure 7.1-5. December 4, 2014 Satellite Imagery off California Coast at Time of Expected MPCV Capsule Recovery (Had Launch Been Successful)

December 5, 2014: The hardware issue associated with a valve on the Delta IV booster was resolved overnight and the decision to proceed toward launch was made by the Launch Flight Director. As per pre-defined timelines, a majority of the NESC assessment mission operations team arrived on console in IPOC at 2:30 a.m. CDT. The entire team was in place several hours before the scheduled launch window that opened at 6:05 am CDT. Winds aloft information off the coast of California provided by SMG permitted the AC to verify that transit times with each aircraft reaching their respective observation locations would permit them to be held on the ground until confirmation of EFT-1 launch was received. As expected, the prognosis for acceptable viewing weather at the thermal observation location was poor. Periodic updates from SMG and JHU-APL reconfirmed the forecast as the launch count preceded forward. Figures 7.1-6 and 7.1-7 provide a graphic-based CFLOS forecast for viewing conditions at the peak heating observation location (designated #1) and the descent observation location (designated #2). In Figure 7.1-6, the colors signify the percentage within any particular cell ($\sim 30 \times 30$ nmi)

	<h1 style="text-align: center;">NASA Engineering and Safety Center</h1> <h2 style="text-align: center;">Technical Assessment Report</h2>	Document #: NESC-RP-12-00795	Version: 1.0
Title:	Remote Imaging of EFT-1 Entry Heating Risk Reduction		
			Page #: 64 of 98

that clouds will prevent a line of site from the Navy NP-3D to the capsule when looking up from 25,000 ft. Poor, if not impossible, viewing conditions were expected at the desired thermal observation location (#1).

The forecast indicated that at the time of reentry, no viable imaging location would allow BH-300 to obtain the desired thermal imagery at the point of maximum heat shield surface temperature. Forecasts from the SMG were consistent with the CFLOS (i.e., in the area where the peak heating observation was to occur, high cirrus appeared to be widespread and uniformly overcast). The satellite imagery confirmed the presence of a widespread cirrus cloud deck. The CFLOS trends indicated acceptable viewing conditions could be located by flying east, further down the ground track toward the recovery sight. This information was relayed to the BH-300 flight crew. The BH-340 stationed in the recovery zone was advised that finding an acceptable up looking viewing location from an altitude of 25,000 ft during their long-range acquisition phase, while challenging, appeared possible.

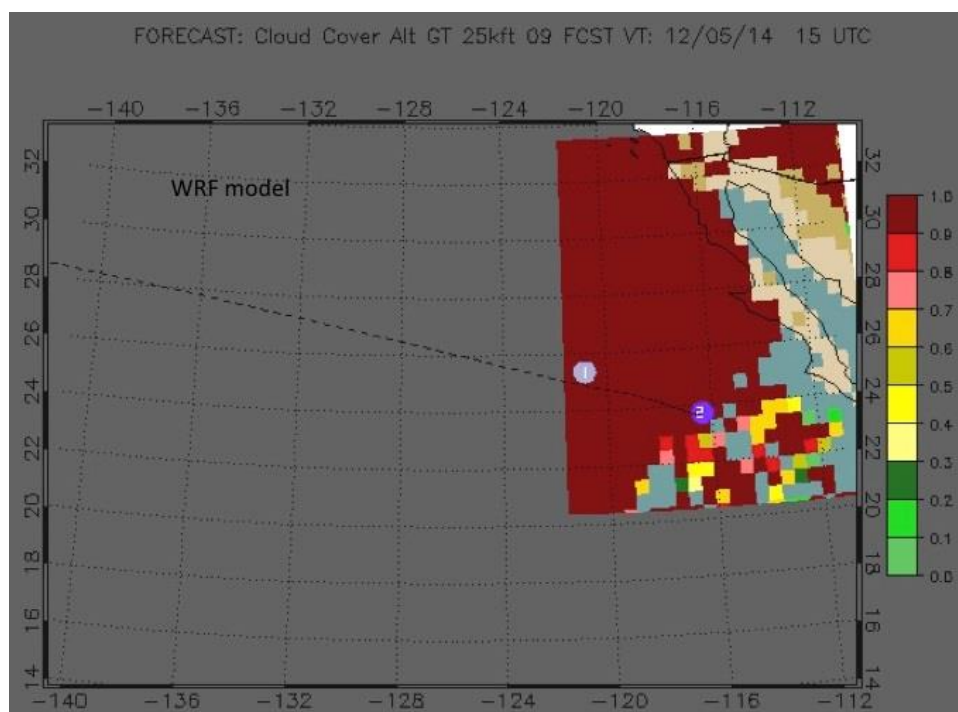



Figure 7.1-6. Forecasted CFLOS for Observer Looking up from 25,000 ft

In Figure 7.1-7, the colors in the CFLOS graphic signify the percentage within any particular cell (~30 × 30 nmi) that clouds will prevent a line of site from the BH-300 NP-3D to the capsule when looking down from an altitude of 25,000 ft. Naturally, the information in this CFLOS forecast is only relevant to the BH-340. The information suggested that if long-range acquisition of the capsule was successful and tracking maintained, acceptable viewing conditions through broken and scattered clouds would likely permit the BH-340 to capture the desired parachute deployment sequence. Acceptable viewing conditions were predicted at the recovery observation location (#2).

	NASA Engineering and Safety Center Technical Assessment Report	Document #: NESC-RP- 12-00795	Version: 1.0
Title:	Remote Imaging of EFT-1 Entry Heating Risk Reduction		Page #: 65 of 98

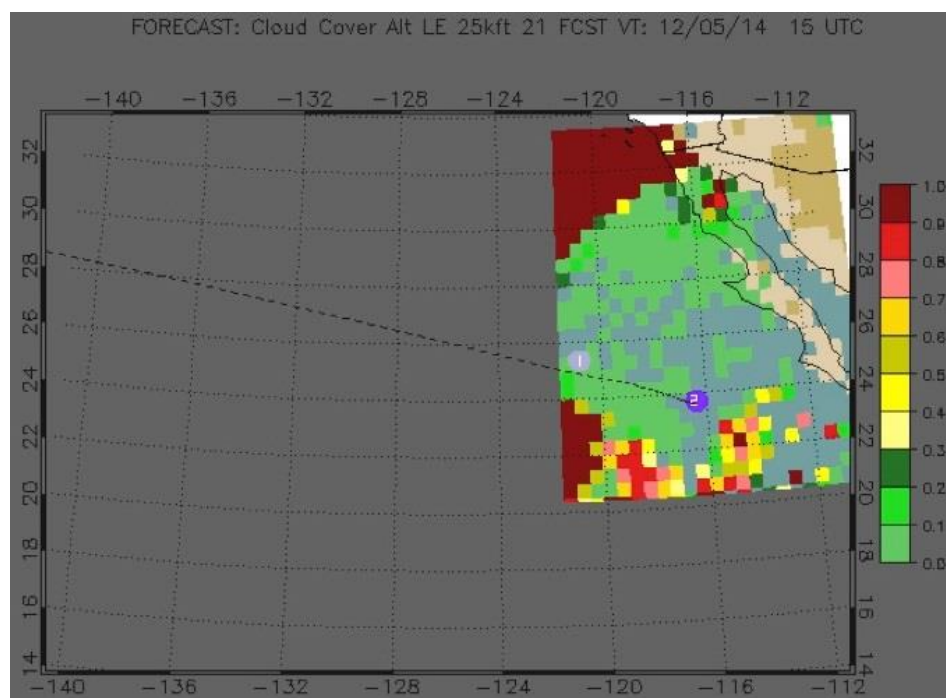



Figure 7.1-7. Forecasted CFLOS for an Observer Looking down from 25,000 ft

In contrast to the first launch attempt on December 4, 2014, the countdown proceeded nominally with no violations or mechanical issue being reported. The Ikhana UAV successfully took off from Edwards AFB approximately 2 hours before the scheduled EFT-1 launch and began transit to its planned observation location south of the anticipated capsule splashdown location. About that same time, the Navy NP-3D flight crews began their preflight briefings. Flight plans were filed with the FAA and no issues with the aircraft were reported. Forecasted weather conditions were relayed to the flight crews by the NESC assessment operations team MC. Approximately 30 minutes before EFT-1 launch, the BH-300 and BH-340 engines were started and the respective crews reported all conditions were green. This information was relayed to the EFT-1 Launch Director in preparation for final polling to proceed with launch. The EFT-1 countdown entered its terminal phase with no issues encountered. Liftoff occurred at the designated time at the beginning of the launch window. With a successful launch confirmation, the MC provided authorization for the aircraft to depart. BH-300 reported wheels up approximately 10 minutes after EFT-1 liftoff with BH-340 following 5 minutes later. Both aircraft proceeded to their designated observation locations to begin scouting the local weather conditions. HF and SatPhone communications were established without difficulty.

BH-340 arrived at its designated TSP approximately 2.5 hours prior to anticipated capsule recovery. BH-300 arrived at its designated observation location approximately 15 minutes later. BH-340 reported broken scattered clouds at the recovery site and remained in the area. As anticipated, the BH-300 reported solid overcast conditions at their desired observation location and began to search for an alternative viewing location. The crew began transiting east toward


	<h1 style="text-align: center;">NASA Engineering and Safety Center</h1> <h2 style="text-align: center;">Technical Assessment Report</h2>	Document #: NESC-RP-12-00795	Version: 1.0
Title:	Remote Imaging of EFT-1 Entry Heating Risk Reduction		
			Page #: 66 of 98

the recovery zone along the EFT-1 ground track, searching for a viable imaging location. SMG and JHU-APL continued to advise that a more probable imaging location with marginal, but acceptable viewing could potentially be found in this easterly direction.

The EFT-1 flight test proceeded nominally. The final deorbit burn of the Delta IV upper stage sending the capsule toward reentry was successful. Aircraft contingencies associated with an off-nominal upper-stage burn were not required. However, the MC continued to monitor the EFT-1 flight in the event of a capsule breakup. Real-time satellite information from SMG suggested breaks in the cloud deck along the transit path of BH-300 180 nmi from its originally planned location. This information was relayed to the crew. Several minutes before EI, BH-300 reported a hole in the clouds in that general area. Monitoring the cabin internal pressure to ensure it was held to a pressure altitude of 10,000 ft or less, the flight crew increased altitude to 33,000 ft in an attempt to get above the clouds and to minimize atmospheric turbulence. The flight crew began to enter into an ad hoc timing pattern to position the optical systems for an observation. This unrehearsed response was only possible because of the crew's skill and expertise, and familiarity with the planned sequence of events. Several minutes after EI, BH-300 reported to the AC the capsule had been successfully acquired with the WFOV SWIR sensor and its sensor operators were actively tracking with the high-spatial-resolution NIR detector. Analysis would later reveal the imagery had been acquired when the capsule was decelerating from approximately Mach 10 to Mach 6. The relative location of the MPCV crew capsule flight path, the originally planned observation location for peak heating at Mach 20 and the location of BH-300 because of the poor viewing conditions is shown in Figure 7.1-8.



Figure 7.1-8. MPCV Crew Capsule Reentry Track and Flight Path of the BH-300 Observation Aircraft (Planned, Yellow; Actual, Green)


	NASA Engineering and Safety Center Technical Assessment Report	Document #: NESC-RP- 12-00795	Version: 1.0
Title:	Remote Imaging of EFT-1 Entry Heating Risk Reduction		Page #: 67 of 98

At nearly the same time, BH-340 reported it was actively tracking the capsule at long range. A few minutes later, the BH-340 provided confirmation to the AC that the parachute deployment sequence had been captured. As viewed from BH-340, the capsule, under chute, dropped below the cloud deck where splashdown was not observed. After the successful observations, both NP-3D aircraft returned to base without incident.

The Ikhana UAV was successful at streaming a live video feed of BH-340 25 nmi distant entering its timing pattern. The UAV sensors acquired the capsule at long range and continued to track the capsule continuously through its parachute deployment sequence. From its more southern viewing location, the capsule, under the three main chutes, was monitored to water impact. The UAV remained on location streaming the recovery operations. The Navy helicopters, flying below 10, 000 ft, monitored the capsule descent through water impact and subsequent recovery operations. The NESC assessment operations team at IPOC stood down after confirmation the NP-3Ds successful landed at their home base, thus removing any airspace separation concerns with the Ikhana UAV. The UAV departed the recovery zone and successfully returned to Edwards AFB.

Several hours after landing back at Point Mugu Naval Air Station, the data hard drives were duplicated and archived. The imagery pertaining to the descent imaging at the recovery zone was provided to the JSC imagery team for analysis. The NESC assessment team was not responsible for analysis of the descent imaging. The hard drive containing the thermal imagery and calibration data was forwarded to JHU-APL for subsequent analysis. The Cast Glance sensor operators provided a quick-look synopsis of the observation with delivery of some selected frames from the unprocessed (raw) NIR intensity imagery. This information was compiled into a slide for general public release 36 hours after landing, Figure 7.1-9. The satellite imagery (upper right quadrant) shows the dynamic and challenging weather the NP-3D flight crews faced. The EFT-1 trajectory and the general location of the repositioned BH-300 were captured in the lower left quadrant. The unprocessed infrared imagery in the lower right quadrant appeared to show the local heating on the heat shield from the compression pads.

The Cast Glance Mission Support Plan (MSP) in Appendix F provides a detailed description of the pre-mission plans, hazard analysis, and planned sensor configurations for both NP-3D imaging aircraft. The companion document, the Cast Glance Final Report and Sensor Operation Notes (see Appendix G), provided 24 hours after the observation, included updated information regarding the “as-flown” flight paths and sensor configurations. Operational notes containing decisional rationale for relocating the BH-300 are included. Samples of the unprocessed imagery are provided in this document.

	<h1>NASA Engineering and Safety Center Technical Assessment Report</h1>	Document #: NESC-RP-12-00795	Version: 1.0
Title: Remote Imaging of EFT-1 Entry Heating Risk Reduction			Page #: 68 of 98

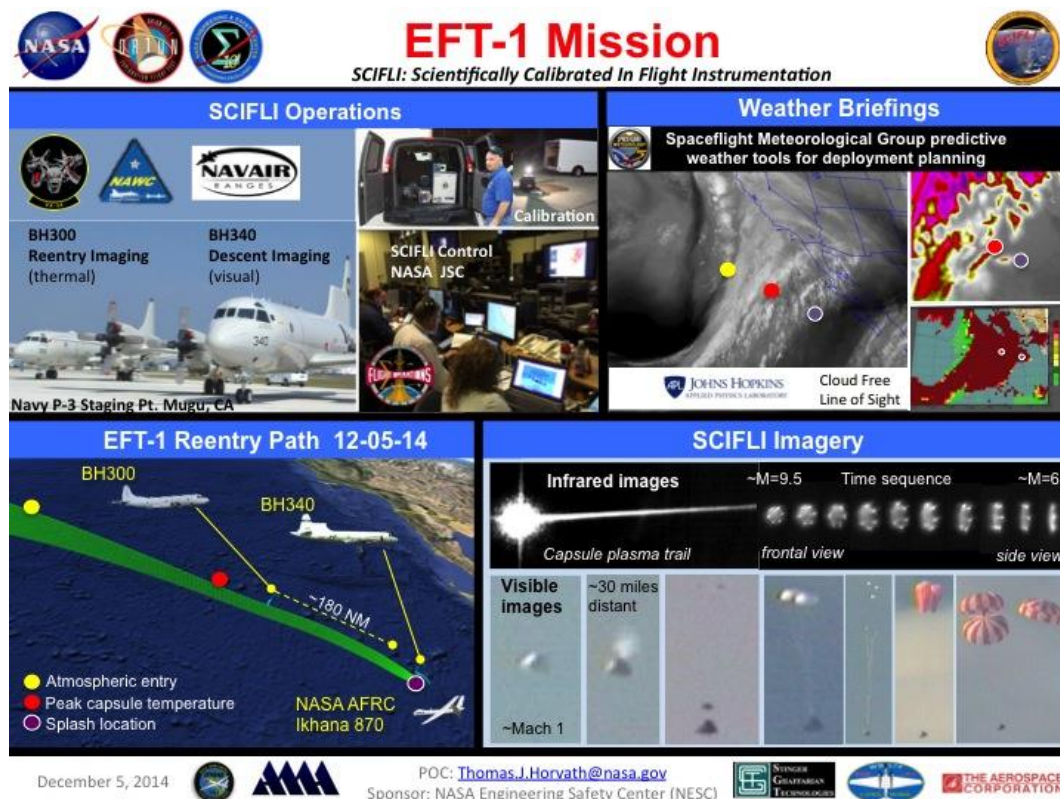



Figure 7.1-9. Synopsis Slide Released to the General Public 24 Hours after Successful Reentry Observations

7.2 Unified Best Estimated Trajectory (BET)

The BET is a data file compiled with information pertaining to EFT-1 performance parameters measured and/or inferred from the flight test. This file was provided to the NESC assessment team and then merged with the BH-300 imaging aircraft data (e.g., position and orientation) and information from the Cast Glance imaging systems (e.g., frame number, exposure times). In its merged form, the file is referred to as the Unified BET (Appendix H). The individual aircraft and sensor data files were parsed and synchronized with reference to UTC and aligned to the nearest EFT-1 flight data time stamp. Placing all of this information into a single organized spreadsheet allowed the engineers and analysts to identify the flight conditions and/or aircraft and sensor parameters for any single frame of observation data. The Unified BET contains descriptive language defining the variable names and units with graphical information on the capsule reference coordinate system.

7.3 Data Processing


Image processing was initially hampered by the fact the the file format of the imagery was not compatible with the analysis software. It was determined that changes to the file format implemented by the Navy were not communicated to the analysis team. The formatting issue

	NASA Engineering and Safety Center Technical Assessment Report	Document #: NESC-RP- 12-00795	Version: 1.0
Title:	Remote Imaging of EFT-1 Entry Heating Risk Reduction		Page #: 69 of 98

was identified and resolved. Six days after the successful observation, the NESC Aerosciences TDT, led by Dr. Schuster, was presented a briefing of the observation and a synopsis of the image quality. It was reported the BH-300 aircraft collected approximately 63 sec of the capsule reentry from ~Mach 13 to Mach 6. This was followed by an additional 195 seconds at subsonic Mach number of the capsule under drogue and main chutes from an extreme range.

Approximately 150 Gb of imagery was recorded with the Cast Glance NIR imager. The initial assessment from the NESC analysis team concluded the operator had managed the sensor configuration effectively during the observation, and that after the initial acquisition little to no saturation existed in the individual frames of thermal imagery. Many “clear” frames free of significant blurring and distortion were found and the six compression pads on the EFT-1 heat shield were distinctly visible. The ability to resolve these features was a testament to the fidelity of the preflight visual and radiance modeling tools. A more extensive review of the calibration data revealed no issues. While the BH-300 aircraft had not obtained the infrared imagery at the desired peak heating point (~Mach 20), the MPCV Program Aerosciences team recommended the quantitative analysis be pursued. A request was made to the NESC and permission granted to move into the optional data analysis phase of the assessment.

This section describes the resulting analysis process. The image processing objective was to first reduce the detrimental effects due to motion (i.e., sensor and capsule), vibration (i.e., jitter), and atmospheric for image quality improvement before performing the conversion of the intensity measurements to engineering units. This image enhancement must be completed without compromising the data quantitative radiometric integrity, especially local intensity (i.e., temperature) variations. First, the approach to selecting the specific time segments during the 63 sec of spatially resolved imagery was outlined. This included the process for selecting and utilizing the highest-quality image frames centered about these times for improving image signal-to-noise. Then, techniques used for improving image quality prior to subsequent thermal analysis were highlighted. Using the preflight calibration data, the process of converting the enhanced infrared intensity images to global surface temperatures was outlined. Figure 7.3-1 summarizes the major steps of this overall process described in Sections 7.3.1 to 7.3.6. The primary data input sources specific to the EFT-1 mission are shown as dashed rectangles with rounded edges, which are calibration data, mission data, weather model data, emissivity estimate, and BET. The solid-lined rectangular boxes show the four main processing areas. Temperature uncertainties will be discussed relative to uncertainties of surface emissivity and atmospheric transmission loss. Comparison of limited onboard surface TC data to the image-derived surface temperature will be presented.

	<h1 style="text-align: center;">NASA Engineering and Safety Center Technical Assessment Report</h1>	Document #: NESC-RP-12-00795	Version: 1.0
Title:	Remote Imaging of EFT-1 Entry Heating Risk Reduction		
			Page #: 70 of 98

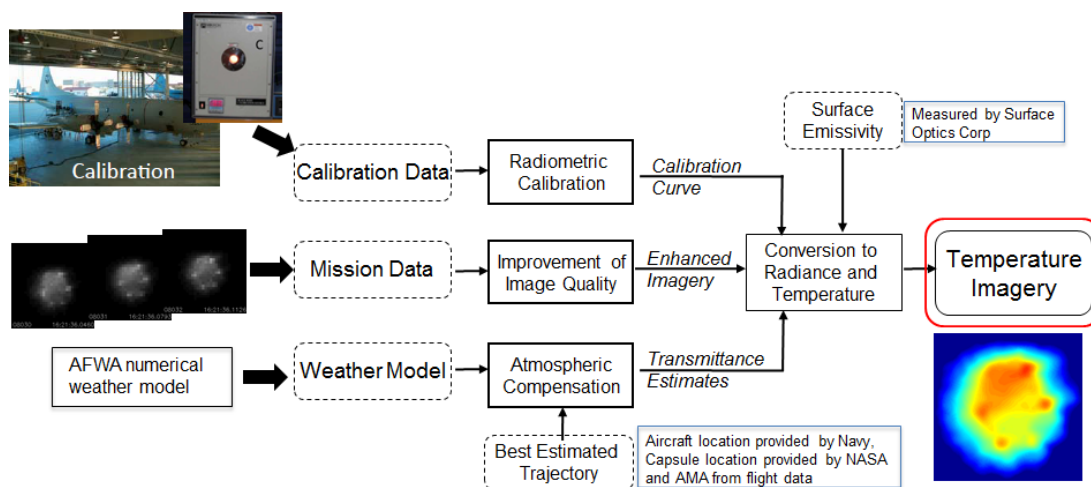



Figure 7.3-1. Summary of Data Sources and Process for Inferring Temperature from Calibrated Imagery

7.3.1 Selection of Time Segments for Processing

Within the 63 sec of total reentry observation time from ~Mach 13 to Mach 6, there were approximately 900 unsaturated NIR image frames to evaluate as the MPCV crew capsule descended from 141,075 to 134,514 ft (43 to 41 km) and decelerated from Mach 9.9 to 7.6. As the capsule was rapidly descending along a parallel path to the observing aircraft, the initial heat shield frontal view progressively transitioned to the expected side-on view at the point of closest approach. Figure 7.3.1-1 provides a sequence of cropped views based on the full-frame raw unprocessed intensity imagery. The Mach number and slant range estimates shown in this figure were based on an EFT-1 pre-flight trajectory and not the BET. This is because the BET took several months to be processed and released to the NESC analysis team. Note the distinct bright areas on the heat shield periphery correspond to the compression pads.

Based upon these sequential views, the selection of image frames for analysis focused on those that presented a reasonable heat shield frontal view (e.g., image frames after #08695 were eliminated from consideration). Frames prior to #7845 were eliminated from consideration as some degree of saturation was evident during this time period. During the initial acquisition phase, the operator configured the sensor with a relatively long integration time to collect as many photons to distinguish the capsule from the sky background.

	<h1 style="text-align: center;">NASA Engineering and Safety Center Technical Assessment Report</h1>	Document #: NESC-RP-12-00795	Version: 1.0
Title: Remote Imaging of EFT-1 Entry Heating Risk Reduction			Page #: 71 of 98

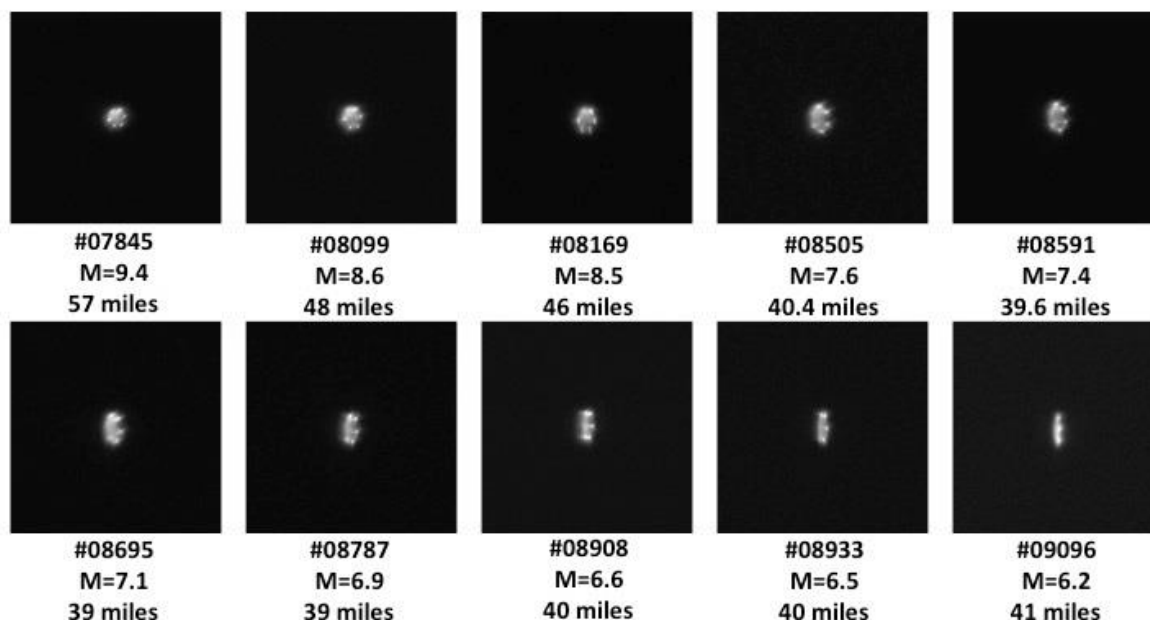


Figure 7.3.1-1. Sequence of Raw NIR Intensity Images Showing Perspective Change of Heat Shield as Capsule Approached the Aircraft

After saturation levels and constraints with the desired view had eliminated frames from the early and late observation phases, other criteria were considered to further remove frames from analysis contention. First, there must be no indication of clouds between the aircraft and the capsule. Second, the imagery must display little to no effects from aircraft motion, tracking jitter, and atmospheric distortion. Third, times when the reaction control system (RCS) thrusters were firing was avoided. To begin this more detailed assessment and elimination process, several key parameters during the observation were plotted as shown in Figure 7.3.1-2. In this figure, the integrated capsule intensity, in raw sensor counts (i.e., left y-axis), is shown with a black line, and the sensor integration time, in milliseconds (msec) (i.e., right y-axis), is shown with a red line. The increasing stair-step nature of the integration time was the result of the Cast Glance operator adjusting the sensor exposure time to accommodate the heat shield's decreasing temperature. In the lower portion of the plot, the blue and light green lines show the average image intensity near the capsule, which was used for background removal of intensity counts. The thicker green vertical lines show selected time segments.

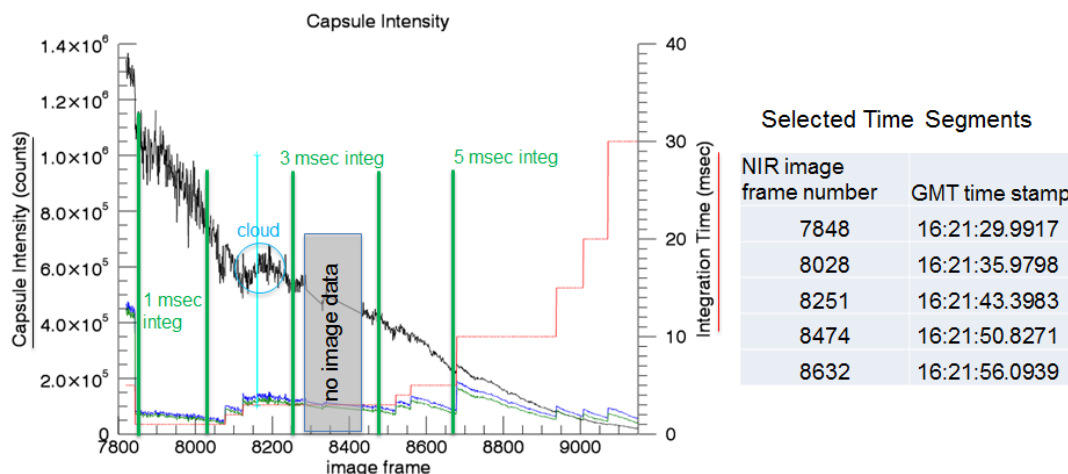



Figure 7.3.1-2. Plot of Several Image-Derived Parameters to Highlight Selection of Imagery for Detailed Analysis

Near frame 8200, a relatively large change in intensity was observed. It was suspected this change was due the presence of a high, thin cloud along the line of sight. The corresponding imagery from the MWIR sensor on Cast Glance, which had a lower magnification, confirmed an abrupt change in the signal and foreground intensity corresponding to a thin cloud. Collecting imagery at 30-Hz frame rate allowed the analysts to identify and eliminate frames showing significant atmospheric effects due to air turbulence, atmospheric density fluctuations, or blurring from tracking motions/jitter. While evidence of RCS thruster firings was not readily observed in the imagery as the backshell-mounted thrusters were obscured from view by the heat shield, the RCS jet duty cycles were identified and the corresponding imagery frames were eliminated.

Given the multitude of considerations, five specific times (i.e., green vertical lines) were identified in Figure 7.3.1-2 for image processing and analysis to infer the heat shield surface temperature. To the right of the plot, frame numbers and the UTC time stamps are listed. Several frames immediately before and after these five selected times were then chosen to enhance imagery. Averaging multiple frames improves the overall signal-to-noise and improves the image quality before radiometric analysis was applied.

In prior SSP orbiter observations, as many as 25 frames centered about the selected time segment were used for subsequent enhancement [refs. 12, 17]. The MPCV capsule was dimensionally smaller than the SSP orbiter (i.e., generating fewer pixels across the heat shield), and the EFT-1 data collected had more image-to-image distortions. As a result, only five frames were considered for each time segment in the post-processing. The best images in the data set (i.e., ones that that appeared relatively undistorted) were selected by evaluating the appearance of the six compression pads. An example of multiple frames, centered about the frame #08028 time segment are shown in Figure 7.3.1-3. The frames shown in this figure are in their unprocessed state with native 32×32 pixel resolution.

	NASA Engineering and Safety Center Technical Assessment Report	Document #: NESC-RP- 12-00795	Version: 1.0
Title: Remote Imaging of EFT-1 Entry Heating Risk Reduction			Page #: 73 of 98

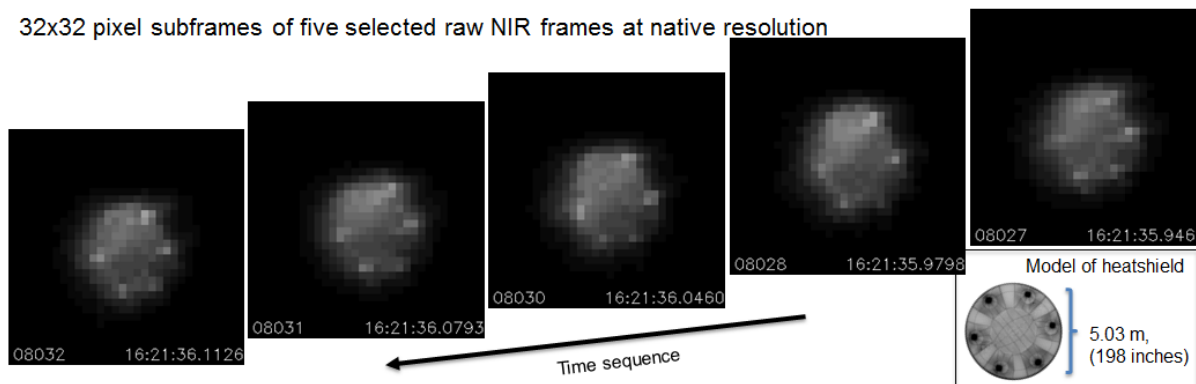


Figure 7.3.1-3. The Selected Five Frames Used to Post-Process Imagery for Frame #8028

The the compression pads physical structure resulted in higher localized heating than the heat shield surrounding area. In the vicinity of each of the six compression pads, there is thickening of the Avcoat TPS creating a shallow ramp and cavity. The pad is circular (~9.5-inch diameter) and made from carbon phenolic with a center stainless steel bolt and insert. The metal bolt/insert is ~2.75 inches in diameter. A resulting oblong planform shape is created by intersection of the ramps with the heat shield outer mold line (OML). The Avcoat on the acreage OML is identical to the ramps surrounding the pads, but there is a material and density difference between the surrounding Avcoat and carbon-phenolic/metal pads. In the intensity imagery, the pads are noticeably brighter as a result of a higher local temperature and/or emissivity difference.


While spatially unresolved, the compression pads acted as indicators to determine the least distorted images. As noted, for a manually tracked image sequence there are often major differences in the image quality frame-to-frame. A relatively few image frames can be better in quality than a majority of the others. These relatively few high-quality images are often referred to as “lucky images.” For the EFT-1 observation, the five image frames showing the best “point-like” response from the compression pads were selected as the “lucky images” for use in the subsequent enhancement process. The thermal signature from the compression pads were used to infer the capsule’s orientation and to serve as a reference point to locate the approximate position of the heat shield DFI TCs.

While not obvious in these linearly scaled images, background variations in the raw intensity imagery existed from ambient light levels and noise within the instrumentation system. Before proceeding to the next level of processing, the background noise (shown in Figure 7.3.1-2) was subtracted from the imagery.

7.3.2 Interpolation, Frame Co-Registration and Averaging

After the five best images for each time segment were selected and the background noise eliminated as described in Section 7.3.1, image resolution and signal-to-noise was improved prior to converting the data to radiometric units (i.e., radiance) in Section 7.3.3.

In Figure 7.3.1-3, the apparent heat shield diameter is approximately 12 to 13 pixels and, as expected for the given slant range, yielded a scale of ~15 inches/pixel. To increase apparent

	NASA Engineering and Safety Center Technical Assessment Report	Document #: NESC-RP- 12-00795	Version: 1.0
Title:	Remote Imaging of EFT-1 Entry Heating Risk Reduction		Page #: 74 of 98

spatial resolution without introducing artifacts or intensity distortions in the image, each of the five 32×32 -pixel “lucky frames” was centered and up-scaled by a factor of 8 through an interpolation process, resulting in 256×256 -pixel images. These images were spatially co-registered such that features overlaid each other from one frame to the next. Finally, the five resolution-enhanced frames were averaged together to form the final intensity-based image using the algorithm developed in reference 34. This final processed frame generally saw a factor of two increase in signal-to-noise, which would improve the temperature accuracy and increase the spatial feature resolution.

Figure 7.3.2-1 shows the five enhanced frames and the resulting single co-registered/averaged image. In the interpolated images, the image-to-image variations in gray-scaled intensity are more apparent with more spatial detail than observed in the corresponding raw images from Figure 7.3.1-3. The resulting co-registered/averaged frame represents an optimally enhanced image while maintaining the radiometric data integrity. This general process was applied to the selected time segments for thermal analysis. A more detailed discussion on this image processing technique has been described in prior publications [refs. 12, 17].

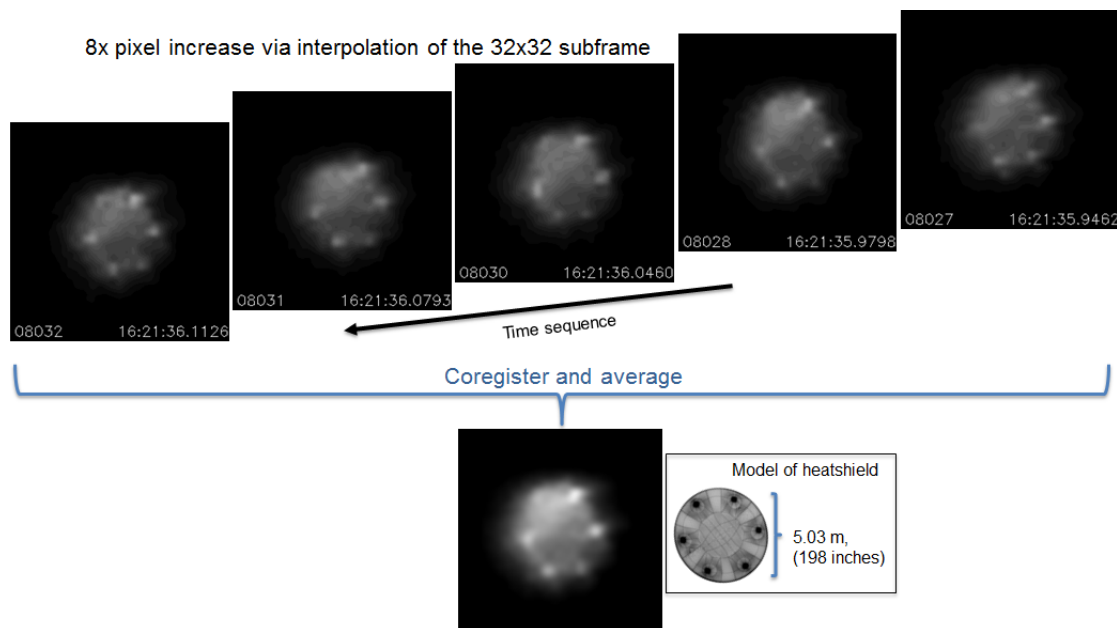



Figure 7.3.2-1. Selected Five Frames Used to Post-Process Imagery for Frame 8028 after 8x Interpolation Has Been Applied

7.3.3 Radiometric Calibration

As described in Section 7.1, the infrared sensor calibrations took place at Point Mugu Naval Air Station, California, 3 days prior to the scheduled EFT-1 launch. The Cast Glance sensor operators captured image-based data from calibrated blackbody temperature sources for integration times likely to be used during the data observation. The calibration data were analyzed to determine the sensor response, counts, or digital numbers (DNs), for each specific integration time. The result of the calibration analysis is a coefficient relating the sensor counts

	NASA Engineering and Safety Center Technical Assessment Report	Document #: NESC-RP- 12-00795	Version: 1.0
Title:	Remote Imaging of EFT-1 Entry Heating Risk Reduction		Page #: 75 of 98


(DN/s) to the in-band radiance, in Watts per centimeter squared per Steradian (W/cm²/sr), at the sensor's aperture for a particular integration time. The analysis details and the coefficient derivation used for analysis are provided in Appendix E. The following represents a synopsis of that report.

The calibration analysis first requires extracting the pixel values in counts generated by the source radiances within the image. In this instance, the calibration sources were two blackbodies whose radiances were controlled by their temperatures and emissivities. Multiple frames at each integration time were recorded and averaged to reduce the errors caused by sensor noise. Sensor background values were calculated and subtracted from the pixel values generated by the source radiance. In addition, the line-of-sight distance of about 500 ft and the atmospheric conditions at the time of calibration were recorded as inputs into MODTRAN[®] to calculate atmospheric transmittance for the EFT-1 calibration measurement configuration. This was necessary to compensate for any atmospheric transmission loss along the line of sight from the blackbodies to the aircraft sensor.

The sensor's background count rate was computed and subtracted for all integration times at each blackbody temperature setting. A check was performed to ensure the sensor's response (i.e., count rate in DN/sec) was linear with in-band radiance. After verifying linearity, a linear least squares fit was performed between the background subtracted count rate and the in-band radiance. For the NIR sensor, the slope (i.e., force zero intercept) was 4.957×10^7 , making the calibration coefficient (i.e., the reciprocal of the slope) 2.017×10^{-8} . The appropriate units for the calibration coefficient were (W/cm²/sr)/(DN/sec). The calibration coefficient when converting directly from count rate into in-band radiance was:

$$\text{Inband Radiance} \left(\frac{\text{Watts}}{\text{cm}^2 \cdot \text{sr}} \right) = 2.017 \times 10^{-8} * \text{Count Rate} \left(\frac{\text{DN}}{\text{sec}} \right)$$

As mentioned, the Cast Glance operators adjusted the NIR sensor's integration time during the mission, attempting to optimize the measured counts from the heat shield for signal-to-noise ratio and to prevent saturation. Accordingly, given the sensor's finite dynamic range imposed by its 12-bit analog-to-digital convertor (ADC), each integration time enables calibrated data on the target of interest to be captured over a limited range of surface temperatures. The blackbody temperature for the entire 12-bit range of ADC counts for three representative integration times is given in Figure 7.3.3-1. This figure represents the range of integration times used during the NIR imagery collection during the EFT-1 observation. This emphasizes the need for changing integration times to yield sufficient signal counts as the heat shield temperature dropped a few hundred degrees Fahrenheit during the 63-second observation period. For a heat shield temperature of 1,800 °F (1,255 K), the 12-bit (0-4095 counts) NIR Cast Glance sensor would reach levels approaching saturation for a 10-msec integration time, where a 1-msec integration time would yield an unacceptably low signal-to-noise ratio.

	NASA Engineering and Safety Center Technical Assessment Report	Document #: NESC-RP- 12-00795	Version: 1.0
Title:	Remote Imaging of EFT-1 Entry Heating Risk Reduction		Page #: 76 of 98

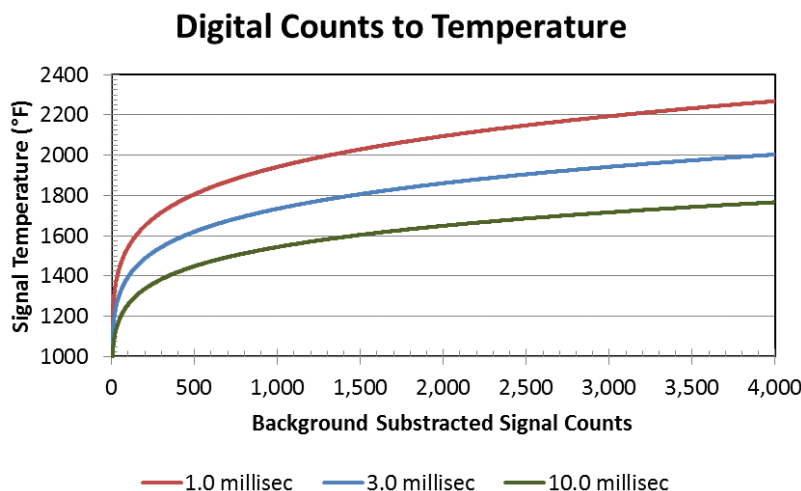



Figure 7.3.3-1. Range of Integration Times Used During Collection of NIR Imagery during EFT-1 Observation

7.3.4 Atmospheric Compensation and Emissivity

The heat shield irradiance was measured at the infrared sensor’s focal plane array after propagating through miles of atmosphere to the imaging system optics. This section outlines the process of estimating the atmospheric transmission. Along the line-of-sight path from the capsule to the sensor, the received light incurs atmospheric transmission loss due to scattering and absorption. The atmospheric data were taken from the Air Force Weather Agency’s 3-D numerical weather model and obtained within the nearest hour of the EFT-1 thermal observation. The NIR sensor spectral band with 850-nm cut-on filter was approximated as a top-hat response (flat) from 0.843 to 1.1 microns, which was adequate for the transmittance calculations.

The average in-band transmittance was computed for each image frame time using MODTRAN® with the observing geometry (i.e., capsule and aircraft locations) and the available atmospheric data. The data contained in the 3-D meteorological data cube were traversed along the line of sight to determine the respective atmospheric transmittance. For typical conditions above 33,000-ft altitude and a nominal 57 nmi slant range at a 17° elevation angle, the atmospheric transmittance was around 0.96. This 4% transmission loss is relatively small, but must be included to accurately estimate the capsule heat shield irradiance. It is this “corrected” irradiance value that was used to infer the heat shield surface temperatures.

The heat shield irradiance is dependent on its emissivity. Prior to the observation, Surface Optics Corporation performed several measurements to determine the heat shield spectral and angular emissivity (Appendix A). During the time of the thermal data collection, the capsule had passed through the point of peak heating and was cooling. The heat shield surface was certainly charred and ablated at this time during the reentry. Figure 7.3.4-1 shows a plot of the estimated emissivity of the charred Avcoat sample in the waveband regions for the three Cast Glance infrared sensors. The blue line shows the result for the NIR used during the spatially resolved observation, which is approximately 0.9 for smaller off-axis angles. The emissivity changes

	NASA Engineering and Safety Center Technical Assessment Report	Document #: NESC-RP- 12-00795	Version: 1.0
Title:	Remote Imaging of EFT-1 Entry Heating Risk Reduction		
			Page #: 77 of 98

slightly as the angle increases, which allows the assumption of a constant emissivity over the entire heat shield even though it is a curved surface. However, as the line-of-sight angle to the heat shield changed during the observation (i.e., from ~11 to 53°), the emissivity value was adjusted accordingly.

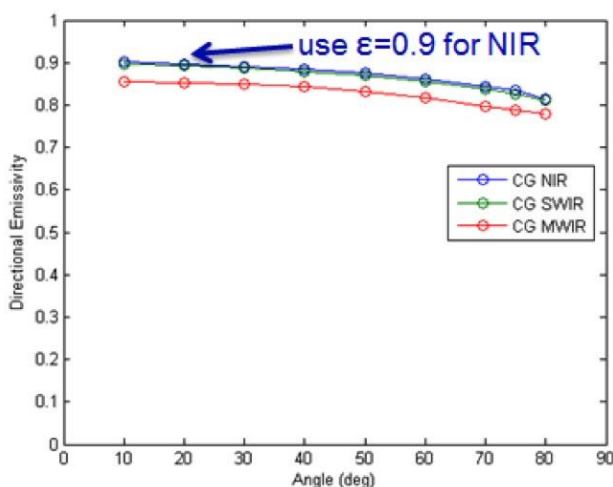


Figure 7.3.4-1. Directional Emissivity Values as Measured on Charred/Ablated Avcoat TPS Sample

7.3.5 Temperature Estimates

The irradiance measured at the detector focal plane array was corrected for atmospheric and other losses to the heat shield irradiance. This heat shield irradiance is divided by the emissivity defined in Section 7.3.4 to adjust to a blackbody equivalent value, which is necessary to convert to a temperature. The radiance can be expressed by the Planck blackbody radiance function. Therefore, to convert the irradiance to temperature, the temperature at each pixel is calculated by iterating the Planck function within the top-hat response from 0.843 to 1.1 microns. An initial temperature is given to calculate an initial radiance, and the difference between the observation-based pixel radiance and initial estimated radiance was determined. The iteration of estimating the temperature and computing the radiance continued until the difference with the image pixel radiance was below the specified 1% tolerance.

Table 7.3.5-1 shows the resulting temperature image estimates for the five selected time segments along with parameters of interest based upon the BET. The imagery-based surface temperatures are shown on the same temperature scale, indicating the rapid heat shield cooling (i.e., ~300 °F in 36 sec) during the observation. The capsule changed orientation as observed by the compression pad locations and from the flight parameters. The primary flight dynamic during the observation was that the capsule was slowing rapidly. The viewing geometry was nearly head-on for the first image shown (i.e., frame 7848) and became more side-on. In this sequence of views, the capsule orientation can be inferred from the compression pad position. The capsule was flying with the hotter area of the heat shield (i.e., the flow stagnation point) at approximately the 11-o'clock position and based upon the BET, at an angle of attack of ~19°.


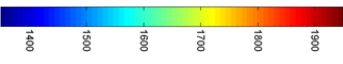
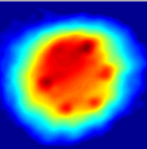
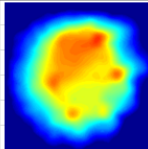
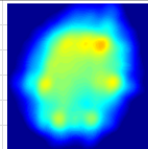
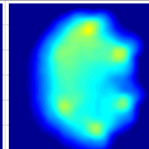
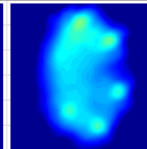

	<h1>NASA Engineering and Safety Center</h1> <h2>Technical Assessment Report</h2>	Document #: NESC-RP-12-00795	Version: 1.0
Title:	Remote Imaging of EFT-1 Entry Heating Risk Reduction		Page #: 78 of 98

Table 7.3.5-1. Final Global Temperature Images for Five Selected Times during EFT-1 Hypersonic Reentry

Image Frame Number:	7848	8028	8251	8474	8632
Image Frame Time Reference (GMT):	16:21:29.9917	16:21:35.9798	16:21:43.3983	16:21:50.8271	16:21:56.0939
Mach number:	9.91	9.33	8.66	8.04	7.63
Target Range (nmi):	65.1	57.2	49.2	43.3	40.6
Target elevation (deg):	15.4	17.4	20.2	22.7	24.1
Raw Image Pixel Footprint (inches):	17.1	15.0	12.9	11.4	10.7
Capsule apparent pitch (angle of attack;deg):	-19.1	-19.1	-19.2	-19.4	-19.4
Capsule "up" (reference to z-axis; deg):	18	18	18	-7	-9
Capsule bank angle (deg):	30.39	22.21	27.85	38.48	46.46
Angle of l.o.s. to heatshield normal(deg):	11.5	33.5	36.0	44.0	53.0
Peak temperature (deg F):	1940	1843	1760	1718	1643
Minimum temperature (deg F):	~1720	~1630	~1520	~1480	~1400
<div> <div>Temperature (deg F):</div>  </div>					
					

A process of mapping a two-dimensional (2-D) temperature map to a 3-D surface as was done for previous SSP observations was not attempted with the EFT-1 temperature maps. The accuracy of the iterative numerical technique developed for the SSP thermal imagery was dependent on vehicle edge definition and the presence of distinct thermal features. While the pixel resolution between the SSP and EFT-1 thermal imagery is reasonably close, the larger SSP orbiter size and the presence of sharp thermal gradients in the 2-D orbiter temperature maps readily facilitated the 3-D mapping process.

The apparent thermal features associated with the compression pads are unresolved, because the compression pads are smaller than the pixel footprint in these images. However, if it was the localized heating from the posts that was observed, then the temperature differences between the compression pad and their immediate surroundings would be in excess of the ~100 °F difference inferred from the imagery. A summary graphic showing the five quantitative thermal temperature maps superimposed on the EFT-1 flight path is shown in Figure 7.3.5-2. These are the same images as shown in Table 7.3.5-1, but with a variable temperature scale to highlight heat shield temperature variation at each time. Two images of the capsule under parachute are as viewed from BH-300 at extreme range are also shown.

	NASA Engineering and Safety Center Technical Assessment Report	Document #: NESC-RP- 12-00795	Version: 1.0
Title:	Remote Imaging of EFT-1 Entry Heating Risk Reduction		
			Page #: 79 of 98

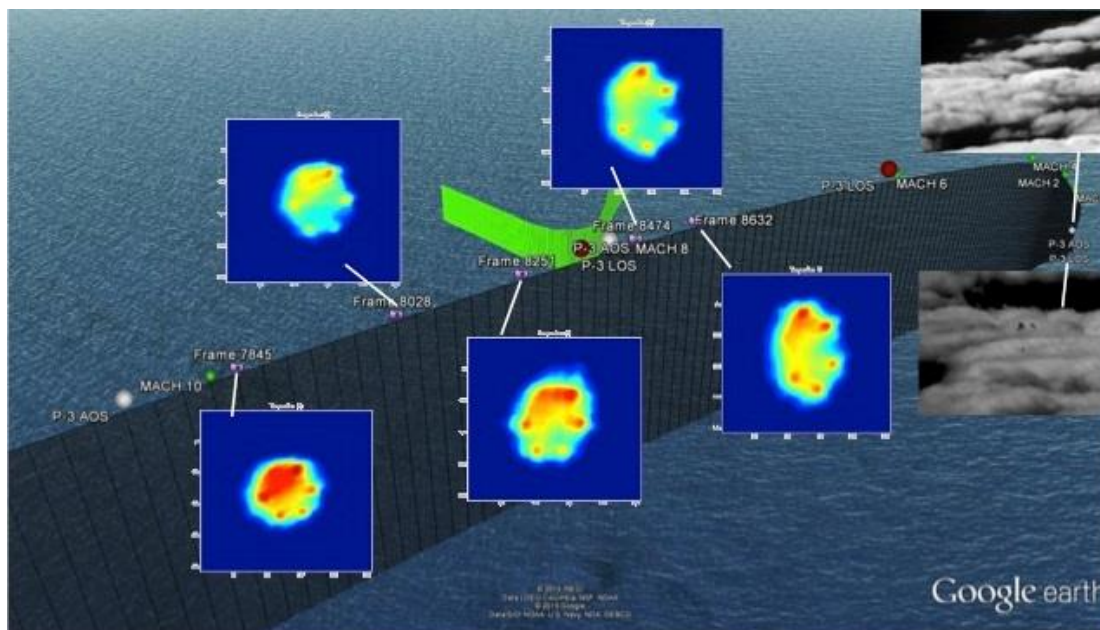



Figure 7.3.5-2. Global Temperature Images Relative to EFT-1 Flight Path. Images of EFT-1 Parachute Deployment (far right)

Consultation with the MPCV Program Aerosciences team indicated the acreage surface temperatures inferred from the infrared imagery were consistent with that inferred from a laminar-based CFD prediction. At no time during the observation when the heat shield was in view (i.e., Mach 9.9 to Mach 7.6) did the thermal imagery indicate the presence of wedge-like thermal footprints associated with hypersonic boundary layer transition as have been observed on the SSP (see Figure 6.2-2). Based upon initial expectations of when hypersonic boundary layer transition was expected to occur on the EFT-1 heat shield during reentry (~Mach 20), a laminar boundary layer this late in the reentry was not expected. In practice, the onset of hypersonic boundary layer transition is difficult to predict, and when additional factors (e.g., surface roughness and mass addition (blowing) from ablation) are present, it is clear that simple engineering methods lack the sophistication to accurately predict when transition will occur. Based upon circumstantial evidence, it is suggested that it is possible the boundary layer initially became unstable (i.e., non-laminar) at higher Mach numbers when the heat shield was not under observation. During this time, the wedge patterns would have been imprinted on the heat shield surface. Soon thereafter, the boundary layer stabilized back to a laminar state as observed during the observation period. After the heat shield was no longer visible to the Cast Glance infrared sensors at lower Mach numbers, the boundary layer would have transitioned to a fully developed turbulent state under this scenario.

A heat shield post-recovery image (Figure 7.3.5-3) suggests this scenario as plausible by revealing what appear to be multiple wedge-like features emanating from the flow stagnation region. The wedge angles of these features are consistent with the spreading angle of flow turbulence at high hypersonic Mach number. The thermal image obtained at Mach 9.9

	NASA Engineering and Safety Center Technical Assessment Report	Document #: NESC-RP- 12-00795	Version: 1.0
Title:	Remote Imaging of EFT-1 Entry Heating Risk Reduction		Page #: 80 of 98

(Figure 7.3.5-3 inset) has been rotated to align with the stagnation region shown in the heat shield image. If these wedges were produced by elevated heating from flow turbulence, then transition or non-laminar flow preceding transition onset had occurred at high Mach number with the flow subsequently returning to a laminar state and the residual heating footprint washed out during the observation time. Alternatively, the transition occurred at supersonic Mach numbers (i.e., less than Mach 7.6) after the observation. However, it is doubtful these wedge-like features would have been imprinted into the heat shield surface as the surface temperatures were greatly reduced at these lower Mach numbers.

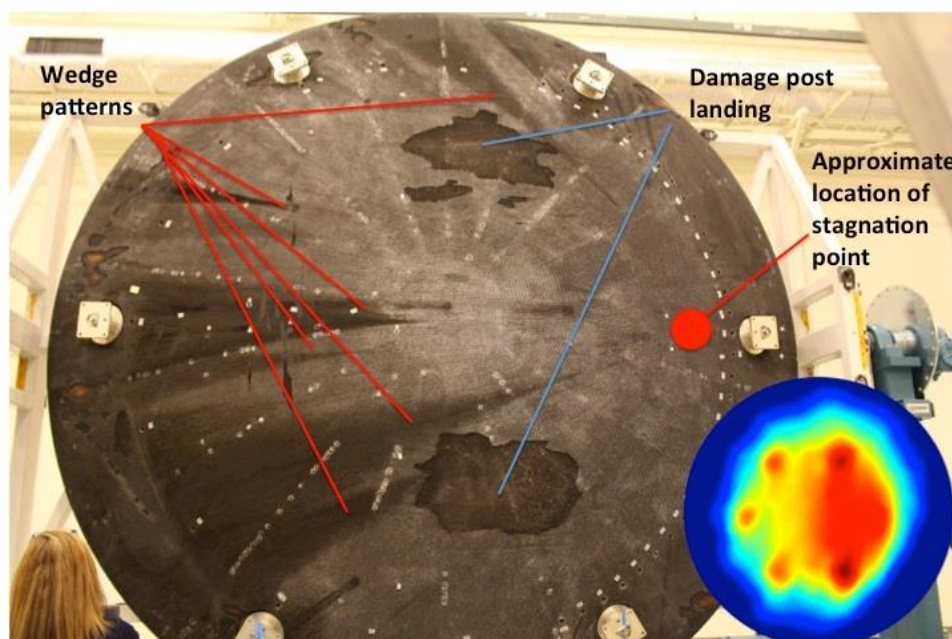



Figure 7.3.5-3. Comparison of Global Temperature Image with Post-Flight Image of the EFT-1 Heat Shield

7.3.6 Uncertainty of Temperature Estimates

The final 2-D temperature mappings were a result of the processes presented in the preceding sections, and most of the inherent data provided as input to these processes have corresponding uncertainties. There are four sources of the uncertainties: sensor noise (i.e., measurement noise), radiometric calibration, heat shield surface emissivity, and atmospheric transmittance.

Because of the image enhancement process where multiple unsaturated frames were registered, co-added, and then averaged, noise statistics were estimated to contribute to approximately 6 °F, based estimates from prior work [ref. 12, 17]. The NIR sensor radiometric calibration was linear, consistent with previous calibration characteristics resulting in an estimated uncertainty of ~2 °F. The emissivity estimate of uncertainty is more difficult to quantify because of the unknowns regarding the Avcoat surface condition during the reentry. It was assumed the charred and ablated TPS sample from the arcjet testing was representative of the reentry condition. The test material showed a consistent emissivity value across the infrared wavebands, and generally

	NASA Engineering and Safety Center Technical Assessment Report	Document #: NESC-RP- 12-00795	Version: 1.0
Title: Remote Imaging of EFT-1 Entry Heating Risk Reduction			Page #: 81 of 98

for different viewing angles. It was therefore presumed that a conservative estimate of emissivity uncertainty would be within 5% of the baseline measured value of 0.9. To characterize this uncertainty in terms of surface temperature, a sensitivity study was performed. As shown in Figure 7.3.6-1, an emissivity variation of a 5% magnitude would account for a temperature error of approximately 10 °F. After analysis of the imagery had been completed, the MPCV TPS community made the NESC team aware of unpublished spectroradiometer-based high-temperature emittance measurements (2010-11) on Avcoat (ref. 35). These measurements have suggested an in band emittance value as low as 0.81. These recently disclosed measurements exhibit some behavior that raise some questions. Never-the-less, an emissivity value of 0.81 would correspond to a 10% emissivity error translating to a ~20 °F increase in the inferred surface temperature as shown in Figure 7.3.6-1

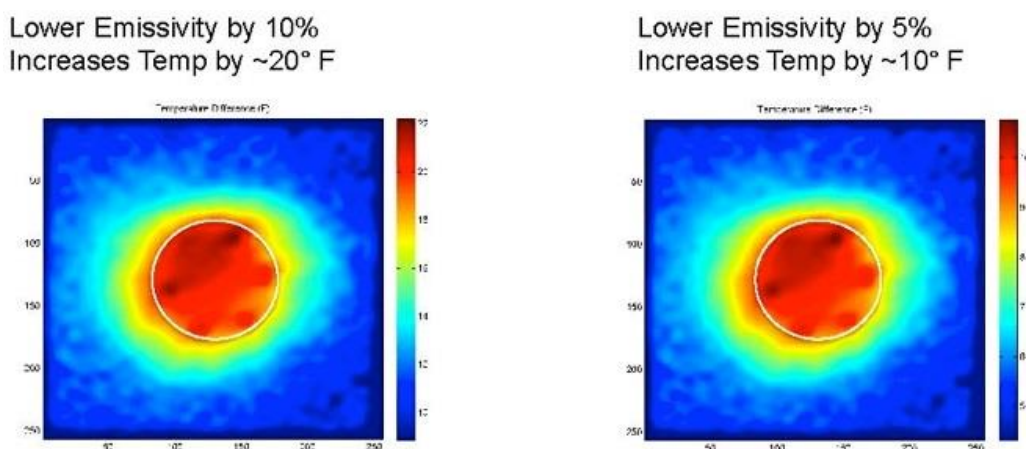

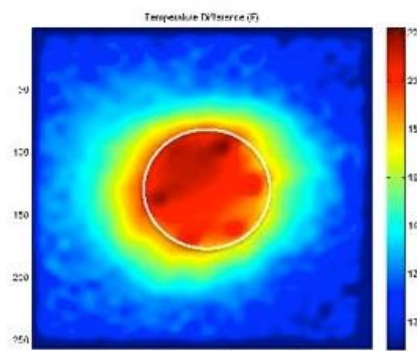


Figure 7.3.6-1. Influence of Emissivity on Computed Surface Temperature

Lastly, the atmospheric transmittance uncertainty is difficult to determine because the conditions during the observation were not measured, but interpolated from limited satellite information where the reentry occurred. However, at the aircraft and capsule altitudes, the transmittance was consistent at approximately 0.96%, and typically does not change more than a few percent. As a worst case, a transmittance uncertainty of 5 and 10% was assumed. As with the emissivity, a sensitivity study was performed. As shown in Figure 7.3.6-2, a variation in transmittance of a 5% magnitude would account for a temperature error of approximately 10 °F. An unrealistic but very conservative 10% error on the transmittance value would increase the error to ~20 °F.

	NASA Engineering and Safety Center Technical Assessment Report	Document #: NESC-RP- 12-00795	Version: 1.0
Title:	Remote Imaging of EFT-1 Entry Heating Risk Reduction		
			Page #: 82 of 98

Lower Transmission by 10%
Increases Temp by ~20° F



Lower Transmission by 5%
Increases Temp by ~10° F

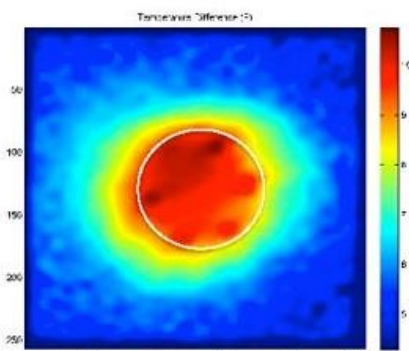



Figure 7.3.6-2. Influence of Atmospheric Transmittance on Computed Surface Temperature.

To assess a total uncertainty, these sources were combined in quadrature. The total uncertainty for the EFT-1 heat shield temperatures was estimated to be ± 15 °F. This is consistent with prior uncertainty estimates for airborne data collections described in earlier work [refs. 9, 12].

7.3.7 Comparison of TC Data to Image-Derived Temperature

As discussed in Section 6.1, instrumented plugs were installed at multiple points on the Avcoat heat shield to measure the in-depth temperatures during the EFT-1 entry. The plugs consisted of two Type-S TCs, two Type-K TCs, and a Hollow aErothermal Ablation and Temperature (HEAT) recession sensor [ref. 36]. The Type-S TC nearest the surface was installed nominally 0.1 inch below the OML, with the remaining TCs installed at progressively deeper locations. According to reference 21, the junction location and TC depths were verified by X-ray prior to heat shield installation. Reconstruction of Avcoat surface temperatures using the near-surface TC measurements were performed using the inverse heat transfer capabilities of the Charring Ablator Response (CHAR) code and the design Avcoat response model [refs. 37, 38]. At the time of this report, uncertainty estimates associated with the TC were not available.

Figure 7.3.7-1 highlights the two EFT-1 heat shield TC locations. These locations (i.e., plug06 and plug08) were selected based their time trace quality (e.g., largely free of apparent non-physical temperature readings observed in several of the near-surface EFT-1 TCs), exhibited a relatively smooth monotonically decreasing temperature with time, and were not located near a large temperature gradient. Based on the TC locations, the corresponding locations in the imagery were estimated by using the pixel size references. The raw imagery for this example had a resolution of ~15 inches/pixel, while the “interpolated” imagery was less than 2 inches/pixel.

	NASA Engineering and Safety Center Technical Assessment Report	Document #: NESC-RP- 12-00795	Version: 1.0
Title:	Remote Imaging of EFT-1 Entry Heating Risk Reduction		Page #: 83 of 98

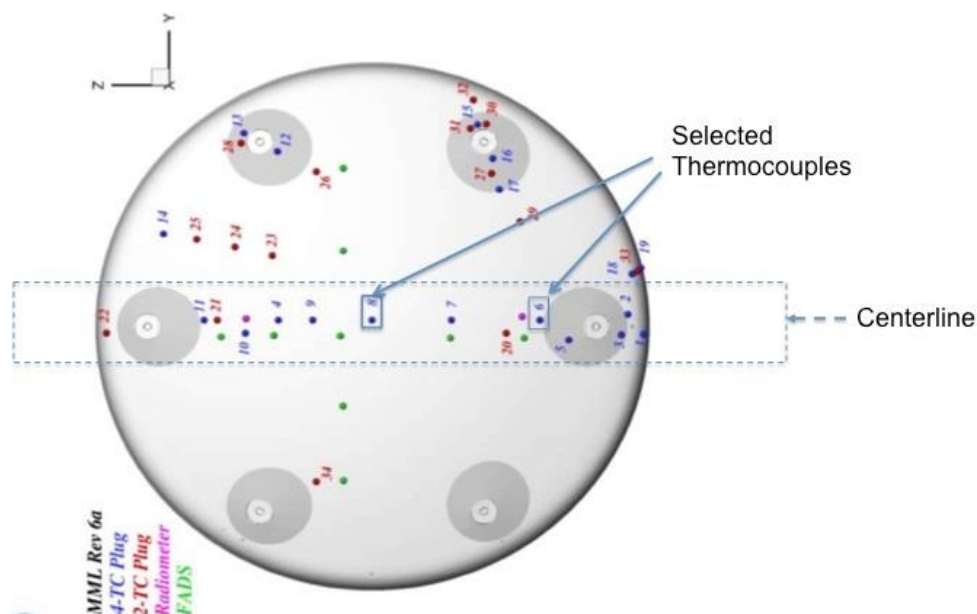


Figure 7.3.7-1. Location of Two DFI In-Depth TCs Selected for Comparison to Image-Derived Surface Temperature

An example of temperatures extracted along the 2-D surface temperature map associated with the thermal image obtained at Mach 9.9 is shown in Figure 7.3.7-2.

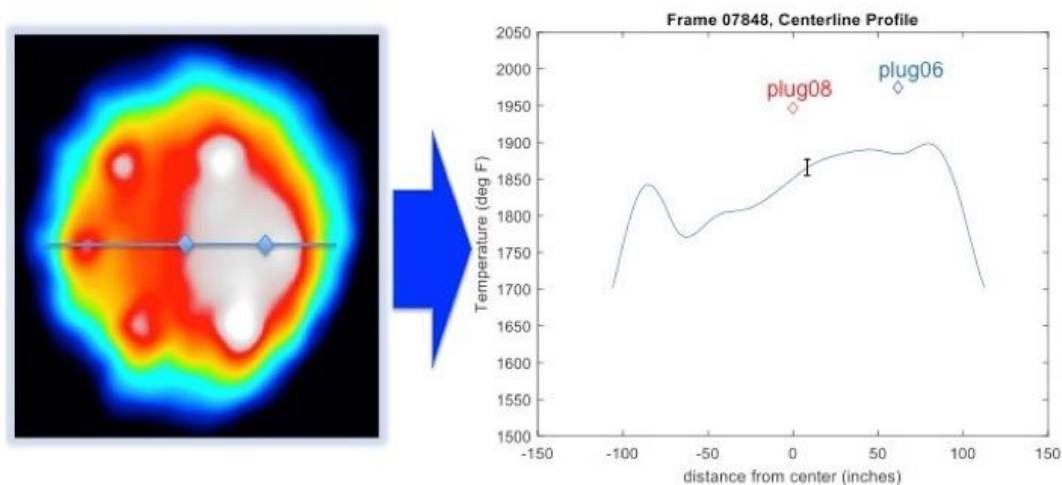



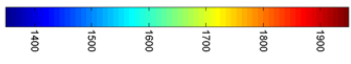
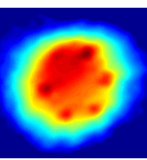
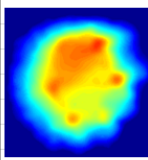
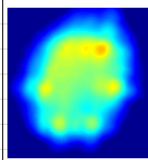
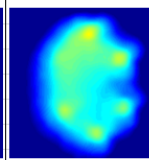
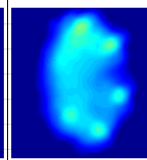
Figure 7.3.7-2. Comparison of Image Derived Surface Temperature Distribution to Surface Temperature Derived from In-Depth TC Measurement Using Inverse Methods

The left side of Figure 7.3.7-2 shows the temperature image for frame 7848 (note different color scale) that has been rotated to correspond to the instrumentation diagram in Figure 7.3.7-1. The right side presents a temperature profile extracted across the dimensional temperature image.

	<h1 style="text-align: center;">NASA Engineering and Safety Center</h1> <h2 style="text-align: center;">Technical Assessment Report</h2>	Document #: NESC-RP-12-00795	Version: 1.0
Title: Remote Imaging of EFT-1 Entry Heating Risk Reduction			Page #: 84 of 98


The diamond symbols represent the in-depth temperatures derived from plug06 and plug08 TCs that have been extrapolated to the recessing heat shield surface. This process was performed at all times the imagery was evaluated and summarized in Table 7.3.7-1. The last two rows of text show the temperature differences between the in-situ and remote observation measurement techniques. The imagery estimates were consistently lower than the TC-derived temperatures. Most of the differences were in the range of 100 °F. The relatively small lateral temperature gradients derived from the heat shield imagery would not account for the large bias.

Table 7.3.7-1. Summary of Temperatures Differences between Plug06 and Plug08 and the Five Selected Imagery Time Segments

Image Frame Number	7848	8028	8251	8474	8632
Image Frame Time Reference (GMT)	16:21:29.9917	16:21:35.9798	16:21:43.3983	16:21:50.8271	16:21:56.0939
Mach number	9.91	9.33	8.66	8.04	7.63
Orion Time Reference (GMT)	16:21:29.846	16:21:35.846	16:21:43.271	16:21:50.696	16:21:55.946
Thermocouple Time (MET_wrt_CMSEP)	3173.526	3179.526	3186.951	3194.376	3199.626
TC Derived Temperature for Plug06 TC (°F)	1975	1891	1797	1712	1659
TC Derived Temperature for Plug08 TC (°F)	1947	1860	1755	1672	1619
Image Derived Temperature for Plug06 (°F)	1886	1798	1702	1655	1596
Image Derived Temperature for Plug08 (°F)	1846	1738	1640	1580	1530
Δ between Plug06 Image and TC estimates (°F)	-89	-93	-95	-57	-63
Δ between Plug08 Image and TC estimates (°F)	-101	-122	-115	-92	-89
Temperature (deg F):					
					

The total uncertainty of the observation based temperature (± 15 °F) is significantly smaller than the observed ~ 100 °F temperature difference between the two measurement techniques. Even a simple addition of the various contributors to uncertainties in the imagery estimates discussed in Section 7.3.6 would only yield a ± 30 °F uncertainty. It was determined that a spectral emissivity value of approximately 0.55 would be required to drive the image-derived temperatures to the values of the TC measurements. This emissivity value is not supported by any laboratory measurement. Naturally, the surface temperatures derived from the in-depth TCs possess uncertainties, due to sensors and the inverse methods utilized to calculate the surface temperature from in-depth measurements. The TC temperature reconstructions are provided in references 36 and 37, and should be considered as a first look. It is beyond the scope of this assessment to determine the origin of a ~ 100 °F bias between the two temperature estimates. The MPCV Program is currently pursuing additional testing to better characterize TC uncertainty.

One of the biggest unknowns regarding TC uncertainty at the present time is the value of the char layer conductivity at high temperature. The large temperature difference suggests the heat shield material property assumptions and uncertainties associated with the inverse method could be re-evaluated and quantified. The inverse method assumed knowledge of the heat shield

	NASA Engineering and Safety Center Technical Assessment Report	Document #: NESC-RP- 12-00795	Version: 1.0
Title:	Remote Imaging of EFT-1 Entry Heating Risk Reduction		Page #: 85 of 98

recession rate with time. Since only post-flight measurements of recession are made, the degree to which the heat shield has recessed at Mach 9.9 remains uncertain. It was likely assumed in the TC reconstruction process that most of the recession had occurred at the time the thermal image was taken. Because of the reconstruction process and the non-physical reading of several of the near surface TCs, comparison of the image-derived surface temperature to other measurements at TC locations was not attempted. Testing sponsored by the NESC is planned to investigate the susceptibility of the TCs to electro-magnetic interference from ionized gases in the plasma during entry.

Even though there was a bias between the two different temperature estimates, there was relative consistency across the five time segments because both measurements indicate a rapidly decreasing temperature during the observation period. To evaluate if the cooling rate inferred from the image data was consistent with that inferred from a TC data, an image-derived temperature time history was evaluated at the plug08 location. The selection of time segments for creating the time history was similar to selecting the best image time segments described in Section 7.3.1. Periods of time were avoided when there was excessive blur, no image data, interference from clouds, and large integration time changes. Figure 7.3.7-3 shows the same plot as shown in Figure 7.3.1-2 and overlays in light blue-gray boxes the two time segments when an acceptable “single point” temperature can be calculated at the plug08 location. For each frame in these time segments, the raw imagery was processed with no imagery enhancement, and the temperature of the heat shield center pixel was computed. The changing transmittance along the line-of-sight path was accounted for even though there were only minor changes.

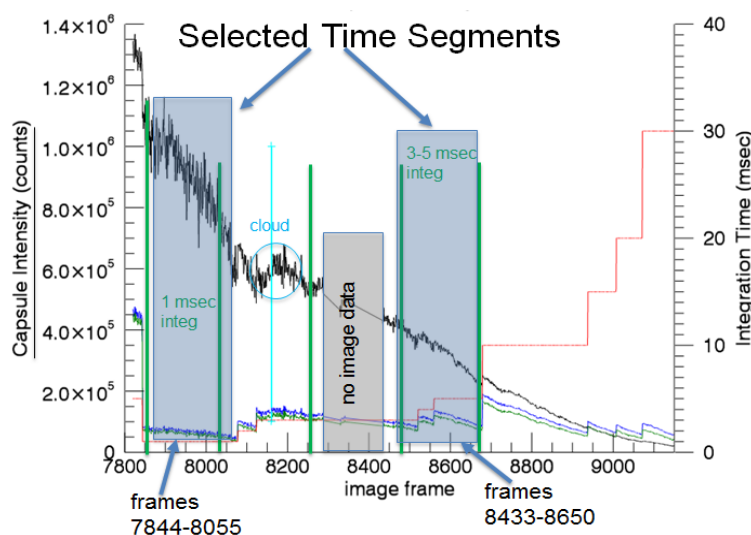



Figure 7.3.7-3. Plot Showing Selection of Two Time Segments Shaded (in blue) for Comparison of Cooling Rates

The image-derived temperature at the plug08 location was compared to the reconstructed TC temperature estimates in Figure 7.3.7-4. The red line represents the TC data (note that some artifacts and spikes were smoothed out) and the blue dots correspond to the temperature inferred

	NASA Engineering and Safety Center Technical Assessment Report	Document #: NESC-RP- 12-00795	Version: 1.0
Title:	Remote Imaging of EFT-1 Entry Heating Risk Reduction		Page #: 86 of 98

from each imagery frame. It was noted the TC temperature did not decrease linearly during the observation. For that reason, a line fit to the two respective temperature time history segments were made. The cyan colored line is the linear fit of the image-derived temperatures, and the bold red line is the linear fit of the plug08 TC-derived temperature. The resulting linear slopes for each time segment correlate, indicating the temperature change, or cooling rate, was represented by both measurement methods.

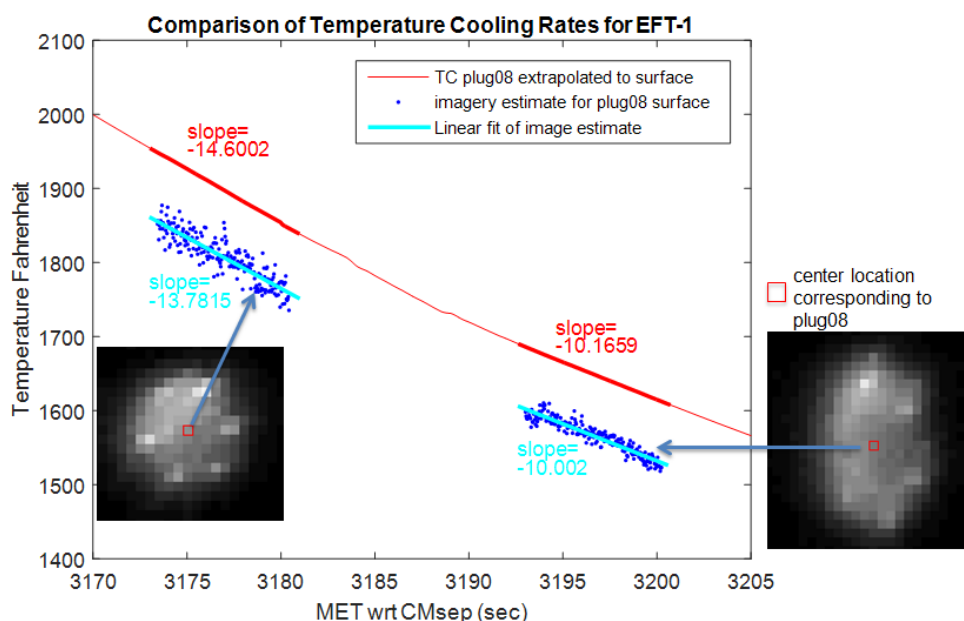



Figure 7.3.7-4. Comparison of Temperature Cooling Rates during Two Selected Intervals of Reentry When Best Imagery Was Acquired

Because the image-derived temperatures (i.e., blue dots in Figure 7.3.7-4) were not derived from the image enhancement process, they were not smoothed. Thus, the temperature data scatter gives a representation of the “noise” in the imagery-derived temperatures using the native data. The first time segment had larger variations than the second time segment for two reasons. The first reason was that there was a larger intensity gradient (i.e., larger temperature change) across the heat shield center during the earlier time segment, so the discretization of pixels along that large gradient caused variations. The second reason was the NIR detector integration time was longer during the second time segment, which tends to reduce or smooth the frame-to-frame “noise,” similar to co-adding frames.

In summary, the reconstructed surface temperature from the TCs appears to have a 100 °F bias high relative to the image derived temperatures. This bias cannot be explained by the uncertainties identified in the factors driving the observation-based temperature. However, the cooling rates inferred from the two measurements were consistent. This suggests further examination into the TC reconstruction process should be considered, including a high-fidelity uncertainty analysis of the charred and ablated Avcoat material properties.

	NASA Engineering and Safety Center Technical Assessment Report	Document #: NESC-RP- 12-00795	Version: 1.0
Title:	Remote Imaging of EFT-1 Entry Heating Risk Reduction		Page #: 87 of 98

8.0 Findings, Observations, and NESC Recommendations

8.1 Findings


The following findings were identified:

Platform and Instrument Capability

- F-1.** Aerial-based optical measurement platforms reduce the attenuating effects of the atmosphere and can provide the necessary range for over water imaging operations.
- F-2.** Ground-based imaging systems were not capable of providing the desired thermal detection capability largely because of the remote broad area of ocean where the desired observation was required.
- F-3.** Sea-based imaging systems, while less restrictive than a ground system regarding deployment location, were not considered due to gyro-stabilization requirements and image degrading effects from viewing through an atmospheric marine layer.
- F-4.** Existing sensor technology is capable of providing sufficient thermal sensitivity and spatial resolution to meet the MPCV FTO OFT1.091 MOP.

Planning

- F-5.** The virtual planning tools were critical in the revelation the capsule heat shield size and temperature would make it difficult to discern from the sky background when first detected from aerial-based optical measurement platforms.
- F-6.** Heat shield TPS material properties provided critical information to optimize the sensors for long-range acquisition.
- F-7.** The metallic film applied to the heat shield would significantly attenuate the MWIR signal, which precluded its use for long-range acquisition.
- F-8.** The metallic film applied to the heat shield would significantly enhance the SWIR signature from solar emissions and increase the probability for a successful long-range acquisition.
- F-9.** Heat shield ablation products in the shock layer during reentry would not significantly attenuate the infrared emissions from the heat shield in the NIR and MWIR waveband.
- F-10.** Pre-mission radiance modeling indicated the emissions from the high-temperature shock layer would not interfere with the heat shield infrared emissions in the NIR and MWIR wavebands.
- F-11.** Mission success was enhanced through pre-observation simulations (e.g., animations, synthetic imagery), which include the entire operational ground, flight, and aerial team.
- F-12.** Multiple pre-observation training and simulation/dress rehearsal exercises permitted the NESC/MPCV Program/Navy team to integrate into the EFT-1 mission timelines,

	NASA Engineering and Safety Center Technical Assessment Report	Document #: NESC-RP- 12-00795	Version: 1.0
Title:	Remote Imaging of EFT-1 Entry Heating Risk Reduction		Page #: 88 of 98

optimize the mission execution plan, and identify errors in the weather tool reporting process.

- F-13.** Unmanned aircraft bring more restrictions than manned aircraft due to the need for compliance with additional FAA regulations and approvals when transiting an unmanned aircraft through the National Airspace System.

Imaging Campaign and Data Processing

- F-14.** Aircraft operational altitude limitations impact the magnitude/quality of imagery data.
- F-15.** The image data files from the aircraft were initially incompatible with the image processing software.
- F-16.** Numerical image reconstruction methods improved image quality while preserving radiometric accuracy from which to infer surface temperature.
- F-17.** Image quality/spatial resolution was affected by atmospheric and operational factors (e.g., manual tracking, magnification/de-magnification-type distortions, atmospheric density changes).
- F-18.** Atmospheric transmission and surface emissivity are the largest contributors to the image-derived temperature uncertainty.
- F-19.** An approximate 100 °F difference was observed between image- and two TC-derived heat shield surface temperature estimates. The two TCs selected exhibited minimal voltage fluctuations observed on other DFI TCs. These voltage fluctuations are currently attributed to electro-magnetic effects from the shock-layer plasma.
- F-20.** The image- and TC-derived heat shield cooling rates were comparable.
- F-21.** Initial TC-derived heat shield temperature values are presently outside the high-confidence error estimate associated with the image-derived surface temperature.

8.2 Observations


The following observations were identified:

Platform and Instrument Capability

- O-1.** The NASA WB-57 was a viable primary or secondary observation platform for MPCV capsule reentry thermal observation.

Planning

- O-2.** Agency delays to the EFT-1 mission required the NESC operations team to go into semi-hibernation to control costs.
- O-3.** Dress rehearsal flights were essential in setting expectations and fostered increased crew proficiency.

	NASA Engineering and Safety Center Technical Assessment Report	Document #: NESC-RP- 12-00795	Version: 1.0
Title:	Remote Imaging of EFT-1 Entry Heating Risk Reduction		Page #: 89 of 98

- O-4.** Concurrently or consecutively aligned observation campaigns (i.e., EFT-1 and Commercial Resupply Services-4) strained the NESC assessment management and mission operations teams.
- O-5.** The operational experience gained and the lessons learned from a series of observations supporting a SpaceX flight test months prior to EFT-1 played an important role in the ability for the assessment operations team to support efficient planning and mission operations of three aircraft during the NASA EFT-1 mission.

Imaging Campaign and Data Processing


- O-6.** Cloud obscuration information concurrently used two weather models (i.e., Global Forecast System and Weather Research and Forecasting) for the first time.
- O-7.** Co-locating the NESC assessment operations imagery team with the MPCV Program imagery team facilitated communication during the hours preceding the observation.
- O-8.** The JSC Flight Operations Division provided invaluable support and infrastructure to facilitate communications and information to make informed decisions.
- O-9.** While not a requirement, the MPCV Program's desire for 48-hour quick-look data (PAO images, movies) were recognized and properly anticipated by the NESC team.
- O-10.** The NESC team anticipated cost (hardware) and schedule (encryption) impacts from Sensitive But Unclassified (proprietary)/International Traffic in Arms Regulations classification requirements.

8.3 NESC Recommendations

The following NESC recommendations are directed toward the MPCV Aerosciences team:

- R-1.** Update the uncertainties of Avcoat material properties and quantify their sensitivity on the reconstructed surface temperature inferred from the in-depth TCs prior to the EM-1 flight test. *(F-19, F-20, and F-21)*
- R-2.** Perform laboratory testing to identify root cause (and mitigation) of the voltage fluctuations as measured by the DFI TCs, which limited opportunities for comparison with image-derived surface temperature. *(F-19)*

Recommendation is being pursued. The NESC has provided funding to the MPCV Program to have the EM-1 heat shield Government-furnished equipment DFI team determine the cause of non-physical temperature readings observed in some of the near-surface EFT-1 thermocouples. A test is being planned to investigate the susceptibility of the thermocouples to EMI from ionized gases in the plasma during entry.

	NASA Engineering and Safety Center Technical Assessment Report	Document #: NESC-RP- 12-00795	Version: 1.0
Title:	Remote Imaging of EFT-1 Entry Heating Risk Reduction		Page #: 90 of 98

The following NESC recommendations are directed toward the MPCV FTMO:

- R-3.** Allocate sufficient lead time for integrating unmanned aircraft into the operations plan and obtaining flight safety approval for co-location with crewed aircraft. **(F-11, F-13)**
- R-4.** Ensure that sufficient monetary reserves are allocated and maintained to cover reasonable slips in a flight test. **(O-2)**


The following NESC recommendations are directed toward the SCIFLI team:

- R-5.** Define image file format requirements to asset providers and verify file/analysis tool compatibility prior to sensor calibration and mission operations. **(F-15)**
- R-6.** Explore utilization of high-altitude, long-endurance platforms to support entire launch window, including multiple day delay, coverage. **(F-1, F-2, F-3, F-14, F-17, F-18, O-1, O-7, and O-8)**

Recommendation has been accepted by the DoD and implemented by the SCIFLI team. The DoD Test Resource Management Center (TRMC) acknowledged the current national capability to support flight T&E is incapable of providing timely and affordable engineering data products (2015 congressional mandate to identify ways to reduce costs/enhance capability). The SCIFLI team is leading a DoD-sponsored study to provide decision makers with a defensible strategic plan for an affordable national High Altitude Long Endurance (HALE) UAV fleet to more efficiently support flight T&E. Such high-altitude capability would have avoided the loss of peak heating imagery as experienced during the EFT-1 observation due to obscuring clouds. The SCIFLI team is also collaborating with the DoD and the conventional Prompt Global Strike Program to support a technology demonstration flight during a hypersonic flight test in 2017 using two NASA aircraft. This next-generation quantitative imaging system (i.e., integrated sensor and platform) would more affordably support civilian and military flight testing to support developing critical and enabling technologies including elements necessary for, but not limited to, hypersonic aerothermodynamics, high-temperature TPS materials, flight dynamics, and range safety including launch, and reentry and spacecraft demise (orbital debris).

- R-7.** Pursue development of a cost-effective enhanced sensor capability using autonomy and sensor-directed flight to increase spatial resolution and accuracy while minimizing tracking motion blur and sensor saturation. **(F-5, F-7, F-8, F-9, F-10, F-13, and F-16)**

Recommendation has been accepted by the DoD and implemented by the SCIFLI team. The SCIFLI team is partnering to support a DoD Broad Agency Announcement to design, develop, and test a next-generation electro-optical imaging system suitable for deployment on a NASA Global Hawk.

	NASA Engineering and Safety Center Technical Assessment Report	Document #: NESC-RP- 12-00795	Version: 1.0
Title:	Remote Imaging of EFT-1 Entry Heating Risk Reduction		Page #: 91 of 98

- R-8.** Ensure an FRR is conducted with the asset providers (sensor operators and flight crews) prior to observation campaign to increase mission success probability. (*F-11 and F-13*)
- R-9.** Ensure a dedicated Project Manager who oversees all of the planning, contracting, execution, and post-mission activities is in place for future observation campaigns. (*O-4, O-9*)

9.0 Alternate Viewpoint

There were no alternate viewpoints identified during the course of this assessment by the NESC team or the NRB quorum.

10.0 Other Deliverables

Data files pertaining to MPCV Avcoat heat shield surface optical properties were provided to MPCV Aerosciences and electronically retained by the JHU-APL to support future infrared observation analyses. The sample material identification are as follows:

Avcoat (Block 113-100556-1 #8 “O”) with white epoxy enamel paint (BiPacco 1839-39 (120-1)

Kapton[®] Tape (P1400173 MS-1E250)

Charred/Ablated Avcoat (ARMSEF #3348)

RCG Tile (C000DE)

11.0 Lessons Learned


No applicable lessons learned were identified for entry into the NASA Lessons Learned Information System (LLIS) as a result of this assessment.

12.0 Recommendations for NASA Standards and Specifications

No recommendations for NASA standards and specifications were identified as a result of this assessment.

13.0 Definition of Terms


Corrective Actions	Changes to design processes, work instructions, workmanship practices, training, inspections, tests, procedures, specifications, drawings, tools, equipment, facilities, resources, or material that result in preventing, minimizing, or limiting the potential for recurrence of a problem.
Finding	A relevant factual conclusion and/or issue that is within the assessment scope and that the team has rigorously based on data from their independent analyses, tests, inspections, and/or reviews of technical documentation.

	NASA Engineering and Safety Center Technical Assessment Report	Document #: NESC-RP- 12-00795	Version: 1.0
Title:	Remote Imaging of EFT-1 Entry Heating Risk Reduction		Page #: 92 of 98


Lessons Learned	Knowledge, understanding, or conclusive insight gained by experience that may benefit other current or future NASA programs and projects. The experience may be positive, as in a successful test or mission, or negative, as in a mishap or failure.
Observation	A noteworthy fact, issue, and/or risk, which may not be directly within the assessment scope, but could generate a separate issue or concern if not addressed. Alternatively, an observation can be a positive acknowledgement of a Center/Program/Project/Organization's operational structure, tools, and/or support provided.
Problem	The subject of the independent technical assessment.
Proximate Cause	The event(s) that occurred, including any condition(s) that existed immediately before the undesired outcome, directly resulted in its occurrence and, if eliminated or modified, would have prevented the undesired outcome.
Recommendation	A proposed measurable stakeholder action directly supported by specific Finding(s) and/or Observation(s) that will correct or mitigate an identified issue or risk.
Root Cause	One of multiple factors (events, conditions, or organizational factors) that contributed to or created the proximate cause and subsequent undesired outcome and, if eliminated or modified, would have prevented the undesired outcome. Typically, multiple root causes contribute to an undesired outcome.
Supporting Narrative	A paragraph, or section, in an NESC final report that provides the detailed explanation of a succinctly worded finding or observation. For example, the logical deduction that led to a finding or observation; descriptions of assumptions, exceptions, clarifications, and boundary conditions.

14.0 Acronyms List


°F	Degrees Fahrenheit
2-D	Two-dimensional
3-D	Three-dimensional
AC	Asset Coordinator
ADC	Analog-to-Digital Converter
AFB	Air Force Base
AFRC	Armstrong Flight Research Center
AOS	Acquisition of Signal
BET	Best Estimated Trajectory
BH	Bloodhound

	NASA Engineering and Safety Center Technical Assessment Report	Document #: NESC-RP- 12-00795	Version: 1.0
Title:	Remote Imaging of EFT-1 Entry Heating Risk Reduction		Page #: 93 of 98

CAD	Computer-Aided Design
CC	Calibration Coordinator
CDT	Central Daylight Time
CFD	Computational Fluid Dynamics
CFLOS	Cloud-Free Line of Sight
ChaPS	Chase Plane Simulator
CHAR	Charring Ablator Response
CMR	Critical Mission Review
DFI	Developmental Flight Instrumentation
DN	Digital Number (counts)
DoD	Department of Defense
DyNAMITE	Day/Night Airborne Motion for Terrestrial Environments
EDL	Entry, Descent, and Landing
EFT-1	Exploration Flight Test-1
EI	Entry Interface
EM-1	Exploration Mission-1
FAA	Federal Aviation Administration
FADS	Flush Air Data System
FDO	Flight Dynamics Officer
FoR	Field of Regard
FOV	Field of View
FRR	Flight Readiness Review
FTMO	Flight Test Management Office
FTO	Flight Test Objective
Gb	Gigabyte
GMT	Greenwich Mean Time (same as UTC)
HALO	High-Altitude Observatory
HEAT	Hollow aErothermal Ablation and Temperature
HF	High Frequency
hr	hour
HYTHIRM	Hypersonic Thermodynamic Infrared Measurements
Hz	Hertz
IPOC	Imagery Payload Operations Center
JHU-APL	Johns Hopkins University Applied Physics Laboratory
JIS	Joint Integrated Simulation
JSC	Johnson Space Center
K	Degrees Kelvin
kft	kilofeet
km	kilometers

	NASA Engineering and Safety Center Technical Assessment Report	Document #: NESC-RP- 12-00795	Version: 1.0
Title: Remote Imaging of EFT-1 Entry Heating Risk Reduction			Page #: 94 of 98


KSC	Kennedy Space Center
KX	JSC Imagery Group
LaRC	Langley Research Center
LOS	Loss of Signal
LSO	Landing Support Officer
LWIR	Longwave Infrared
m	meter
M	Mach number
MC	Mission Coordinator
MCC	Mission Control Center
MDA	Missile Defense Agency
MEP	Mission Execution Plan
mi	mile
min	minute
mm	millimeter
MODTRAN®	Moderate Resolution Atmospheric Transmission
MOP	Measure of Performance
MPCV	Multi-Purpose Crew Vehicle
msec	milliseconds
MSP	Mission Support Plan
MWIR	Midwave Infrared
NEQAIR	Nonequilibrium Air Radiation code
NESC	NASA Engineering and Safety Center
NIR	Near-Infrared
nm	nanometers
nmi	nautical mile
NOAA	National Oceanic and Atmospheric Administration
NRB	NESC Review Board
OML	Outer Mold Line
PAO	Public Affairs Office
q	dynamic pressure
RCS	Reaction Control System
SCIFLI	Scientifically Calibrated In-Flight Imagery
sec	second
SMG	Spaceflight Meteorology Group
SOFIA	Stratospheric Observatory for Infrared Astronomy
SPURC	Standard Plume Ultraviolet Radiation Code
SSP	Space Shuttle Program
SWIR	Shortwave Infrared

	NASA Engineering and Safety Center Technical Assessment Report	Document #: NESC-RP- 12-00795	Version: 1.0
Title:	Remote Imaging of EFT-1 Entry Heating Risk Reduction		Page #: 95 of 98


T&E	Test and Evaluation
TC	Thermocouple
TDT	Technical Discipline Team
TPS	Thermal Protection System
TSP	Test Support Point
UAS	Unmanned Aerial System
UAV	Unmanned Aerial Vehicle
UTC	Coordinated Universal Time (same as GMT)
ViDI	Virtual Diagnostics Interface
W/cm ² /sr	Watts per centimeter squared per Steradian
WFOV	Wide Field of View

15.0 References

1. NESC Assessment: Orbiter Boundary Layer Transition (BLT) Testing for Development of Aeroheating Prediction Methodology, Task 5: Remote Entry Imaging (Phase A), NESC-TI-07-00413.
2. Horvath, T.; Berry, S.; Alter, S.; Blanchard, R.; Schwartz, R.; Ross, M.; and Tack, S.: "Shuttle Entry Imaging Using Infrared Thermography," AIAA-2007-4267, June 2007.
3. Ross, M.; Werner, M.; Mazuk, S.; Blanchard, R.; Horvath, T.; Berry, S.; Wood, W.; and Schwartz, R.: "Infrared Imagery of the Space Shuttle at Hypersonic Entry Conditions," AIAA-2008-0636, *46th AIAA Aerospace Sciences Meeting and Exhibit*, Reno, NV, January 7–10, 2008.
4. Schwartz, R.; Ross, M.; Baize, R.; Horvath, T.; Berry, S.; and Krasa, P.: "A System Trade Study of Remote Infrared Imaging for Space Shuttle Re-entry," AIAA-2008-4023, June 2008.
5. Splinter, S.; Daryabeigi, K.; Horvath, T.; Mercer, C. D.; Ghanbari, C.; Tietjen, A.; and Schwartz, R.: "Solar Tower Experiments for Radiometric Calibration and Validation of Infrared Imaging Assets and Analysis Tools for Entry Aero-Heating Measurements," AIAA-2008-4025, June 2008.
6. Horvath, T.; Berry, S.; Splinter, S.; Daryabeigi, K.; Wood, W.; Schwartz, R.; and Ross, M.: "Assessment and Mission Planning Capability for Quantitative Aerothermodynamic Flight Measurements Using Remote Imaging," AIAA-2008-4022, June 2008.
7. Berry, S.; Horvath, T.; Schwartz, R.; Ross, M.; Campbell, C.; and Anderson, B.: "IR Imaging of Boundary Layer Transition Flight Experiments," AIAA-2008-4026, June 2008.
8. Gibson, D. M.; Spisz, T. S.; Taylor, J. C.; Zalameda, J. N.; Horvath, T. J.; Tomek, D. M.; Tietjen, A. B.; Tack, S.; and Bush, B. C.: "HYTHIRM Radiance Modeling and Image Analyses in Support of STS-119, STS-125, and STS-128 Space Shuttle Hypersonic Re-entries," AIAA Paper 2010-244, January 2010.


	NASA Engineering and Safety Center Technical Assessment Report	Document #: NESC-RP- 12-00795	Version: 1.0
Title:	Remote Imaging of EFT-1 Entry Heating Risk Reduction		Page #: 96 of 98

9. Zalameda, J. N.; Horvath, T. J.; Tomek, D. M.; Tietjen, A. B.; Gibson, D. M.; Taylor, J. C.; Tack, S.; Bush, B. C.; Mercer, C. D.; and Shea, E. J.: "Application of a Near Infrared Imaging System for Thermographic Imaging of the Space Shuttle during Hypersonic Re-entry," AIAA Paper 2010-245, January 2010.
10. Tack, S.; Tomek, D. M.; Horvath, T. J.; Verstynen, H. A.; and Shea, E. J.: "Cast Glance Near Infrared Imaging Observations of the Space Shuttle during Hypersonic Re-entry," AIAA Paper 2010-243, January 2010.
11. Horvath, T. J.; Tomek, D. M.; Berger, K. T.; Splinter, S. C.; Zalameda, J. N.; Krasa, P. W.; Tack, S.; Schwartz, R. J.; Gibson, D. M.; and Tietjen A. B.: "The HYTHIRM Project: Flight Thermography of the Space Shuttle during Hypersonic Re-entry," AIAA Paper 2010-241, January 2010.
12. Spisz, T. S.; Taylor, J. C.; Gibson, D. M.; Kwame, O. W.; Horvath, T. J.; Zalameda, J. N.; Tomek, D. M.; Berger, Tietjen, A. B.; Tack, S.; and Schwartz, R. J.: "Processing Near-Infrared Imagery of Hypersonic Space Shuttle Reentries," *Thermosense XXXII Conference at 2010 SPIE Defense, Security, and Sensing Symposium*, April 5–9, 2010, Orlando, FL, Paper#7661-17.
13. Taylor, J. C.; Spisz, T.; Kennerly, S.; Gibson, D.; Horvath, T.; Zalameda, J.; Splinter, S.; Kerns, R.; and Schwartz, R.: "Global Thermography of the Space Shuttle during Hypersonic Re-entry," AIAA 2011-3324, June 2011.
14. Schwartz, R. J.; McCrea, A. C.; Gruber, J. R.; Hensley, D. W.; Verstynen, H. A.; Oram, T.; Berger, K. T.; Splinter, S.; Horvath, T. J.; and Kerns, R. V.: "Remote Infrared Imaging of the Space Shuttle during Hypersonic Flight: HYTHIRM Mission Operations and Coordination," AIAA 2011-3326, June 2011.
15. Horvath, T. J.; Kerns, R. V.; Jones, K. M.; Grinstead, J. H.; Schwartz, R. J.; Gibson, D. M.; Tack, S.; and Dantowitz, R. F.: "A Vision of Quantitative Imaging Technology for Validation of Advanced Flight Technologies," AIAA-2011-3325, June 2011.
16. Horvath, T. J.; Zalameda, J. J.; Wood, W. A.; Berry, S. A.; Swartz, R. J.; Dantowitz, R. F.; Spisz, T. S.; and Taylor, J. C.: "Time Resolved Global Infrared Observations of Roughness Induced Boundary Layer Transition on the Space Shuttle Orbiter During STS-134 Reentry," NATO RTO-MP-AVT-200-27, *Applied Vehicle Technology Panel and Specialist's Meeting on Hypersonic Laminar-Turbulent Transition*, San Diego, CA, April 16–19, 2012.
17. Spisz, T. S.; Taylor, J. C.; Gibson, D. M.; Kennerly, S. W.; Kwame, O.; Horvath, T. J.; Zalameda, J. N.; Kerns, R. V.; Shea, E. J.; Mercer, C. D.; Schwartz, R. J.; Dantowitz, R. F.; and Kozubal, M. J.: "Processing Ground-Based Near-Infrared Imagery of Space Shuttle Reentries," *Thermosense XXXIV Conference at 2012 SPIE Defense, Security, and Sensing Symposium*, April 23–27, 2012, Baltimore, MD, Paper 8354-15.
18. Zalameda, J. N.; Horvath, T. J.; Kerns, R. V.; Taylor, J. C.; Spisz, T. S.; Gibson, D. M.; Shea, E. J.; Mercer, C. D.; Schwartz, R. J.; Tack, S.; Bush, B. C.; and Dantowitz, R. F.: "Thermographic Imaging of the Space Shuttle during Re-Entry Using a Near Infrared

	NASA Engineering and Safety Center Technical Assessment Report	Document #: NESC-RP- 12-00795	Version: 1.0
Title:	Remote Imaging of EFT-1 Entry Heating Risk Reduction		Page #: 97 of 98

Sensor,” *Thermosense XXXIV Conference at 2012 SPIE Defense, Security, and Sensing Symposium*, April 23-27, 2012, Baltimore, MD, Paper 8354-14.

19. Horvath, T. J.; Cagle, M. F.; Grinstead, J. H.; and Gibson, D. M.: “Remote Observations of Reentering Spacecraft Including the Space Shuttle Orbiter,” *IEEE-2013-2707*, March 2013.
20. Morring, F., Jr.: “NASA, SpaceX Share Data on Supersonic Retropropulsion,” *Aviation Week & Space Technology*, October 20, 2014.
21. Orion-MPCV Aerothermodynamics Team, “Supporting Aerothermal Data for EFT-1 90-Day Post-Flight Report,” NASA JSC, March 2015.
22. Schwartz, R. J.; and McCrea, A. C.: “Virtual Diagnostic Interface: Aerospace Experimentation In The Synthetic Environment,” *MODSIM World Conference and Expo.*, October 14, 2009.
23. Schwartz, R. J.: “ViDI: Virtual Diagnostics Interface Volume 1—The Future of Wind Tunnel Testing” Contractor Report NASA/CR-2003-212667, December 2003.
24. Schwartz, R. J.; and Fleming, G. A.: “LiveView3D: Real Time Data Visualization for the Aerospace Testing Environment,” *AIAA-2006-1388, 44th AIAA Aerospace Sciences Meeting and Exhibit*, Reno, NV, January 9–12, 2006.
25. Schwartz, R. J.; and McCrea, A. C.: “Virtual Diagnostic Interface: Aerospace Experimentation in the Synthetic Environment,” *MODSIM World 2009 Conference and Expo.*, Virginia Beach, VA, October 14–16, 2009.
26. Crow, D.; Coker, C.; and Keen, W.: “Fast Line-of-Sight Imagery for Target and Exhaust-Plume Signatures (FLITES) Scene Generation Program,” *Technologies for Synthetic Environments: Hardware-in-the-Loop Testing XI*. Edited by Murrer, and Robert Lee, Jr., *Proceedings of the SPIE*, Vol. 6208, June 2006.
27. Oguz, H. N.; and O’Neil, J. M.: “EZMSLRAD Users Manual,” JHU/APL, A1C-04-067, May 13, 2004.
28. Berk, A.; Bernstein, L. S.; and Robertson, D. C.: “MODTRAN: A Moderate Resolution Model for LOWTRAN7,” Report GL-TR-89-0122, Air Force Geophys. Lab., Bedford, MA, April 1989.
29. Kelly, M. A.; Osei-Wusu, K.; Spisz, T. S.; Strong, S.; Setters, N.; and Gibson, D. M.: “Assimilation of Nontraditional Datasets to Improve Atmospheric Compensation,” *2012 SPIE Defense Security & Sensing Symposium, Atmospheric Propagation IX*, SPIE-8380.
30. Wright, M. L.; Candler, G. V.; and Bose, D.: “Data-Parallel Line Relaxation Method for the Navier-Stokes Equations,” *AIAA Journal*, Vol. 36, No. 9, September 1998.
31. “Standard Plume Ultraviolet Radiation Code (SPURC2.0) User’s Manual,” Air Force Research Lab, Edwards AFB, CA 93524, AFRL/PRSA-PS, January 2007.
32. Whiting, E.; Park, C.; Liu, Y.; Arnold, J.; and Paterson, J.: “NEQAIR96, Nonequilibrium and Equilibrium Radiative Transport and Spectra Program: User’s Manual,” NASA RP-1389, 1996.

	NASA Engineering and Safety Center Technical Assessment Report	Document #: NESC-RP- 12-00795	Version: 1.0
Title:	Remote Imaging of EFT-1 Entry Heating Risk Reduction		Page #: 98 of 98

33. EFT-1 Imagery Operations Post Flight Report, JSC-66799, April 27, 2015.
34. Periaswamy, S.; and Farid, H.: "Elastic Registration in the Presence of Intensity Variations," *IEEE Transactions on Medical Imaging*, Vol. 22, No. 7, July 2003.
35. Personal communication, Stan Bouslog, NASA JSC, April 2016.
36. Santos, J.; Oishi, T.; and Martinez, E.: "Isotherm Sensor Calibration Program for Mars Science Laboratory Heat Shield Flight Data Analysis," *42nd AIAA Thermophysics Conference*, June 27–30, 2011, Honolulu, HI, AIAA 2011-3955.
37. Oliver, A. B.; Amar, A. J.; Droba, J.; Lessard V.; and Mahzari, M.: "EFT-1 Heatshield Aerothermal Environment Reconstruction," *46th AIAA Thermophysics Conference*; June 13–16, 2016, Washington, DC.
38. Oliver, A. B.; and Amar, A. J.: "Inverse Heat Conduction Methods in the CHAR Code for Aerothermal Flight Data Reconstruction," *46th AIAA Thermophysics Conference*; June 13–16, 2016; Washington, DC.

16.0 Appendices (separate volume)

Because the Appendices to this report contain restricted materials, they will not be included in the publication.

- Appendix A: Surface Optics Emissivity Measurement Final Report
- Appendix B: EFT-1 Mission Execution Plan (MEP)
- Appendix C: Critical Events Timeline
- Appendix D: Aircraft Contingency Matrix
- Appendix E: Cast Glance Sensor Calibration Final Report
- Appendix F: Cast Glance Mission Support Plan (MSP)
- Appendix G: Cast Glance Final Report & Sensor Operational Notes
- Appendix H: Unified Best Estimated Trajectory (BET)

REPORT DOCUMENTATION PAGE					Form Approved OMB No. 0704-0188	
<p>The public reporting burden for this collection of information is estimated to average 1 hour per response, including the time for reviewing instructions, searching existing data sources, gathering and maintaining the data needed, and completing and reviewing the collection of information. Send comments regarding this burden estimate or any other aspect of this collection of information, including suggestions for reducing this burden, to Department of Defense, Washington Headquarters Services, Directorate for Information Operations and Reports (0704-0188), 1215 Jefferson Davis Highway, Suite 1204, Arlington, VA 22202-4302. Respondents should be aware that notwithstanding any other provision of law, no person shall be subject to any penalty for failing to comply with a collection of information if it does not display a currently valid OMB control number.</p> <p>PLEASE DO NOT RETURN YOUR FORM TO THE ABOVE ADDRESS.</p>						
1. REPORT DATE (DD-MM-YYYY)		2. REPORT TYPE		3. DATES COVERED (From - To)		
01-06-2016		Technical Memorandum		June 2012 - May 2016		
4. TITLE AND SUBTITLE Remote Imaging of Exploration Flight Test-1 (EFT-1) Entry Heating Risk Reduction				5a. CONTRACT NUMBER		
				5b. GRANT NUMBER		
				5c. PROGRAM ELEMENT NUMBER		
6. AUTHOR(S) Schuster, David M.; Horvath, Thomas J.; Schwartz, Richard J.				5d. PROJECT NUMBER		
				5e. TASK NUMBER		
				5f. WORK UNIT NUMBER 869021.05.07.09.18		
7. PERFORMING ORGANIZATION NAME(S) AND ADDRESS(ES) NASA Langley Research Center Hampton, VA 23681-2199				8. PERFORMING ORGANIZATION REPORT NUMBER L-20727 NESC-RP-12-00795		
9. SPONSORING/MONITORING AGENCY NAME(S) AND ADDRESS(ES) National Aeronautics and Space Administration Washington, DC 20546-0001				10. SPONSOR/MONITOR'S ACRONYM(S) NASA		
				11. SPONSOR/MONITOR'S REPORT NUMBER(S) NASA/TM-2016-219214		
12. DISTRIBUTION/AVAILABILITY STATEMENT Unclassified - Unlimited Subject Category 16-Space Transportation and Safety Availability: NASA STI Program (757) 864-9658						
13. SUPPLEMENTARY NOTES						
14. ABSTRACT A Measure of Performance (MOP) identified with an Exploration Flight Test-1 (EFT-1) Multi-Purpose Crew Vehicle (MPCV) Program Flight Test Objective (FTO) (OFT1.091) specified an observation during reentry through external ground-based or airborne assets with thermal detection capabilities. The objective of this FTO was to be met with onboard Developmental Flight Instrumentation (DFI), but the MOP for external observation was intended to provide complementary quantitative data and serve as a risk reduction in the event of anomalous DFI behavior (or failure). The Entry, Descent, and Landing Phase Engineer for the MPCV Program requested a risk-reduction assessment from the NASA Engineering and Safety Center (NESC) to determine whether quantitative imagery could be obtained from remote aerial assets to support the external observation MOP. This document contains the outcome of the NESC Assessment.						
15. SUBJECT TERMS Measure of Performance; Exploration Flight Test-1; Multi-Purpose Crew Vehicle; NASA Engineering and Safety Center; Remote Imaging; Risk Reduction						
16. SECURITY CLASSIFICATION OF:			17. LIMITATION OF ABSTRACT	18. NUMBER OF PAGES	19a. NAME OF RESPONSIBLE PERSON	
a. REPORT	b. ABSTRACT	c. THIS PAGE			STI Help Desk (email: help@sti.nasa.gov)	
U	U	U	UU	103	19b. TELEPHONE NUMBER (Include area code) (443) 757-5802	